

Responses to Comments by the Referees and Readers

C. Ye (c.ye@pku.edu.cn) and X. Zhou (xianliang.zhou@health.ny.gov)

(1) Response to the Interactive comment by Anonymous Referee #1 on “Tropospheric HONO Distribution and Chemistry in the Southeast U.S.”

The manuscript “Tropospheric HONO distribution and chemistry in the Southeast U.S.” by Ye et al. presents HONO measurements made during the NOMADSS campaign. The two main claims presented here are: (1) there is more HONO observed than can be explained by known chemistry, and (2) photolysis of particle nitrate accounts for this so-called missing HONO source. The analysis used to make both claims are weak, therefore, unconvincing. Moreover, the analysis on nighttime chemistry and production in power plant exhaust were hastily done and written. This work can be considered for publication only after significant improvements.

Response: We thank the Anonymous Referee #1 for pointing out the shortcomings in our analysis and presentation of the data. We have significantly revised the manuscript accordingly to address the referee’s comments and concerns. Here are our responses to the referee’s specific comments.

As for (1), the authors claim that because HONO photo-lifetime is 8 minutes, that direct emission of HONO can be disregarded. This is a misinterpretation of the concept of lifetime. Lifetime represents an e-folding time, meaning that ~36% of the original amount still remains after 8 minutes since time zero, or time since emission. If HONO at the emission source is 10 ppb, approximately 50 to 60 minutes is required for HONO to reach 11 ppt, the median HONO level reported. Judging by figure 2, the median HONO value of 11 ppt (what the authors claim is anthropogenic-free HONO) is observed in close proximity to urban plumes (20 to 30 ppt, identified in figure 2). This 50 to 60 minute period is an underestimate since it does not account for re-formation of HONO by OH + NO, both of which are likely to be elevated in urban plumes. Bottom line is that the authors need to demonstrate convincingly that the 11 ppt HONO is not derived from anthropogenic sources (by quantitatively accounting for mixing, emissions, and chemistry), because the case for this so-called ‘extra’ HONO is the difference between 11 ppt and 2 ppt (amount of HONO expected assuming PSS without this ‘extra’ source). The analysis as it currently stands is inadequate.

Response: The referee is correct that ~36% of the original HONO remains after one photolysis lifetime. However, we did not “disregard” the contribution from ground HONO source simply because HONO photo-lifetime is 8 minutes. We would first like to point out that there has not been any report in literature for 10 ppbv daytime HONO on the ground level, as the referee assumed. The daytime HONO/NO_x ratio is in the range of 0.05-0.1 in the low-NO_x rural atmosphere (Zhou et al., 2002) and ~ 0.02 in high-NO_x urban environment (Villena et al., 2011). The direct emission HONO/NO_x ratios are even lower, ≤0.01 in automobile exhausts (Kirchstetter et al., 1996; Li et al., 2008) and ~0.002 in power plant plumes (Neuman et al., 2016). The NO_x levels that we observed in the Southeast U.S. was mostly under 0.5 ppbv in the background area and even in the urban plumes; the initial HONO concentration associated with the observed levels of NO_x would be ≤ 50 pptv even if

an upper limit HONO/NO_x ratio of 0.1 is assumed. With a transport time of ~1 h from the source, i.e., ~ 5 times of the HONO photolysis lifetime, the contribution from the source would be well below the detection limit of 1 pptv of our HONO instrument. Therefore, we argued that the measured HONO was mostly produced *in situ* from precursors such as NO_x and pNO₃ within the air masses during the transport, not from the ground HONO sources.

Our conclusion of no significant contribution from the ground HONO source was also based on the vertical profile of HONO. We examined the vertical profiles of HONO, its precursor, isoprene and potential temperature (Figure 4) in section “3.2 HONO contribution from ground-level sources”. Isoprene is a biogenic VOC emitted from ground vegetations (trees) and has a lifetime of ~1 hr. Based on isoprene vertical distribution information, a TBL mixing time can be estimated. The photolysis lifetime of HONO was much shorter than that of isoprene during the daytime NOMADSS flights. If the ground source contributed significant to the TBL HONO budget, a much steeper vertical concentration gradient than that of isoprene should be expected. However, we observed relatively uniform vertical concentration profiles (Figs. 3 and 4), suggesting that contribution from ground HONO source was not important.

We did not randomly assign an air mass as “background” or “urban” just based on HONO concentrations. In the four daytime research flights (RFs #4, #5, #11 and #17) reported in this manuscript, we conducted our airborne HONO measurements mostly over the rural regions in Southeast U.S., and only sampled urban and power plumes sometimes in RF #11 (Figure 2). A large suite of chemical and metrological parameters were measured onboard the C-130. The identifications of plumes and background air masses were done with the help of plumes tracers like NO_x, and benzene (Figure 7) in original manuscript, further with SO₂, CO, and acetonitrile (Figure S1) in the revised manuscript. And in RF #18, we performed back trajectory calculations to examine the impact of urban plume from Nashville metropolitan area. Indeed, HONO was being produced from its precursors (including the OH-NO reaction the referee mentioned) in the air mass during the transport. The HONO is considered *in situ* produced, not directly emitted. When an air mass was influenced by the urban emission, concentrations of HONO precursors and urban tracers (NO_x, CO, benzene) were higher, and *in situ* HONO production would be higher.

We have significantly revised the discussion in the manuscript in both “3.2 HONO contribution from ground-level sources” and “3.4 HONO chemistry in plumes”, to address referee’s concerns and to make our argument more clearly.

As for (2), the authors conclude a causal relationship between photolysis of particulate nitrate and HONO based on rather weak correlation (figure 5). That is less than convincing. Moreover, a photolysis rate of 2e-4 sec-1 means a photo-lifetime less than 1.5 hours for particulate nitrates. What are these nitrates? inorganic or organic? Has there been any reports of particle-phase nitrates exhibiting photo-lifetimes on the order of 1.5 hours? Is there a mechanism proposed? What remains in the particle-phase as the nitrate is released as HONO? Is all of the nitrate turn into HONO, or NO or NO2 or HNO3? I am concerned the photolysis conducted in the laboratory is not atmospherically relevant. More information on this lab photolysis experiment may help. How do the nitrate abundances measured with this filter method compare to what other instruments (AMS? PILS?) have measured for particle nitrates? And as for the power plant analysis, the same concerns I have for claim (1) applies here. You cannot assume just because the plume has been transported over 1 hour that none of the HONO observed is anthropogenic in origin. You need to know what the mixing ratio was near the emission point to know whether the HONO measured downwind was or was not directly emitted because the photo-lifetime is an e-folding time, it does not just disappear after

8 minutes. Lastly, citing previous work on the subject could be useful. Recent work by Neuman et al. 2016 comes to mind (<https://agupubs.onlinelibrary.wiley.com/doi/abs/10.1002/2016JD025197>).

Response: We disagree with the referee that our conclusion was based on weak correlation. The conclusion that inorganic particulate nitrate (pNO₃) photolysis is a major HONO source in the air column in Southeast U.S. was first based on directly field observation and HONO budget analysis. With comprehensive parameters related to HONO chemistry were directly measured in our study, we were able to conduct HONO budget analysis. The analysis suggested that known NO_x-related reactions can only sustain a minor fraction of the observed HONO source and there was a major fraction of HONO source strength unaccounted in the air column. If particulate nitrate behaves similarly to surface HNO₃ photochemically, i.e., with a photolysis rate constant 2-3 order of magnitude higher than that in the gas phase (e.g., Baergen and Donaldson, 2013; Reed et al., 2017; Ye et al., 2016b, 2017a; Zhou et al., 2003, 2011; Zhu et al, 2010, 2015), it could be a potentially important HONO precursor. To examine the potential role of pNO₃ as a HONO precursor, we collected aerosol samples on Teflon filters on the C-130 during the NOMADSS field study and determined the photolysis rate constants of particulate nitrate leading to the productions of HONO (a major product) and NO₂ (a minor product). High and highly variable $J_{pNO_3}^N$ values were obtained, from $8.3 \times 10^{-5} \text{ s}^{-1}$ to $3.1 \times 10^{-4} \text{ s}^{-1}$, with a median of $2.0 \times 10^{-4} \text{ s}^{-1}$ and a mean (± 1 standard deviation) of $1.9 (\pm 1.2) \times 10^{-4} \text{ s}^{-1}$, when normalized to tropical noontime conditions at ground level (solar zenith angle = 0 °) (Ye et al., 2017b). The laboratory measurement of J_{pNO_3} has been described and discussed in detail in our previous paper (Ye et al., 2017b). HONO budget analysis using the median $J_{pNO_3}^N$ value of $2.0 \times 10^{-4} \text{ s}^{-1}$ suggests that pNO₃ photolysis can account for most of the remaining HONO source strength (the original Figures 6b and 7b, and now the revised Figures 5b and 6).

The correlation between HONO and its potential precursor pNO₃ (the original Figure 5, and now the revised Figure S1) is quite weak ($r^2 \sim 0.17$), as pointed out by the referee. The correlation between the required HONO source and the contribution from particulate nitrate photolysis ($[pNO_3] \times J_{pNO_3}$) improved somewhat ($r^2 = 0.34$) (the original Figures 6b, now the revised Figure 5b), but is still not as strong as to be expected from pNO₃ photolysis being the major HONO source. As we explained in the manuscript (lines 338-343), “It may be in part due to the use of a single median $J_{pNO_3}^N$ value of $\sim 2.0 \times 10^{-4} \text{ s}^{-1}$ in the calculations of the ambient J_{pNO_3} and the production rates of HONO in Figure 5b; the actual $J_{pNO_3}^N$ values are highly variable, ranging from $8.3 \times 10^{-5} \text{ s}^{-1}$ to $3.1 \times 10^{-4} \text{ s}^{-1}$ (Ye et al., 2017). HONO source contribution from particulate nitrate photolysis in Figure 5b are thus estimates of the *in situ* HONO production rates from pNO₃ photolysis in different air masses.”

The photolysis lifetime of pNO₃ was short using the median value of laboratory determined J_{pNO_3} , as the referee pointed out. Many laboratory and field studies have shown the high photolysis rate constant of surface HNO₃ (Baergen and Donaldson, 2013; Ye et al., 2016a; Zhou et al., 2003, 2011; Zhu et al, 2010, 2015) and pNO₃ (Reed et al.; Ye et al., 2017a, 2017b), lending support to our argument that pNO₃ photolysis can be an effective renoxification pathway to recycle nitric acid to photochemically reactive NO_x and HONO. However, we would like to point out that particulate nitrate is in a dynamic equilibrium with gas-phase HNO₃, and that the later accounts for a larger (or even dominant) fraction of total nitrate (pNO₃+HNO₃) and is photochemically inert. The overall photolysis of total nitrate (pNO₃+HNO₃) would be much slower than indicated by J_{pNO_3} . In addition, oxidation of NO_x via several pathways will replenish the pNO₃+HNO₃ reservoir. The results reported in this manuscript and in earlier papers (Reed et al., 2017; Ye et al., 2016a) suggest that there is an

effective cycling in reactive nitrogen species in the low-NO_x atmosphere, sustaining the observed levels of HONO and pNO₃.

Some mechanisms have been proposed to explain the large enhancement of photolysis rate constant for surface HNO₃ and pNO₃, by 2-3 orders of magnitude compared to that of gas-phase HNO₃. The light absorption by HNO₃ in the UV range has been found to be 1-4 orders of magnitude higher on surfaces of silicon and ice than in the gas phase, with a significant red shift to long wavelength (Du et al., 2011; Zhu et al., 2008, 2015), probably resulting from bond stretching and/or bond deformation (Svoboda et al., 2013). Since the photolysis yield stays relatively high, 0.8-0.9 (Zhu et al., 2010), the resulting effect of the catalytic surface is the enhancement of photolysis rate constant over that in gas phase. In addition, organic and inorganic chromophores on ambient surfaces and in aerosol particles can enhance the photolysis of the associated HNO₃ and nitrate through photosensitization (Ye et al., 2016b, 2017b). We also hypothesized that NO₂ is the dominant primary product of the photolysis of surface HNO₃ and pNO₃, and the produced NO₂ (adsorbed) may react quickly with organics and water molecules on the surface and in aerosol particles to produce HONO as the secondary product. The proposed mechanism explains the laboratory results showing NO₂ as the dominant product from HNO₃ photolysis on clean and dry laboratory surfaces (Zhou et al., 2003; Zhu et al., 2010), while HONO as the major product on natural surfaces and in ambient aerosols (Ye et al., 2016a, 2017b).

We have not got the chance to compare our LPAS pNO₃ method with other instruments. We would like to do that as soon as we have the opportunity.

As to the issue of power plant plumes raised by the referee, the answer is similar to what we just provided for urban plumes. That is, the power plant plumes we encountered were small and relatively diluted with NO_x levels up to 1.8 ppbv (Figures 2 and 7), and the directly emitted HONO would be ≤ 18 pptv ppbv even if a high HONO/NO_x emission ratio of 0.01 is assumed (Neuman et al., 2016). During the 1-h transport time, the remaining HONO concentration from the direct emission would be well below our detection limit of 1 pptv. Therefore, the HONO concentrations in the power plant plumes were mostly produced within the air mass during the transportation, from elevated HONO precursors from anthropogenic sources. In fact, the HONO measured in fresh power plant plumes has been found to be mostly secondarily produced (Neuman et al., 2016).

Lastly, we regret the omission to reference the recent paper by Neuman et al. (2016). We finished our first draft of this manuscript over two years ago, before the publication of the mentioned paper. Although we have made significant changes to the draft during the subsequent revisions, we failed to update the references. The paper by Neuman et al. (2016) has been referenced and discussed in the revised manuscript.

References

- Baergen, A. M., and Donaldson, D. J.: Photochemical renoxification of nitric acid on real urban grime, *Environ. Sci. Technol.*, 47, 815-820, 10.1021/es3037862, 2013.
- Du, J., and Zhu, L.: Quantification of the absorption cross sections of surface-adsorbed nitric acid in the 335-365 nm region by Brewster angle cavity ring-down spectroscopy, *Chem. Phys. Lett.*, 511, 213-218, 10.1016/j.cplett.2011.06.062, 2011.
- Kirchstetter, T. W, Harley, R.A., and Littejohn, D.: Measurements of nitrous acid in motor vehicle exhaust, *Environ. Sci. Technol.*, 30 (9), 2843–2849, 1996.
- Li, Y. Q., Schwab, J. J., and Demerjian, K. L.: Fast time response measurements of gaseous nitrous acid using a tunable diode laser absorption spectrometer: HONO emission source from vehicle exhausts, *Geophys. Res. Lett.*, 35, 2008.

- Neuman, J. A., et al.: HONO emission and production determined from airborne measurements over the Southeast U.S., *J. Geophys. Res. Atmos.*, 121, 9237–9250, doi:10.1002/2016JD025197, 2016
- Reed, C. et al.: Evidence for renoxification in the tropical marine boundary layer, *Atmos. Chem. Phys.*, 17, 4081–4092, 2017.
- Svoboda, O.; Kubelova, L.; Slavicek, P.: Enabling forbidden processes: Quantum and solvation enhancement of nitrate anion UV absorption, *J. Phys. Chem. A*, 117, 12868-12877, 2013.
- Villena, G., Kleffmann, J., Kurtenbach, R., Wiesen, P., Lissi, E., Rubio, M. A., Croxatto, G., and Rappengluck, B.: Vertical gradients of HONO, NO_x and O₃ in Santiago de Chile, *Atmos. Environ.*, 45, 3867-3873, 2011.
- Ye, C., et al.: Rapid cycling of reactive nitrogen in the marine boundary layer, *Nature*, 532, 489-491, 2016a.
- Ye, C., Gao, H., Zhang, N., and Zhou, X.: Photolysis of nitric Acid and nitrate on natural and artificial surfaces, *Environ. Sci. Technol.*, 50, 3530-3536, 2016b.
- Ye, C., Heard, D.E., and Whalley, L.K.: Evaluation of novel routes for NO_x formation in remote regions, *Environ. Sci. Technol.*, DOI: 10.1021/acs.est.6b06441, 2017a.
- Ye, C., Zhang, N., Gao, H., and Zhou, X.: Photolysis of particulate nitrate as a source of HONO and NO_x, *Environ. Sci. Technol.*, DOI: 10.1021/acs.est.7b00387, 2017b.
- Zhou, X., Civerolo, K., Dai, H., Huang, G., Schwab, J., and Demerjian, K.: Summertime nitrous acid chemistry in the atmospheric boundary layer at a rural site in New York State, *J. Geophys. Res.*, 107, doi:10.1029/2001JD001539, 2002.
- Zhou, X., Gao, H., He, Y., Huang, G., Bertman, S. B., Civerolo, K., and Schwab, J.: Nitric acid photolysis on surfaces in low-NO_x environments: Significant atmospheric implications, *Geophys. Res. Lett.*, 30, 2217, 10.1029/2003gl018620, 2003.
- Zhou, X., Zhang, N., TerAvest, M., Tang, D., Hou, J., Bertman, S., Alaghmand, M., Shepson, P. B., Carroll, M. A., Griffith, S., Dusanter, S., and Stevens, P. S.: Nitric acid photolysis on forest canopy surface as a source for tropospheric nitrous acid, *Nature Geosci.*, 4, 440-443, 10.1038/NGEO1164, 2011.
- Zhu, C. Z., Xiang, B., Zhu, L., and Cole, R.: Determination of absorption cross sections of surface-adsorbed HNO₃ in the 290-330 nm region by Brewster angle cavity ring-down spectroscopy, *Chem. Phys. Lett.*, 458, 373-377, 2008.
- Zhu, C., Xiang, B., Chu, L.T., and Zhu, L.: 308 nm Photolysis of nitric acid in the gas phase, on aluminum surfaces, and on ice films, *J. Phys. Chem. A*, 114, 2561-2568, 2010.
- Zhu, L., Sangwan, M., Huang, L., Du, J., and Chu, L.T.: Photolysis of nitric acid at 308 nm in the absence and in the presence of water vapor, *J. Phys. Chem. A*, 119, 4907-4914, 2015.

(2) Response to the Interactive comment by Anonymous Referee #2 on “Tropospheric HONO Distribution and Chemistry in the Southeast U.S.”

General Comments

This manuscript explores the generation and fate of HONO above and within the planetary boundary layer over the southeastern United States during NOMADSS 2013 from several research flights aboard the NCAR C-130 aircraft. The vertical distribution of HONO throughout this layer is clearly demonstrated to be derived from volume sources, with a robust testing of the known mechanisms of HONO formation against parameterizations of particulate nitrate photolysis, which is emerging as an important source of tropospheric HONO. The Author’s find that previously established volume-based mechanisms of HONO formation cannot account for the observed quantities and that the photolysis nitrate in the condensed phase can possibly explain the majority of the observed quantities. The Authors demonstrate that HONO is a minor OH source at these altitudes when its production is driven solely from volume production and also that it is an important intermediate in the renoxification pathways of tropospheric trans- port of nitrogen oxides. Overall, this manuscript is well written with a solid analysis of the dataset. There are minor modifications necessary to make the manuscript more clear and concise in its purpose and findings. The removal of some figures and text by the production of a supporting information document would easily facilitate this.

Response: We thank Anonymous Referee #2 for the positive and encouraging comments. The detailed and insightful comments and suggestions have greatly helped us in revising and improving the manuscript. A supplement document has been generated to include supporting content as suggested.

Specific Comments

Page 2, Lines 7-10: The detailed analysis of the isoprene transport and subsequent lifetime calculations for HONO are a quantitative assessment of the decoupling of surface emissions from the observed HONO. The Authors should consider using their quantitative assessment as the basis for their statement here instead of the more qualitative observation of no vertical gradient.

Response: The abstract has been revised and reorganized, as the referee suggested.

Page 2, Lines 14-15: Please provide the average +/- SD of the actual fraction of the observed HONO that was generated by pNO₃ photolysis from the presented calculations instead of ‘appeared to be the major daytime HONO source’.

Response: The abstract has been revised and reorganized, as the referee suggested.

Page 2, Lines 20-25: Provide the quantitative findings from each section of the detailed analysis here over the general statements of relative importance. This will generate greater impact for this work.

Response: The abstract has been revised and reorganized, as the referee suggested.

Page 3, Line 39: Remove ‘, as an important OH precursor,’ as it is redundant.

Response: The phrase has been removed as suggested.

Page 3, Lines 51-57: I would suggest removing this length section and replacing it with a single sentence following the statements on combustion HONO sources (Line 48). This level

of detail in the introduction is not really relevant to the tropospheric chemistry discussed in this work.

Response: Revision has made as the referee suggested.

Page 4, Lines 75-84: The last two sentences demonstrate that R4 is unnecessary and it should likely be removed from here and from the presented data analysis, since it has been show to be a two-photon process. It should be removed here and the section on the hydroperoxyl-water complex mechanisms should be replaced with one sentence on its existence and low yield of HONO.

Response: As the referee pointed out, both reactions (R4) and (R5) are not important as HONO sources. Since we intend to conduct HONO budget analyses in the later sections, to include all NO_x-related reactions. We feel that a brief discussion of reactions (R4) and (R5) here is justified.

Page 5, Lines 104-107: It would be useful to guide the readers through the major explorations of this dataset here. Consider listing the major sections of this work here in the order that they are presented in the abstract, manuscript, and conclusions, to improve clarity.

Response: We did provide some field campaign and measurement information in the first paragraph in section “2 Experimental”, right after the paragraph.

Page 5, Line 108: The experimental section could use subsections to improve clarity.

Response: Revision has made as the referee suggested.

Page 5, Line 126: The baseline subtraction of interferences from particulate nitrite here does not acknowledge that there is a size-dependent collection efficiency in these style of instruments. For example, fog droplets would be effectively captured in the primary channel to appear as HONO and not be corrected for in the secondary channel. This has been demonstrated in other works with this analytical approach (e.g. (Sörgel et al., 2011) and references therein). Is there any potential for droplet nitrite interferences in these measurements where clouds may have been encountered?

Response: As pointed out by the referee, cloud droplets may be collected at significant efficiency and be an interference in our measurement. We have excluded the in-cloud measurement data from our data analysis, due to lack of valid way to correct the data. The following sentences have been added in the revised manuscript (lines 163-166): “Noisy baselines were observed when the C-130 was flying in the clouds, due to the sampling of cloud droplets by our sampling systems. Because of the lack of a valid way to correct for this interference, all in-cloud measurement data of HONO and pNO₃ have been excluded from the data analysis.”

Page 6, Lines 138-139: It is confusing to follow the logic of this estimation. Was the maximum possible interference determined in some sections of the dataset to set the limit at 0.2? If possible, add the quantitative approach used to a section in a Supporting Information document. If not, please improve the clarity here.

Response: We have not determined the collection efficiency for HO₂NO₂ experimentally. The upper limit HO₂NO₂-to-HONO conversion efficiency of 0.2 was estimated from the ratio of the observed [HONO] to the calculated [HO₂NO₂]_{ss} in cold, high altitude air masses under our measurement conditions, assuming ambient HONO concentration approaching zero. We found that the correction was not necessary in the TBL. The discussion has been revised to:

“Potential interference from peroxyntic acid (HO_2NO_2) was suppressed by heating the PFA sampling line to 50 °C. The HO_2NO_2 steady state concentration ($[\text{HO}_2\text{NO}_2]_{\text{SS}}$) was estimated to be less than 1 pptv at temperatures of 20 - 30 °C in the background PBL (Gierczak et al., 2005), and thus interference from HO_2NO_2 was negligible. Whereas in power plant and urban plumes in the PBL or biomass burning plumes in the upper free troposphere (FT), HO_2NO_2 interference was not negligible and thus a correction for HONO measurement was made. An upper-limit HO_2NO_2 response efficiency was estimated to be 0.2 for our HONO measurement systems. The estimation was made from the lowest ratio of the measured HONO to the corresponding $[\text{HO}_2\text{NO}_2]_{\text{SS}}$ in cold air masses at high altitude, assuming no HONO existed. HONO concentration were then corrected by subtracting a term of “ $0.2 \times [\text{HO}_2\text{NO}_2]_{\text{SS}}$ ”. The correction was below 10% of the measured HONO concentrations in the PBL plumes. However, there may be over-corrections in the cold free troposphere.” (lines 13-143)

Page 6, Lines 142-144: Provide the correlation coefficient, slope, and intercept here to improve clarity and validity of analytical approach.

Response: The intercomparison of HONO measurements from the two instruments (the DOAS and the LPAP) was made by overlaying the concentration time-series on each other (Extended Data Fig. S3 in Ye et al., 2016). The measured concentrations closely tracked each other, and the agreements were within the assessed uncertainties. The readers are encouraged to read the paper for more information.

Page 6, Line 149: The order of the used apparatus is not clear. Presumably the denuder followed the filter? Please clarify.

Response: As the referee suggested, the sentence has been revised as suggested to ““Zero- pNO_3 ” air was generated to establish measurement baselines for pNO_3 by passing the ambient air through a Teflon filter to remove aerosol particles and then a NaCl-coated denuder to remove HNO_3 before reaching the sampling unit of LPAP.” (lines 155-158).

Page 6, Line 160: Delete ‘NCAR’s’

Response: Revision has made as the referee suggested.

Page 7, Line 161: What are ‘state parameter measurements’?

Response: The NSF/NCAR C-130 aircraft comes equipped with a package of standard instrumentation that flies on all C-130 research missions. The measurements made by these sensors form the core of any research program and provide the information necessary to place the aircraft in space and time while characterizing the basic “**state**” of the local environment. The parameters include aircraft longitude, latitude, altitude, flight speed, pressure, temperature, dew point, and many more.

Page 7, Lines 183-184: Remove this from here. It is discussed in sufficient detail later and distracts from the results.

Response: Indeed, the vertical HONO distribution is discussed in the following section in more details. However, we feel that in the “General data description” section, this sentence provides some contrast to the horizontal inhomogeneity of HONO distribution, and thus we keep the sentence as it is.

Page 7, Lines 186-188: Remove these statements. The information is already presented in the Table and does not need repeating.

Response: The readers can obtain the information directly from these statements without going the tables and Figures. We feel that some degree of redundancy may be needed. Thus we keep the sentence as it is.

Page 7, Lines 191-192: Delete the sentence on the future paper.

Response: Revision has made as referee #2 suggested.

Page 8, Lines 194-196: Delete these and direct the reader to the relevant section at the end of the preceding sentence by adding '(Section 3.4)'

Response: Revision has made as the referee suggested.

Page 8, Lines 201-203: Remove these statements. The information is already presented in the Table and does not need repeating.

Response: Again, the readers can obtain the information directly from these statements without going the tables and Figures. We feel that some degree of redundancy may be needed. Thus we keep the sentence as it is.

Page 8, Lines 210-212: Remove these statements. The information is already presented in the Table and does not need repeating.

Response: Again, the readers can obtain the information directly from these statements without going the tables and Figures. We feel that some degree of redundancy may be needed. Thus we keep the sentence as it is.

Page 9, Line 236: Here is the first definition of the altitudes considered to by the PBL versus the FT. The Authors should add their criteria for distinguishing between the PBL and FT to the methods section. If it would be a lengthy addition, then a condensed description with supporting details could be placed in the Supporting Information document.

Response: The discussion in this section was focused on the transport and contribution of HONO from ground level to the overlying PBL, based on the vertical distributions of HONO and other species in the PBL (300 -1200 m). Transport into the FT would be much slower and was not discussed in the section. The PBL height can be estimated by the temperature inversion in the vertical potential temperature profile.

Page 9, Lines 238-250: This is a fantastic analysis of the vertical mixing and transport of surface-emitted species, but it is outside the focus of this work. Consider relocating this detailed analysis to the Supporting Information document.

Response: The main discussion of this manuscript is on HONO daytime budget and chemistry. HONO is a unique species mainly produced by heterogeneous processes on surfaces. Ground surfaces provide the sites for the heterogeneous processes to produce HONO. We feel that it is important to examine the input from ground HONO source to the HONO budget in the PBL. Therefore, we keep the equation (Eq. 1), vertical profiles in Figure 4, and discussion of vertical transport in the main section.

Page 9, Lines 250-254: Distinguish between ground-emitted and volume-produced HONO here to improve clarity.

Response: We have significantly modified the discussion in that paragraph. The two sentences have been changed to “With a photolytic lifetime of ~ 11 min for HONO, about 11% of the HONO originated from the ground level is expected to reach the altitude of 300 m,

the lowest flight altitude of the C-130 aircraft between 11:00 – 12:15 LT in RF #4.” (lines 266-268).

Page 9, Line 256: ‘of its precursors’ should be ‘of its potential precursors’ since this work is yet to demonstrate this quantitatively (although it is shown quite well later).

Response: Revision has made as the referee suggested.

Page 10, Lines 286-287: This was stated in the introduction as insignificant (and potentially invalid), so why have the authors chosen to include this in their analysis? Suggest removing throughout.

Response: We intended to include in our calculation all the NO_x-related reactions reported in literature. While the importance of R4 and R5 are still under debate in literature, our HONO budget analysis does suggest they were insignificant under the conditions we encountered in the Southeast U.S., as stated in the Introduction.

Pages 10-11, Lines 289-291: Consider providing a justification for selecting all upper limits in these calculations to improve clarity.

Response: As suggested by the referee, the following sentence has been added after equation (Eq. 2): “It should be noted that the upper limit values of rate constants were used in the calculation to avoid the underestimation of [HONO]_{ps} value.” (line 307-309)

Page 11, Line 302: Remove ‘, such as pNO₃.’ As it is redundant for the transition between paragraphs.

Response: The phrase has been removed as suggested.

Page 11, Lines 309-310: Remove ‘over the terrestrial areas’, ‘on Teflon filters. . . summer field study’. This information is already presented in the methods.

Response: The redundant information has been removed as suggested.

Page 12, Lines 326-330: This is a single sentence and is difficult to follow. Consider breaking into 2-3 sentences to improve clarity.

Response: The long sentence has been changed to “However, the r² of 0.34 is not as strong as expected from pNO₃ photolysis being the major volume HONO source. It may be in part due to the use of a single median $J_{pNO_3}^N$ value of $\sim 2.0 \times 10^{-4} \text{ s}^{-1}$ in the calculations of the ambient J_{pNO_3} and the production rates of HONO in Figure 5b; the actual $J_{pNO_3}^N$ values are highly variable, ranging from $8.3 \times 10^{-5} \text{ s}^{-1}$ to $3.1 \times 10^{-4} \text{ s}^{-1}$ (Ye et al., 2017).” (line 337-341)

Page 12, Line 331: Delete ‘only rough’. Redundant. Also see comments on Figure 6 regarding weighted error analysis.

Response: The redundant phrase has been deleted as suggested.

Page 13, Line 357: What is the error on this ratio of 0.02? Is it statistically different from the fresh power plant emissions?

Response: Standard deviations of the HONO/NO_x ratio have been added in the revised manuscript. The sentence has been revised and expanded to “The observed HONO/NO_x ratio was 0.019 ± 0.004 in the power plant plumes (e.g., P4) and 0.057 ± 0.0019 in urban plumes, significantly higher than the typical HONO/NO_x emission ratio of ~ 0.002 in the fresh power plant plumes (Neuman et al., 2016) and ≤ 0.01 in automobile exhaust (Kurtenbach et al., 2001; Li et al., 2008b).” (lines 380-383)

Page 13, Line 370: Since plume G is the only case study from these labels, consider a uniform label for the urban emissions (A) and the remainder of the power plant plumes (B). The increasing lettered format makes it seem that each instance will be discussed.

Response: We have revised Figures 2 and the text, as the referee suggested, and have labeled the plumes according to their sources.

Page 15, Line 439: The conclusions section of this manuscript is similarly qualitative, as the abstract is, despite the excellent quantitative analysis presented throughout the results and discussion. Suggest revisiting this section with more quantitative information to improve clarity and impact.

Response: We have followed the referee's suggestion, and have revised the conclusions.

Page 25, Table 2: The +/- SD is in brackets in one part of the table and not the other. Please correct this. The terms PBL and FT are not defined anywhere in the manuscript and should be given at least an operational definition somewhere in the methods section. Lastly, the number of data points being used in each of these calculations should be provided in a column or in the caption.

Response: Revision has made as the referee suggested.

Page 27, Figure 2: Consider moving this figure to the supporting information or removing it entirely from the manuscript. The only specific features necessary here are the plumes which are presented again in Figure 7. With respect to the urban and power plant plumes, it could be simpler to assign the urban plumes a single letter (such as A), and similarly assign all the power plant plumes with a single letter excepting the one plume discussed in detail, which could be assigned a third letter. With each plume having a different letter, the figure suggests that there is something different between these, when there is nothing in the discussion that suggests this is the case. It would improve the clarity to simplify this.

Response: The figure has been referred 8 times in the main text. We feel that it is important to keep this figure in the main manuscript so that the reader can get to it quickly. The plumes have been re-labeled according to their sources, as the referee suggested.

Page 28, Figure 3: This figure does not seem necessary for inclusion in the main manuscript and should be considered to be moved to the supporting information. Figure 4 and Table 2 provide redundant and better insight into the measurements.

Response: Again we feel that it is important to keep Figure 3 in the main manuscript; it was referred three times in the discussion. Only a few vertical HONO concentration profiles have been reported so far in literature. They provide important information to understand the budget, the chemistry and the transport of HONO in the troposphere. Figure 3 contains far more data points from 5 research flights over different environments in the southeast U.S., while Figure 4 shows many more parameters from only one race-track over one area, and Table 2 only summarizes the statistics of the measurements. Therefore, they are not really redundant, but rather complementary.

Page 29, Figure 4: It could be useful to add the typical PBL to FT height as a shaded area (if it has some variability) or horizontal line in each panel to facilitate clarity between the figure data and the discussion.

Response: As stated in the figure caption, Figure 4 shows the vertical distributions of concentrations of HONO, NO_x, pNO₃, isoprene and potential temperature in the PBL during

the first race-track of RF#4. According to the potential temperature and isoprene profiles, the PBL height was around 1200 m.

Page 30, Figure 5: The two sentences in the paper communicate all the information contained in this figure. Suggest removing this figure altogether or relocating to the supporting information. Further, the correlation analysis undertaken here is unclear and may be subject to some error if an error-weighted analysis is not being used (Wu and Zhen Yu, 2018). Is the error in both datasets being taken into account when calculating the regression coefficient? Please update the analysis and discussion to reflect the approach and ensure it is robust for the presented data.

Response: The figure has been moved to the supporting information, as the referee suggested. And more robust Deming least-squares regression (Wu and Yu, 2018) has been used in the data analysis, as suggested.

Page 31, Figure 6: The same regression questions from Figure 5 also apply here. Please clarify the approach utilized and ensure that the appropriate regression analysis and statistics have been used when interpreting the data.

Response: As the reviewer suggested, more robust Deming least-squares regression (Wu and Yu, 2018) has been used in the data analysis.

Page 32, Figure 7: Panel (a) here can be move to the supporting information or re- moved altogether.

Response: We have moved the panel (a) to the supporting information as the referee suggested, and have also added SO₂ as power plant plume tracer and acetonitrile as a biomass burning tracer to the revised Figure S1, as Andy Neuman suggested in his Short Comments.

Page 33, Figure 8: This information in this figure is presented concisely in the discussion and the figure does not add anything further. Consider removing this figure from the manuscript.

Response: The figure has been moved to the supporting information as suggested.

Page 34, Figure 9: The lines are very hard to see on this figure and the green line does not print well. Suggest using two black lines that are thicker than those currently used, with different dashing to distinguish them. The markers are also defined by very thin lines that could be made thicker for clarity.

Response: The figure has been revised as suggested.

References

- Gierczak, T., Jimenez, E., Riffault, V., Burkholder, J. B., and Ravishankara, A. R.: Thermal decomposition of HO₂NO₂ (peroxynitric acid, PNA): Rate coefficient and determination of the enthalpy of formation, *J. Phys. Chem. A*, 109, 586-596, 2005.
- Kurtenbach, R., Becker, K. H., Gomes, J. A. G., Kleffmann, J., Lorzer, J. C., Spittler, M., Wiesen, P., Ackermann, R., Geyer, A., and Platt, U.: Investigations of emissions and heterogeneous formation of HONO in a road traffic tunnel, *Atmos. Environ.*, 35, 3385-3394, Doi 10.1016/S1352-2310(01)00138-8, 2001.
- Li, Y. Q., Schwab, J. J., and Demerjian, K. L.: Fast time response measurements of gaseous nitrous acid using a tunable diode laser absorption spectrometer: HONO emission source from vehicle exhausts, *Geophys. Res. Lett.*, 35, 2008.

- Neuman, J.A., Trainer, M., Brown, S.S., Min, K.-E., Nowak, J.B., Parrish, D.D., Peischl, J., Pollack, I.B., Roberts, J.M., Ryerson, T.B., and Veres, P.R.: HONO emission and production determined from airborne measurements over the Southeast U.S., *J. Geophys. Res.-Atmos.*, 121, 9237–9250, 2016.
- Wu, C., and Yu, J.Z.: Evaluation of linear regression techniques for atmospheric applications: the importance of appropriate weighting, *Atmos. Meas. Tech.*, 11, 1233–1250, 2018.
- Ye, C. X., Zhou, X. L., Pu, D., Stutz, J., Festa, J., Spolaor, M., Tsai, C., Cantrell, C., Mauldin, R. L., Campos, T., Weinheimer, A., Hornbrook, R. S., Apel, E. C., Guenther, A., Kaser, L., Yuan, B., Karl, T., Haggerty, J., Hall, S., Ullmann, K., Smith, J. N., Ortega, J., and Knote, C.: Rapid cycling of reactive nitrogen in the marine boundary layer, *Nature*, 532, 489-491, 2016.
- Ye, C., Zhang, N., Gao, H., and Zhou, X.: Photolysis of particulate nitrate as a source of HONO and NO_x, *Environ Sci Technol*, DOI: 10.1021/acs.est.7b00387, 2017.

(3) Response to interactive comment on manuscript on “Tropospheric HONO Distribution and Chemistry in the Southeast U.S.” by A. Neuman

General comments: The manuscript "Tropospheric HONO Distribution and Chemistry in the Southeast U.S" by Ye et al. presents airborne measurements of reactive nitrogen compounds in the troposphere. They measure HONO to be larger than can be explained by known formation processes and find that known mechanisms explain only 20% of the daytime HONO source in background air masses. Understanding HONO formation and loss is important to understanding the photochemistry of the atmosphere, but the results here require further support to be useful in constraining reactions that produce HONO. Some specific concerns are detailed below.

Response: We would like to thank Andy Neuman for his time and efforts in preparing this detailed and comprehensive comment. We have revised the manuscript accordingly to address his questions and concerns. Specific concerns and questions are addressed below in this Response .

Major concerns:

Q1: The discussion of the measurements and their uncertainties are insufficient, and many of the experimental descriptions are qualitative. Substantially greater quantitation is required to support the stated 1 ppt detection limit. For example, zeros were performed "periodically" (line 125), and the baselines were subtracted from the total signal. How frequently were these backgrounds performed, and how was the back- ground determined outside of the zero periods? Was a single value used for a flight, or was the background determined by interpolating between zeroes?

Response: HONO measurement technique has been described in detail in the previous method paper (Zhang et al., 2012), therefore only brief description of the instrument was given in the manuscript to provide the key pieces of information (lines 117 – 144 in the original manuscript). We have added significant amount of information to the revised manuscript as suggested. To answer the reviewer’s questions, more details are provided below; please refer to the method paper (Zhang et al., 2012) for instrumental details, such as HONO sampling, baseline subtraction and interference correction, nitrite derivatization, and absorbance measurement of azo dye derivative by LPAP technique.

HONO was measured by two separate LPAP (long-path absorbance photometer) systems. Each system ran a 30-min measurement and zero cycle, with 20 min sampling ambient air and 10 min sampling “zero-HONO” air for baseline correction, and with a 15-min time offset between the two sampling cycles (Figure 1a). The “zero-HONO” air was generated by directing the ambient air stream through a Na₂CO₃-coated denuder to remove HONO while allowing most of interfering species (NO_x, PAN, and particulate nitrite) to pass through. The combination of overlapping ambient signals from the two systems provide a continuous HONO concentration measurement (Figure 1b, solid black circles). The absorbance signals were sampled at a rate of 1 Hz (Figure 1a, blue and red circles), and were averaged into 1-min or 3-min data (Figure 1b, blue and red circles, 1-min averaging). The averaged signals were converted into concentrations based on calibration slope and air sampling and liquid flow rate information. The baseline correction was made by subtracting the ambient signals by the extrapolated line between the two adjacent stable “zero-HONO” air signals (Figure 1b, blue and red lines). The “zero-HONO” air signals were stable most of the time, and the slow drift in the baseline can be easily corrected for. The baseline was sometimes found to change rapidly in two circumstances: when the aircraft was transacting through a high NO_x plume, and when the ambient pressure changed rapidly and significantly

during the rapid ascending to or descending from high altitudes. For the first case, the interference from other reactive nitrogen species in high NO_x plumes can be corrected by subtracting from the ambient air signals the increases in the “zero-HONO” air signals measured by the other HONO system. However, this correction was rarely needed, since the increases in the “zero-HONO” air signals were usually quite small even in the urban and power plant plumes (Figure 2). In the second circumstance, large baseline drifts were observed when the flow state of the scrubbing solution was disturbed by rapid pressure fluctuations. The up-shifting or down shifting of the baseline may result in over-correction or under-correction; the over-correction could then result in negative concentration numbers, as Andy Neuman pointed out. Fortunately, altitude changes in the PBL during the race-track profiling did not disrupt the liquid flow pattern enough to cause rapid baseline shift (Figure 1a). If the baseline shift was found to be caused by rapid pressure fluctuations and if reasonable baseline correction could not be made, the data points were excluded from analysis, regardless of the sign or magnitude of the data.

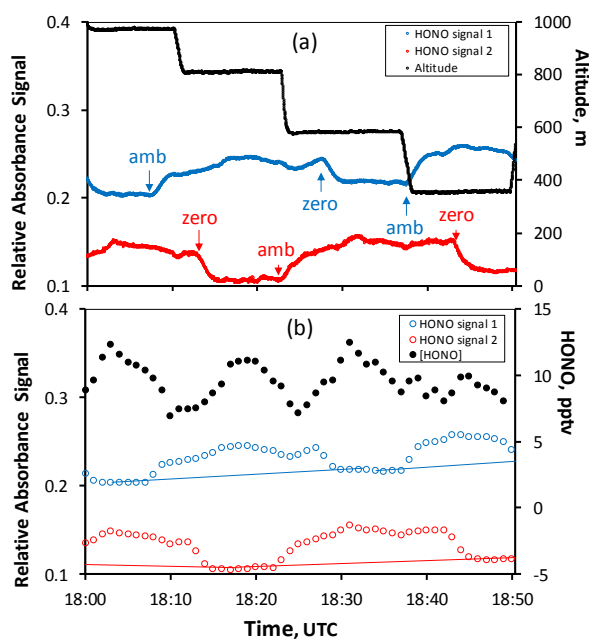


Figure 1. Time series of 1-Hz raw absorbance signals (blue and red circles) and flight altitude (black circles) (a) and of 1-min averaged absorbance signals ((blue and red circles) and calculated HONO concentrations (black solid circles) (b), during NOMADSS RF#4 on June 12, 2013. The blue and red lines in panel (b) are the baselines extrapolated from the two adjacent “zero-HONO” air measurements.

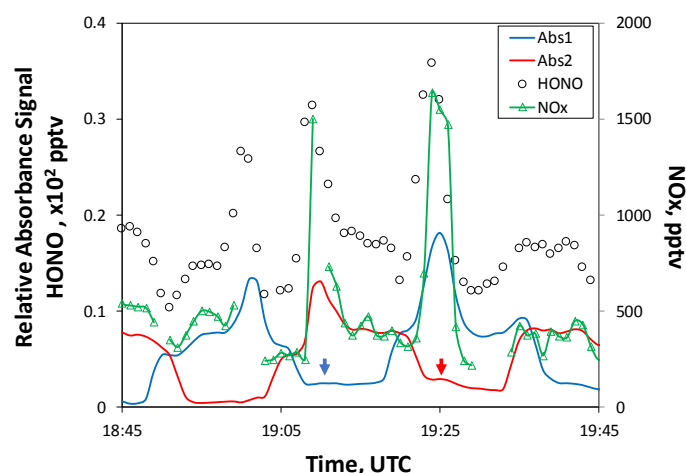


Figure 2. One-hour time series of 1-Hz absorbance signals from two HONO systems (blue and red lines), 1-min averaged HONO (black circles) and NO_x (green triangles with line) during NOMADSS RF11 on June 29, 2013. The blue and red arrows indicate the slight increases in the “zero-HONO” air signals due to potential interferences from NO_x, particulate nitrite and PAN in the power plant plumes.

The time resolution is defined as the 90% response time based on the signal transition from “zero-HONO” air to ambient air. The lowering of the flow rates of scrubbing and reagent solutions and increase in the length of liquid plumbing tubing resulted in a longer response time (200 s) compared to that reported for the ground-based system (110 s) (Zhang et al., 2012). The lower detection limit of the method was estimated to be ≤ 1 pptv, based on 3 times the standard deviation of the zero air signal ($N > 10$). An overall uncertainty of $\pm(1 + 0.2 [\text{HONO}])$ pptv was estimated, combining the uncertainties in signal acquisition and processing, air and liquid flow rates, standard preparation, and baseline correction. Again, the estimated overall uncertainty of $\pm(1 + 0.2 [\text{HONO}])$ pptv is significantly higher for the aircraft HONO measurements than that of $\pm(1 + 0.05 [\text{HONO}])$ pptv for the ground HONO measurements (Zhang et al., 2012), in part due to pressure fluctuation and baseline drifting on the aircraft.

Q2: The inlet residence time of 0.8 s is very large. What happens in a NO_x plume? Wouldn't there be a contribution from NO₂ conversion to HONO on the inlet? A description of the inlet length and flow would be helpful.

Response: Andy Neuman has made some fair comments regarding the long inlet deployed on the C-130 for HONO measurement. It was only during the instrument integration when we learned that there were exhaust vents next the inlet ports near our instrument location. The vented aircraft cabin air might significantly contaminate our HONO measurement. To avoid the potential contamination artifacts, the inlet port on the other side of the aircraft was used. A heated 7-m long 3/8"-ID PFA inlet line was thus needed and used, and a high flow rate (210 L min⁻¹) ambient air was drawn by an auxiliary blower to reduce the air sample residence time in the inlet line. The resulting residence time in the inlet line is 0.14 s, not 0.8 s stated in the original manuscript. We regret the error and have made the correction in the revised manuscript.

Our group has examined the potential interference from heterogeneous NO₂ reactions on the inlet wall surface on HONO measurements many times and in different environments, and have found it not to be significant. Figure 3 shows the result of such an experiment conducted recently in downtown Albany. HONO in the ambient air was measured by two HONO systems, one with a regular inlet, and the other with or without adding long piece of

heated PFA tubing (10 m long, 1/4-OD and 1/8"-DI). At a sampling flow rate of 2 L min⁻¹, the residence time of air sample in the PFA tubing was ~2.4 s, about 17 times longer than 0.14 s for the aircraft systems. The ambient NO₂ concentration varied from ~1 to ~6 ppbv during the measurement period. The comparison of the two time series by measured the two HONO systems shows no discernible difference within the estimated uncertainty, regardless if the extra long tubing was added or removed (Figure 3).

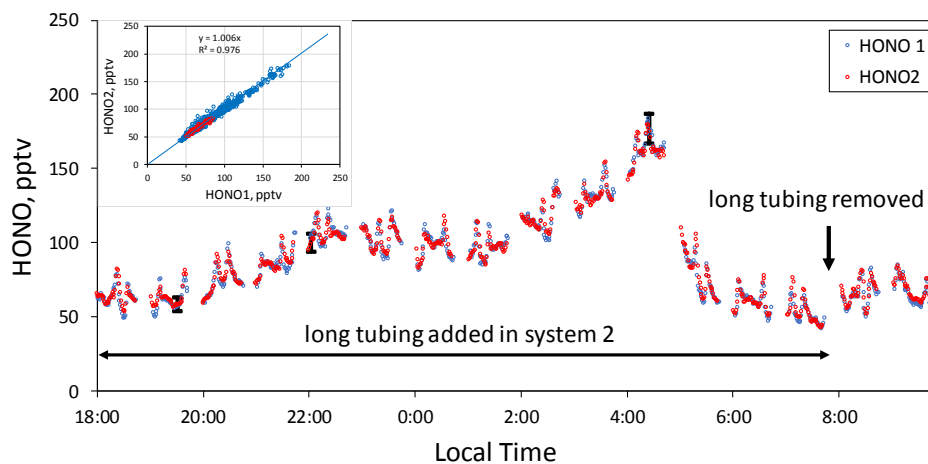


Figure 3. Ambient HONO concentrations measured by two HONO systems in Downtown Albany during April 19-20, 2016. A 10-m PFA tubing (1/8"-DI) was added to the inlet of system 2 (red circles) from at 17:00 on April 19, and was removed at 7:53 on April 20, as indicated by the black arrow. The three black bars at 19:31 and 22:02 on April 19 and at 4:25 on April 20 indicate estimated measurement uncertainties at the measured concentrations. The insert is the scatter plot of the measured HONO concentrations by the two systems. The red symbols represent the measurements by the two systems with the same short inlets (10-cm long, 1/16"-ID), and the blue symbols represent the measurements when an additional 10-m tubing (1/8"-ID) was added to system 2. The line is the linear best fit for the data.

The accuracy of HONO measurements was also confirmed by comparison with a limb-scanning differential optical absorption spectroscopy (DOAS) (Ye et al., 2016a). When measuring in wide power plant plumes where HONO mixing ratios exceeded the lower detection limits of both instruments, the agreement between these two instruments was very good, within the assessed uncertainties (Extended Data Fig. 3 in Ye et al., 2016a).

Q3: *If the HONO measurement is a difference between total signal and background, I am surprised that there are no values below zero in Figures 2 and 3. Are there really never any instances when HONO falls to zero? Perhaps the interferences are underestimated.*

Response: The signals for the “zero-HONO” air were quite stable, and ambient signals were well above the baselines, even at the data sampling rate of 1 Hz (Figure 1a). As explained in the response to Q1, ambient signals are always higher than the baseline signals extrapolated from the adjacent “zero-HONO” signals, except during the rapid ascending to and descending from high altitudes; large baseline drifts were observed when the flow state of the scrubbing solution was disturbed by rapid pressure fluctuations. Overcorrection of the upward-shifting baseline may sometimes result in negative values in HONO concentration. However, the data were excluded from analysis if the baseline shifts caused by rapid pressure fluctuations could not be reasonably corrected, regardless of the sign or magnitude of the data.

Q4: *Please mention briefly how surface area density was determined from SMPS data. Wouldn't SMPS also provide a constraint on aerosol mass that could be useful for verifying*

the pNO₃ measurements? Some of values of pNO₃ in remote regions are very large - up to 0.5 and Have similarly large nitrate values been measured outside of urban plumes over the SE US in other studies?

Response: The surface area density was calculated by the following equation:

$$S/V = \sum(4\pi r_i^2) \times n_i$$

where r_i and n_i represent the radius and number density of aerosol particles. A perfect sphere was assumed for aerosol particle in the calculation.

The mean (± 1 std) and median of pNO₃ in the Southwest US were 76 (± 45) pptv and 66 pptv in the PBL, and 35 (± 39) pptv and 15 pptv in the free troposphere, within the range of reported particulate nitrate in rural atmosphere (Heald et al., 2012 and paper therein). The high pNO₃ concentrations were observed in the PBL during the first racetracks of the RFs #4 and #5 west of Centreville, AL, and during the RF 11 around Auburn, AL (Figures 1 and 2). Agricultural activities in this region may release enough NH₃ to convert some of the gaseous HNO₃ into pNO₃, as observed by Neuman et al. (2003). We have calculated the aerosol mass using the SMPS data as suggested. However, no robust relationship was found between aerosol mass and the concentration of pNO₃. We were not able to do the same analysis as that in Neuman et al. (2003) due to poor resolution and missing data points of HNO₃ and the lack of NH₃ data.

Q5: I cannot find the mentioned UHSAS data or DOAS data in the project archive. What does a "very good" agreement mean (line 142)? Again, quantifying the agreement and showing data would strengthen the paper.

Why is OH estimated using a prior study (line 246), when the OH measurements listed in Table 1 could be used?

Response: No HONO data from DOAS is available in the project archive, because the ambient HONO concentrations (11.2 ± 4.3 pptv in the PBL and 5.6 ± 3.4 in the FT as measured by LPAP) were mostly below the lower detection limits of the DOAS instrument (30 pptv) during the NOMADSS study. Good HONO measurements were made by both the DOAS and the LPAP in wide power plant plumes during RF 7 over Ohio River Valley, and results have been intercompared (Extended Data Fig. 3 in Ye et al., 2016a). We found the HONO concentrations from the two instruments closely tracks each other, and the agreements were within the assessed uncertainties. The readers are encouraged to read the paper for more information.

Both this manuscript and the "prior" paper by Kaser et al. (2015) were based on results from the NOMADSS study, and the same OH measurement dataset was shared and used by the two papers. Since the information on OH levels during the flight had been published, it is appropriate to reference the paper.

Q6: A very large photolysis rate for pNO₃ is used to explain HONO formation, but this rate isn't consistent with the data shown. It is difficult for me to understand the difference between "determined photolysis rate" and "ambient photolysis rate" (section 3.3), but both are extremely large and comparable to the loss rate for isoprene. The nitrate photolysis rates give a nitrate lifetime of approx. one hour, which is less than the lifetime of NO_x. How can nitrate ever accumulate in the atmosphere if its lifetime is so short? Are there any other studies that find a very short lifetime for nitrate? The large nitrate photolysis rate is inconsistent with the nitrate abundance and distribution reported here and cannot explain the HONO abundance.

Response: Indeed, a very large photolysis rate constant was used for pNO₃ in our calculation. The pNO₃ photolysis rate constant was determined in the laboratory using the aerosol samples collected on board the C130 during the NOMADSS field study (Ye et al., 2017a). Several

recent laboratory studies have demonstrated that surface nitric acid and particulate nitrate can be photolyzed at much higher rates than gaseous nitric acid, by 2-3 orders of magnitudes (Baergen and Donaldson, 2013; Du and Zhu, 2011; Ye et al., 2016b, 2017a; Zhou et al., 2003; Zhu et al., 2010, 2015). While NO_2 has been found to be the dominant product from HNO_3 photolysis on clean and dry laboratory surfaces (Ye et al., 2016b; Zhou et al., 2003; Zhu et al., 2010, 2015), HONO is the major product on natural surfaces and in ambient aerosols (Ye et al., 2016b, 2017a).

The “determined photolysis rate constant” ($J_{p\text{NO}_3}^N$) is the laboratory determined photolysis rate constant using the ambient aerosol samples. It has been normalized to tropical noontime conditions at ground level (solar zenith angle = 0°), so that it can be compared with results in other studies. The $J_{p\text{NO}_3}^N$ value varies over a wide range, from $8.3 \times 10^{-5} \text{ s}^{-1}$ to $3.1 \times 10^{-4} \text{ s}^{-1}$ among the samples, with a median of $2.0 \times 10^{-4} \text{ s}^{-1}$ and a mean (± 1 standard deviation) of $1.9 (\pm 1.2) \times 10^{-4} \text{ s}^{-1}$. A median $J_{p\text{NO}_3}^N$ value of $2.0 \times 10^{-4} \text{ s}^{-1}$ was used in the calculation.

The “ambient photolysis rate constant” is the $p\text{NO}_3$ photolysis rate constant ($J_{p\text{NO}_3}$) under the ambient conditions. It varies with the time of the day, the location, and the cloud coverage. $J_{p\text{NO}_3}$ was calculated by scaling $J_{p\text{NO}_3}^N$ ($\sim 2.0 \times 10^{-4} \text{ s}^{-1}$) to ambient light conditions using the measurement-derived J_{HNO_3} (Eq. 3).

Yes, some recent studies also showed the short lifetime of particulate nitrate in low- NO_x environments (Reed et al., 2017; Ye et al., 2016a, 2017b). Many laboratory studies have also shown fast photolysis rate constant for surface HNO_3 and $p\text{NO}_3$ (Baergen and Donaldson, 2013, Ye et al., 2016b, 2017a; Zhou et al., 2003; Zhu et al., 2010; Zhu et al., 2015), lending support to our argument that $p\text{NO}_3$ photolysis can be an effective renoxification pathway. However, particulate nitrate is in a dynamic equilibrium with gas-phase HNO_3 , the later accounts for a larger (or even dominant) fraction of total nitrate ($p\text{NO}_3 + \text{HNO}_3$) and is photochemically inert. The overall photolysis of $p\text{NO}_3 + \text{HNO}_3$ would be much slower than indicated by $J_{p\text{NO}_3}$. In addition, oxidation of NO_x via several reactions will replenish the $p\text{NO}_3 + \text{HNO}_3$ reservoir. Our results reported in this manuscript and in an earlier paper (Ye et al., 2016a) suggest that there is a rapid cycling in reactive nitrogen species in the low- NO_x atmosphere, sustaining the observed levels of HONO and $p\text{NO}_3$.

Q7: The different air mass types are not explained, and it isn't clear if or how they were separated. Benzene is used to identify urban plumes, but how are power plant plumes and biomass burning plumes identified? Could there be a large biomass burning plume contribution to the observations? Were some plumes a combination of sources? CO or acetonitrile measurements could be used to identify air mass influences. Similarly, SO₂ was measured and could be used to identify power plant plumes. I could find no mention of any meteorological conditions. Without a more thorough description of the ambient conditions and ancillary measurements, it is very difficult to compare these results with other studies.

Response: As suggested, we have added CO, acetonitrile and SO₂ as tracers to identify plumes in the revised manuscript (Figure S1). Based on the low levels of acetonitrile during the reported flights in this manuscript, we did not observe any significant contribution from biomass burning (Figure S1). The original assignments of plumes are further confirmed by these tracers: The CO peaks in plumes U1, U2 and U3 (A, B, C in the original Figures 2 and 7) suggest that they were under influenced by urban activities, and the lack of CO peaks in plumes P1-P4 (D, E, F, G in the original Figures 2 and 7) suggest that they were power plant plumes. A high SO₂ peak also accompanied a high NO_x peak in the power plant plume P4 (G in the original Figures 2 and 7).

We did employ the meteorological information in our discussions, for examples, using the wind speed and wind direction to calculate the transport time of plumes from a power plant (original lines 358-362) and back trajectories in explaining horizontal HONO variations (original lines 401-409). Ancillary measurements, including OH, NO, NO₂, aerosol number and size distribution, isoprene, *J* values, ..., were used in calculations and discussion throughout the manuscript.

Q8: The large reduction in PBL mixing time (line 262) between noon and afternoon is very surprising and differs from previous studies. By noon in the summer, the mixing time should be much less than 1.5 h.

Response: The mixing time can be influenced by several factors, such as the surface albedo and cloud coverage. The longer than expected mixing time was calculated using the vertical isoprene profile and may be due to the combined effect of these factors. We have also found significant variations in mixing time in RF #4, #5 and #17. Nevertheless, HONO photolytic lifetime was still much shorter than the mixing time even if the later was reduced by half; the conclusion of this section remains unchanged, i.e., the contribution of ground HONO source was not important to the overall HONO budget in the PBL, due to low ground source strength and/or slower transport than its photolysis loss.

Q9: Relevant literature is not referenced, and the differences with previous measurements are not discussed. We published a very similar paper, using aircraft HONO measurements at the same time and location and under the same SAS umbrella (Neuman et al., HONO emission and production determined from airborne measurements over the Southeast U.S., JGR, 2016), but oddly, that paper is not referenced. We found that known HONO production mechanisms explained the HONO abundance, and we did not need to invoke unknown sources. In contrast, the studies referenced in the introduction (lines 29-30, line 103) report much larger values ranging from 100s of pptv to ppb levels. Why do the HONO values reported here differ from previous measurements, which range from indistinguishable from zero to ppbv levels? Meaningful comparisons to previous studies (some conducted at the same time and location) are essential for understanding the findings reported here.

Response: We finished our first draft of this manuscript over two years ago, before the publication of the mentioned paper (Neuman et al., 2016). Although we have made significant changes to the draft during the subsequent revisions, we failed to update the references. We regret the omission. The paper by Neuman et al. (2016) has been referenced and discussed in the revised manuscript (lines 64, 95, 211, 215, 239, 282, 403).

We agree that meaningful comparisons to previous studies are essential for understanding the reported data. We compared our results with those from other two airborne studies (Zhang et al., 2009; Li et al., 2014) in the original manuscript, and have added more discussions and comparisons with Neuman et al. (2016) in the revised manuscript.

Although the two aircraft studies, SENEX on NOAA's WP-3D and NOMADSS on NSF/NCAR's C-130, were conducted at the same time and location and under the same SAS umbrella, they had been focused on somewhat different objectives. The main objective of TROPHONO project (one of the three projects in NOMADSS) was to investigate daytime HONO formation mechanisms and the role of nitrate photolysis in aerosol particles in the cycling of reactive nitrogen species in the troposphere. All the C-130 flights were conducted in the daytime during NOMADSS except the RF#18 (from late-afternoon to midnight). And the results reported in this manuscript were mostly from rural background air masses, with only a few small urban and power plant plumes in RE#11. On the other hand, the WP-3D spent far more time in various plumes and at nights during the SENEX (Neuman et al., 2016).

We would like to point out that there are actually no major disagreements between the two aircraft-based studies when the overlapped measurements are compared. Similar to what reported by Neuman et al. (2016), we found that the NO_x-related reactions (mainly the NO+OH reaction) accounted for nearly all the required HONO source in the large fresh power plant plume (NO_x ~ 20 ppbv) encountered during the RF #7 to Ohio River Valley (lines 375-378 in the original manuscript). In the low-NO_x background air masses, the mean HONO concentration was 11.2 ± 4.3 pptv in the PBL and 5.6 ± 3.4 in the free troposphere (Table 2), which is within the range from -15 pptv to 10 pptv (± 15 pptv uncertainty) (Neuman et al., 2016).

As pointed out by Andy Neuman, the studies referenced in Section “1. Introduction” reported significantly higher HONO concentrations, up to hundreds of pptv in the rural environments and several ppbv in the urban environments. The reported values include lower daytime and higher nighttime HONO concentrations. Most of these measurements were made on ground stations, and thus under direct influence of the ground HONO sources, including direct emissions (combustion sources and soil emission sources), heterogeneous and photochemical reactions of precursors (e.g., NO₂, PAN and HNO₃) on ground surfaces, and gaseous reactions with elevated reactant concentrations. The measurements on aircrafts, on the other hand, minimized the influence of the ground HONO sources, as we discussed on section 3.2. Therefore, the airborne measurement data would provide a better insight into the HONO chemistry within an air parcel.

Q10: Line 85 states that nearly all HONO measurements have been made at ground sites, but that dismisses the many studies of HONO vertical gradients using DOAS and from towers (e.g. Young et al, Vertically Resolved Measurements of Nighttime Radical Reservoirs in Los Angeles and Their Contribution to the Urban Radical Budget, ES&T, 2012; Stutz et al., Simultaneous DOAS and mist-chamber IC measurements of HONO in Houston, TX, Atmospheric Environment, 2010; Vandenoer 2013 in the references). And the authors themselves have many papers that detail airborne measurements.

Response: We would like to point out that the HONO gradient measurements using DOAS and from towers are still ground-based, and that we did reference many of the related literatures (Kleffmann et al., 2003; Li et al., 2014; Stutz et al., 2002; Villena et al., 2011; Wong et al., 2011, 2012, 2013; Ye et al., 2015; Zhang et al., 2009) when discussing HONO vertical measurements and airborne measurements in the introduction (the paragraph starting line 85 in the original manuscript).

Q11: smaller points I don't know what an N(V) level is (line 216)

Response: We have much few data points of HNO₃, due to poor time resolution and more technical difficulties with the system (bubble formation/baseline shift, especially at high altitudes). The HNO₃ levels in the PBL were 305 ± 87 pptv in RF4, 291 ± 81 pptv in RF 5, 342 ± 108 pptv in RF11, 105 ± 38 pptv in RF 17, and 206 ± 73 pptv in RF18, accounting for 70% - 85% of (N(V)).

Q12: Data averaging is not explained. The time resolution of HONO and pNO3 are listed as 3 min and 6 min, yet 1 min data are shown. How are the data averaged in figure 3? The values do not match those shown in Figure 2, but the binning and averaging are never described.

Response: The absorbance signals were sampled at 1 Hz, much higher rate than the time resolutions of HONO and pNO₃ (see Figure 1 in this Response). The 1-min or 3-min averages were used to convert absorbance signals to concentrations, based on flow rate and calibration

information (please see our responses to Q1 and Q2 for more details on method and data processing). We have added the above information to the revised manuscript and have used 3-min HONO data and 6-min pNO₃ data for the revised figures, as suggested.

Q14: Figure 2 shows pNO₃ in ppbv, which is in error.

Response: Thank you for pointing out the error; the error has been corrected.

References

- Baergen, A. M., and Donaldson, D. J.: Photochemical renoxification of nitric acid on real urban grime, *Environ. Sci. Technol.*, 47, 815-820, 10.1021/es3037862, 2013.
- Du, J., and Zhu, L.: Quantification of the absorption cross sections of surface-adsorbed nitric acid in the 335-365 nm region by Brewster angle cavity ring-down spectroscopy, *Chem. Phys. Lett.*, 511, 213-218, 10.1016/j.cplett.2011.06.062, 2011.
- Heald, C. L., et al.: Atmospheric ammonia and particulate inorganic nitrogen over the United States, *Atmos. Chem. Phys.*, 12, 10295–10312, 2012.
- Kaser, L., et al.: chemistry-turbulence interactions and mesoscale variability influence the cleansing efficiency of the atmosphere, *Geophys. Res. Lett.*, 42, doi:10.1002/2015GL066641, 2015.
- Kleffmann, J., Kurtenbach, R., Lorzer, J., Wiesen, P., Kalthoff, N., Vogel, B., and Vogel, V.: Measured and simulated vertical profiles of nitrous acid - Part I: Field measurements, *Atmos. Environ.*, 37, 2949-2955, 2003.
- Li, X., et al.: Missing gas-phase source of HONO inferred from Zeppelin measurements in the troposphere, *Science*, 344, 292-296, 2014.
- Neuman, J. A., et al.: Variability in ammonium nitrate formation and nitric acid depletion with altitude and location over California, *J. Geophys. Res.*, 108(D17), 4557, doi:10.1029/2003JD003616, 2003.
- Neuman, J. A., et al., HONO emission and production determined from airborne measurements over the Southeast U.S., *J. Geophys. Res. Atmos.*, 121, 9237–9250, doi:10.1002/2016JD025197, 2016
- Reed, C. et al.: Evidence for renoxification in the tropical marine boundary layer, *Atmos. Chem. Phys.*, 17, 4081–4092, 2017.
- Stutz, J., Alicke, B., and Neftel, A.: Nitrous acid formation in the urban atmosphere: Gradient measurements of NO₂ and HONO over grass in Milan, Italy, *J. Geophys. Res.-Atmos.*, 107, Artn 8192, 10.1029/2001jd000390, 2002. Wong, K. W., Oh, H. J., Lefer, B. L., Rappengluck, B., and Stutz, J.: Vertical profiles of nitrous acid in the nocturnal urban atmosphere of Houston, TX, *Atmos. Chem. Phys.*, 11, 3595-3609, 2011.
- Villena, G., Kleffmann, J., Kurtenbach, R., Wiesen, P., Lissi, E., Rubio, M. A., Croxatto, G., and Rappengluck, B.: Vertical gradients of HONO, NO_x and O₃ in Santiago de Chile, *Atmos. Environ.*, 45, 3867-3873, 2011.
- Wong, K. W., Tsai, C., Lefer, B., Haman, C., Grossberg, N., Brune, W. H., Ren, X., Luke, W., and Stutz, J.: Daytime HONO vertical gradients during SHARP 2009 in Houston, TX, *Atmos. Chem. Phys.*, 12, 635-652, 2012.
- Wong, K. W., Tsai, C., Lefer, B., Grossberg, N., and Stutz, J.: Modeling of daytime HONO vertical gradients during SHARP 2009, *Atmos. Chem. Phys.*, 13, 3587-3601, 2013.
- Ye, C. X., Zhou, X. L., Pu, D., Stutz, J., Festa, J., Spolaor, M., Cantrell, C., Mauldin, R. L., Weinheimer, A., and Haggerty, J.: Comment on "Missing gas-phase source of HONO

- inferred from Zeppelin measurements in the troposphere", *Science*, 348, 10.1126/science.aaa1992, 2015.
- Ye, C., et al.: Rapid cycling of reactive nitrogen in the marine boundary layer, *Nature*, 532, 489-491, 2016a
- Ye, C., Gao, H., Zhang, N., and Zhou, X.: Photolysis of nitric Acid and nitrate on natural and artificial surfaces, *Environ. Sci. Technol.*, 50, 3530-3536, 2016b.
- Ye, C., Zhang, N., Gao, H., and Zhou, X.: Photolysis of particulate nitrate as a source of HONO and NO_x, *Environ. Sci. Technol.*, DOI: 10.1021/acs.est.7b00387, 2017a.
- Ye, C., Heard, D.E., and Whalley, L.K.: Evaluation of novel routes for NO_x formation in remote regions, *Environ. Sci. Technol.*, DOI: 10.1021/acs.est.6b06441, 2017b.
- Zhang, N., Zhou, X., Shepson, P. B., Gao, H., Alaghmand, M., and Stirm, B.: Aircraft measurement of HONO vertical profiles over a forested region, *Geophys. Res. Lett.*, 36, L15820, 10.1029/2009gl038999, 2009.
- Zhang, N., Zhou, X., Bertman, S., Tang, D., Alaghmand, M., Shepson, P. B., and Carroll, M. A.: Measurements of ambient HONO concentrations and vertical HONO flux above a northern Michigan forest canopy, *Atmos. Chem. Phys.*, 12, 8285-8296, 2012.
- Zhou, X., Gao, H., He, Y., Huang, G., Bertman, S. B., Civerolo, K., and Schwab, J.: Nitric acid photolysis on surfaces in low-NO_x environments: Significant atmospheric implications, *Geophys. Res. Lett.*, 30, 2217, 10.1029/2003gl018620, 2003.
- Zhu, C., Xiang, B., Chu, L.T., and Zhu, L.: 308 nm Photolysis of nitric acid in the gas phase, on aluminum surfaces, and on ice films, *J. Phys. Chem. A*, 114, 2561-2568, 2010.
- Zhu, L., Sangwan, M., Huang, L., Du, J., and Chu, L.T.: Photolysis of nitric acid at 308 nm in the absence and in the presence of water vapor, *J. Phys. Chem. A* 2015, 119, 4907-4914, 2015.

(4) Response to interactive comment on manuscript on “Tropospheric HONO Distribution and Chemistry in the Southeast U.S.” by D. Parrish

General comments

"Extraordinary claims require extraordinary evidence" is a phrase made popular by Carl Sagan [Rational Wiki]. This is particularly relevant to the Ye et al. [2018] paper. The authors make the extraordinary claim that “. . .the sum of all known NO_x-related HONO formation mechanisms was found to account for less 20% of the daytime HONO source in the background terrestrial air masses, . . .”. If this claim were true, it would possibly force a reassessment of our understanding of HO_x and NO_x budgets of the troposphere, depending on the details of the other 80% of the (unknown) sources. However, the evidence presented Ye et al., [2018] does not justify that claim. In fact, Neuman et al. [2016] conclude: “Outside of recently emitted plumes from known combustion sources, HONO mixing ratios measured several hundred meters above ground level were indistinguishable from zero within the 15 parts per trillion by volume measurement uncertainty. The results reported here do not support the existence of a ubiquitous unknown HONO source that produces significant HONO concentrations in the lower troposphere.” The conclusion of these two studies disagree strongly, yet the reported measurements were made from different aircraft with different instrumentation, but in the same region of the country over the same time period, summer 2013. Unfortunately, Ye et al., [2018] do not discuss or even cite Neuman et al. [2016]. The differences in the results reported in these two papers point to clear experimental problems in the measurements. Until these problems are resolved, the extraordinary claim of Ye et al. [2018] should not be published.

References

Neuman, J. A., et al. (2016), HONO emission and production determined from airborne measurements over the Southeast U.S., J. Geophys. Res. Atmos., 121, 9237–9250, doi:10.1002/2016JD025197.

Rational Wiki, [tps://rationalwiki.org/wiki/Extraordinary_claims_require_extraordinary_evidenceh](https://rationalwiki.org/wiki/Extraordinary_claims_require_extraordinary_evidenceh)

Ye, C., et al. (2018), Tropospheric HONO distribution and chemistry in the Southeast U.S., Atmos. Chem. Phys. Discuss., <https://doi.org/10.5194/acp-2018-105>.

Response: We completely agree with David Parrish that “Extraordinary claims require extraordinary evidence.” However, we disagree that our finding that “. . .the sum of all known NO_x-related HONO formation mechanisms was found to account for less 20% of the daytime HONO source in the background terrestrial air masses, . . .” is an extraordinary claim. In high NO_x environments, such as urban atmosphere and power plant and biomass burning plumes, NO_x is known to be the dominant precursor to HONO. However, in low NO_x environments, such as the rural regions in the Southeast US, other precursors become more important. In fact, there have been many reports in literature, based on both field and laboratory results, demonstrating that several processes other than reactions involving ambient NO_x can lead to the production of HONO. Nitrate photolysis in snowpack has been found to be a major source for HONO and NO_x during the polar spring and summer in the polar regions (Beine et al., 2002, 2008; Honrath et al., 2000, 2002; Zhou et al., 2001). In low-NO_x rural and forested regions, photolysis of nitric acid on the forest canopy surface has been found to be the major daytime HONO source (Ye et al., 2016a; Zhou et al., 2002, 2003, 2011). Photolysis of particulate nitrate has been found to be the major HONO source in the low-NO_x marine boundary layer (Reed et al, 2017; Ye et al., 2016b). And in agricultural regions, biochemical process in the soils (denitrification or nitrification) has been found to

account for the majority of HONO budget (Oswald et al., 2013; Su et al., 2012; Meusel et al., 2018).

We estimated the HONO formation rates from known homogeneous and heterogeneous NO_x reactions, with a suit of parameters measured on board the C-130, and found the sum of these mechanisms to contribute less than 20% of the total HONO source strength in the background air masses. Most of the remaining so-called “unknown” 80% can actually be accounted for by the photolysis of particulate nitrate (lines 302 - 331 in the original manuscript). This finding is consistent with several reported laboratory studies that the photolysis of surface nitric acid and particulate nitrate is 2 - 3 orders faster than that of gaseous nitric acid (Baergen and Donaldson, 2013, Ye et al., 2016a, 2017a; Zhou et al., 2003; Zhu et al, 2010, 2015), producing mostly NO_2 on clean dry surface (Ye et al., 2016a; Zhou et al., 2003; Zhu et al, 2010) and mainly HONO on natural surfaces and ambient aerosols (Ye et al., 2016a, 2017a).

We would also like to point out that while HONO photolysis can be a significant or even a major HO_x source on the ground level in both rural and urban atmosphere (Acker et al., 2006a,b; Elshorbany et al., 2010; Kleffmann et al., 2003, 2005; Villena et al., 2011), it was found unimportant compared to photolyses of O_3 and HCHO in the background air masses **aloft** over the Southeast US. At the observed levels of 5-11 pptv, the answer to the HONO source question is unlikely to significantly affect our understanding of HO_x chemistry in the rural troposphere. On the other hand, since HONO was found to be mainly produced from photolysis of particulate nitrate, it is an important intermediate product of a photochemical renoxification process recycling nitric acid and nitrate back to NO_x .

We regret that we did not reference the recent paper by Neuman et al. (2016). We prepared and finished our first draft of this manuscript over two years ago, before the publication of the mentioned paper. Although we have made significant changes to the first draft during the subsequent revisions, we failed to update the references. We have referenced and discussed the paper in the revised manuscript (lines 64, 95, 211, 215, 239, 282, 403).

It is important to point out that there is no major disagreement in the results between the two aircraft-based studies. Similar to what reported by Neuman et al. (2016), we found that the NO_x -related reactions (mainly $\text{NO}+\text{OH}$ reaction) accounted for nearly all the required HONO source in the large fresh power plant plume ($\text{NO}_x \sim 20$ ppbv) encountered during the RF #7 to Ohio River Valley (lines 375-378 in the original manuscript). In the smaller and more diluted power plant plume G in the original Figures 2c and 7b ($\text{NO}_x \sim 1.8$ ppb), NO_x -related reactions contribute to a major fraction (52%) of the total required HONO source (the original Figure 7b). In the low- NO_x background air masses, the mean HONO concentration was 11.2 ± 4.3 pptv in the PBL and 5.6 ± 3.4 in the free troposphere (Table 2), which is again in agreement the value reported by Neuman et al (2016) “indistinguishable from zero **within the 15 parts per trillion by volume measurement uncertainty.**”

We would further argue that while the CIMS instrument, with detection limits of 40 pptv for 1-s data and 15 pptv for 30-min averaging, is capable of producing high quality data in the plumes, it does not have the sensitivity to measure low levels of HONO in the low- NO_x background atmosphere. The conclusion based on its below-detection-limit measurements and on the extrapolations from combustion plumes to low- NO_x background atmosphere is not reliable and thus should not be used to rule out the findings based on our measurement in the low- NO_x rural atmosphere. The relative contribution of NO_x -related reactions is in the order of power plant plume ($\text{NO}_x \sim 1-20$ ppb) > urban plume ($\text{NO}_x \sim 1$ ppb) > background terrestrial air masses ($\text{NO}_x \sim 100-300$ pptv). That is, the relative contribution from NO_x -related reactions to the required HONO source is highly dependent on the NO_x regimes. While the conclusion we draw in the high NO_x regime in large power plant plumes is not different from

that by Neuman et al. (2016), our measurements have added new and valuable HONO budget information in low NO_x regime to the literature.

We appreciate the question regarding potential problems with experimental design/measurement technique. More detailed descriptions and discussions on HONO measurement technique and set up have been provided in our response to Andy Neuman's comment (#1 and #2). The wet chemistry-based techniques, including the LPAP used in this study, can provide exceptionally high sensitivity for HONO. However, the measurements by these techniques have been treated with caution and suspicion due to potential interferences from ambient constituents. We have made major and continued efforts in the past two decades to minimize and correct for the potential interferences. For examples, we found that shielding the inlet line from sunlight could prevent photochemical formation of HONO on the inlet wall surface (Zhou et al., 2002b). Results from many field and laboratory tests we conducted so far have indicated that heating the inlet line can effectively minimize the HONO loss to and/or HONO formation from heterogeneous NO₂ reactions on inlet wall surface (see Figure 3 in the response to Andy Neuman's comment). We have used Na₂CO₃-coated denuder to generate "zero-HONO" air by selectively removing HONO (and acidic species) from ambient air to established measurement baselines. The subtraction of "zero-HONO" air baselines from ambient signals effectively eliminate the potential interference from HONO precursors, such as NO_x, PAN and particulate nitrite (Zhang et al., 2012; Figures 1 and 2 in the Response to A. Neuman's Comment). To check the effectiveness of our background correction procedure and to validate the LPAS technique, we have compared the HONO concentrations measured by the LPAS and by a limb-scanning differential optical absorption spectroscopy (DOAS) instruments on board the C-130 in large power plant plumes during the NOMADSS campaign, and found very good agreement between the two measurements (Ye et al., 2016b). Therefore, we have high confidence with our HONO data measured on the C-130 during the NOMADSS field study, and we stand by our findings that the photolysis of particulate nitrate is the major daytime HONO source and NO_x-related reactions is an only minor HONO contributor in the low-NO_x TBL over Southeast U.S.

References

- Acker, K., Moller, D., Wieprecht, W., Meixner, F. X., Bohn, B., Gilge, S., Plass-Dulmer, C., and Berresheim, H.: Strong daytime production of OH from HNO₂ at a rural mountain site, *Geophys. Res. Lett.*, 33, L02809, 10.1029/2005gl024643, 2006.
- Acker, K., et al.: Nitrous acid in the urban area of Rome, *Atmos. Environ.*, 40, 3123-3133, 2006b.
- Baergen, A. M., and Donaldson, D. J.: Photochemical renoxification of nitric oxide on real urban grime, *Environ. Sci. Technol.*, 47, 815-820, 10.1021/es3037862, 2013.
- Beine, H., Domine, F., Simpson, W., Honrath, R.E., Sparapani, R., Zhou, X., and King, M.: Snow-pile and chamber experiments during the Polar Sunrise Experiment 'Alert 2000': exploration of nitrogen chemistry. *Atmos. Environ.* 2002, 36, 2707-2719, 2002.
- Beine, H., Colussi, A.J., Amoroso, A., Esposito, G., Montagnoli, M., and Hoffmann, M.R.: HONO emissions from snow surfaces, *Environ. Res. Lett.*, 3, 045005, 2008.
- Elshorbany, Y. F., Kleffmann, J., Kurtenbach, R., Lissi, E., Rubio, M., Villena, G., Gramsch, E., Rickard, A. R., Pilling, M. J., and Wiesen, P.: Seasonal dependence of the oxidation capacity of the city of Santiago de Chile, *Atmos. Environ.*, 44, 5383-5394, 10.1016/j.atmosenv.2009.08.036, 2010.

- Honrath, R. E., Peterson, M. C., Dziobak, M. P., Dibb, J. E., Arsenault, M. A., and Green S. A.: Release of NO_x from sunlight-irradiated midlatitude snow, *Geophys. Res. Lett.*, 27, 2237-2240, 2000.
- Honrath R. E., Lu, Y., Peterson, M.C., Dibb, J.E., Arsenault, M.A., Cullen, N.J., and Steffen, K.: Vertical fluxes of NO_x, HONO, and HNO₃ above the snowpack at Summit, Greenland *Atmos. Environ.*, 36 2629-40, 2002.
- Kleffmann, J., Kurtenbach, R., Lorzer, J., Wiesen, P., Kalthoff, N., Vogel, B., and Vogel, V.: Measured and simulated vertical profiles of nitrous acid - Part I: Field measurements, *Atmos. Environ.*, 37, 2949-2955, 2003.
- Kleffmann, J., et al.: Daytime formation of nitrous acid: A major source of OH radicals in a forest, *Geophys. Res. Lett.*, 32, doi:10.1029/2005GL022524, 2005.
- Meusel, H. et al.: Emission of nitrous acid from soil and biological soil crusts represents an important source of HONO in the remote atmosphere in Cyprus, *Atmos. Chem. Phys.*, 18, 799–813, 2018.
- Neuman, J. A., et al.: HONO emission and production determined from airborne measurements over the Southeast U.S., *J. Geophys. Res. Atmos.*, 121, 9237–9250, doi:10.1002/2016JD025197, 2016.
- Oswald, R., et al.: HONO emissions from soil bacteria as a major source of atmospheric reactive nitrogen, *Science*, 341, 1233-1235, DOI: 10.1126/science.1242266, 2013.
- Reed, C. et al.: Evidence for renoxification in the tropical marine boundary layer, *Atmos. Chem. Phys.*, 17, 4081–4092, 2017.
- Ren, X., et al.: OH and HO₂ chemistry in the urban atmosphere of New York City. *Atmos. Environ.* 37, 3639-3651, 2003.
- Su, H., Cheng, Y. F., Oswald, R., Behrendt, T., Trebs, I., Meixner, F. X., Andreae, M. O., Cheng, P., Zhang, Y., and Poschl, U.: Soil Nitrite as a Source of Atmospheric HONO and OH Radicals, *Science*, 333, 1616-1618, 10.1126/science.1207687, 2011.
- Villena, G., et al.: Vertical gradients of HONO, NO_x and O₃ in Santiago de Chile, *Atmos. Environ.*, 45, 3867-3873, 2011.
- Ye, C., Gao, H., Zhang, N., and Zhou, X.: Photolysis of nitric Acid and nitrate on natural and artificial surfaces, *Environ. Sci. Technol.*, 50, 3530-3536, 2016a.
- Ye, C., et al.: Rapid cycling of reactive nitrogen in the marine boundary layer, *Nature*, 532, 489-491, 2016b.
- Ye, C., Zhang, N., Gao, H., and Zhou, X.: Photolysis of particulate nitrate as a source of HONO and NO_x, *Environ. Sci. Technol.*, DOI: 10.1021/acs.est.7b00387, 2017a.
- Ye, C., Heard, D.E., and Whalley, L.K.: Evaluation of novel routes for NO_x formation in remote regions, *Environ. Sci. Technol.*, DOI: 10.1021/acs.est.6b06441, 2017b.
- Zhou, X., H. J. Beine, H.J., Honrath, R.E., Fuentes, J.D., Simpson, W., Shepson, P.B., and J. W. Bottenheim, J.W.: Snowpack photochemical production as a source for HONO in the Arctic boundary layer in spring time, *Geophys. Res. Lett.*, 28:4087-4090, 2001.
- Zhou, X., Civerolo, K., Dai, H., Huang, G., Schwab, J., and Demerjian, K.: Summertime nitrous acid chemistry in the atmospheric boundary layer at a rural site in New York State, *J. Geophys. Res.*, 107, doi:10.1029/2001JD001539, 2002a.
- Zhou, X., He, Y., Huang, G., Thornberry, T.D., Carroll, M.A., and Bertman, S.B.: Photochemical production of HONO on glass sample manifold wall surface, *Geophys. Res. Lett.*, 29, doi:10.1029/2002GL015080, 2002b.
- Zhou, X., Gao, H., He, Y., Huang, G., Bertman, S. B., Civerolo, K., and Schwab, J.: Nitric acid photolysis on surfaces in low-NO_x environments: Significant atmospheric implications, *Geophys. Res. Lett.*, 30, 2217, 10.1029/2003gl018620, 2003.

- Zhou, X., G. Huang, G., Civerolo, K., Roychowdhury, U., and Demerjian, K.L.: Summertime observations of HONO, HCHO, and O₃ at the summit of Whiteface Mountain, New York, *J. Geophys. Res.*, 112, doi:10.1029/2006JD007256, 2007.
- Zhou, X., Zhang, N., TerAvest, M., Tang, D., Hou, J., Bertman, S., Alaghmand, M., Shepson, P. B., Carroll, M. A., Griffith, S., Dusanter, S., and Stevens, P. S.: Nitric acid photolysis on forest canopy surface as a source for tropospheric nitrous acid, *Nature Geosci.*, 4, 440-443, 10.1038/NGEO1164, 2011.
- Zhu, C., Xiang, B., Chu, L.T., and Zhu, L.: 308 nm Photolysis of nitric acid in the gas phase, on aluminum surfaces, and on ice films, *J. Phys. Chem. A*, 114, 2561-2568, 2010.
- Zhu, L., Sangwan, M., Huang, L., Du, J., and Chu, L.T.: Photolysis of nitric acid at 308 nm in the absence and in the presence of water vapor, *J. Phys. Chem. A* 2015, 119, 4907-4914, 2015.

Tropospheric HONO Distribution and Chemistry in the Southeast U.S.

Chunxiang Ye^{1,2}, Xianliang Zhou^{2,3}, Dennis Pu³, Jochen Stutz⁴, James Festa⁴, Max Spolaor⁴, Catalina Tsai⁴, Christopher Cantrell⁵, Roy L. Mauldin III^{5,6}, Andrew Weinheimer⁷, Rebecca S. Hornbrook⁷, Eric C. Apel⁷, Alex Guenther⁸, Lisa Kaser⁷, Bin Yuan⁹, Thomas Karl¹⁰, Julie Haggerty⁷, Samuel Hall⁷, Kirk Ullmann⁷, James Smith^{7,11}, John Ortega⁷

[1] State Key Joint Laboratory of Environmental Simulation and Pollution Control, College of Environmental Sciences and Engineering, the Key Joint Laboratory of Environment

[2] Wadsworth Center, New York State Department of Health, Albany, NY

[3] Department of Environmental Health Sciences, State University of New York, Albany, NY

[4] Department of Atmospheric and Oceanic Sciences, University of California, Los Angeles, CA

[5] Department of Atmospheric and Oceanic Sciences, University of Colorado-Boulder, Boulder Colorado

[6] Department of Physics, University of Helsinki, Helsinki, Finland

[7] National Center for Atmospheric Research, Boulder, Colorado

[8] Department of Earth System Science, University of California, Irvine, CA

[9] Institute for Environmental and Climate Research, Jinan University, Guangzhou, 511443

[10] Institute of Atmospheric and Cryospheric Sciences-, University of Innsbruck, Innsbruck, Austria

[11] University of Eastern Finland, Kuopio, Finland

Correspondence to: Chunxiang Ye (c.ye@pku.ed.u.cn) and Xianliang Zhou (xianliang.zhou@health.ny.gov)

1 Abstract

2 Here we report the measurement results of nitrous acid (HONO) and a suite of relevant
3 parameters on the NCAR C-130 research aircraft in the Southeast U.S. during the NOMADSS
4 2013 summer field study. ~~Daytime~~ The daytime HONO concentrations ranged from low parts
5 per trillion by volume (pptv) in the free troposphere (FT) to mostly within 5 - 15 pptv in the
6 background planetary boundary layer (PBL), ~~and to up to 34.4 pptv in the power plant plumes~~
7 ~~and urban plumes.~~ Above the lower flight altitude of 300 m in the PBL of background
8 Southeast U.S., ~~There~~ There was no discernible vertical HONO ~~distribution trend~~ gradient
9 above the lower flight altitude of 300 m in the PBL, ~~in the PBL,~~ and ~~t.~~ The transport of ground
10 surface HONO source was found not a significant contributor to the in situ tropospheric
11 HONO budget ~~source budget~~ in the measurement PBL above the lower flight altitude between
12 of 300 m and 4.7 km. ~~The total in situ HONO source,~~ mean (± 1 SD) was calculated 48-53 (\pm
13 29-21) pptv h⁻¹ in the background Southeast U.S., during the day. ~~verse an~~ The upper limit
14 contribution from NO_x-related reactions was 10 (± 5) pptv h⁻¹ of 11-10 ($\pm 9-5$) pptv h⁻¹, and
15 and the contribution from photolysis of particulate nitrate (pNO₃) was 38 (± 23) pptv h⁻¹, of 31
16 38 ($\pm 25-23$) pptv h⁻¹, based on estimated from the measured pNO₃ concentrations and the
17 median pNO₃ photolysis rate constant value of 2.0×10^{-4} s⁻¹ for determined in laboratory pNO₃
18 photolysis rate constant determined in the laboratory using ambient aerosol samples ~~collected~~
19 ~~during the field study.~~ Specifically within the diluted and aged power plant and urban plumes
20 encountered, NO_x-related reactions contributed up to 52% of the total HONO source,
21 depending on NO_x concentration. ~~While~~ The photolysis of HONO only contributed to less
22 than 10% ~~to of~~ the primary OH budget ~~source.~~ ~~;~~ ~~while~~ However, The regenerating
23 rate renoxification of NO_x of about 52 pptv h⁻¹ via HONO an recycling NO_x source via pNO₃
24 photolysis ~~photolysis is~~ was equivalent to an air column NO_x source of $\sim 32.3 \times 10^{-6}$ mol m⁻² h⁻¹
25 in the 1.5-km PBL, in the air column within the PBL, a considerable supplementary NO_x
26 source in the low-NO_x background area. Up to several tens pptv of HONO were observed in
27 power plant and urban plumes during the day, mostly produced in situ from precursors
28 including NO_x and pNO₃. ~~it was an important intermediate product of a photochemical~~
29 ~~renoxification process recycling nitric acid and nitrate back to NO_x.~~ Finally, there was no
30 observable accumulation of HONO in the nocturnal residual layer and the nocturnal FT in the
31 background Southeast U.S., with an increase in HONO/NO_x ratio of \leq less than 3×10^{-4} hr⁻¹
32 after sunset.

33

34

35 1 Introduction

36 Extensive field studies at ground sites have shown that gas-phase nitrous acid (HONO)
37 exists at much higher levels than expected during the day, with a mixing ratio of HONO up to
38 several parts per billion by volume (ppbv) in the urban atmosphere (Acker et al., 2006;
39 Villena et al., 2011) and up to several hundred parts per trillion by volume (pptv) in rural
40 environments (Acker et al., 2006; Kleffmann et al., 2003; Zhang et al., 2009; Zhou et al.,
41 2002, 2011). At the observed concentrations, HONO photolysis (R1) becomes an important or
42 even a major OH primary source in both urban (Elshorbany et al., 2010; Villena et al., 2011)
43 and rural environments near the ground surface (Acker et al., 2006; He et al., 2006;
44 Kleffmann et al., 2003; Zhou et al., 2002, 2011).

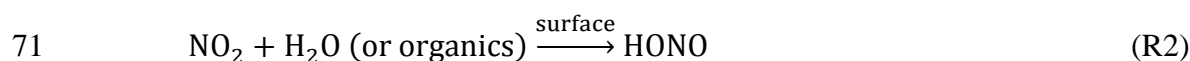


46 The OH radical is responsible for the removal of primary pollutants, and plays a crucial role in
47 the formation of secondary pollutants, such as O₃ and aerosol (Finlayson-Pitts and Pitts,
48 2000), and thus HONO, ~~as an important OH precursor,~~ plays an important role in atmospheric
49 chemistry.

50 The removal processes of HONO from the troposphere are relatively well understood,
51 including mainly photolysis, reaction with the OH radical and surface deposition. Photolysis
52 is the dominant sink for HONO during the day (Kleffmann et al., 2003; Oswald et al., 2015;
53 Zhang et al., 2009, 2012), and dry deposition is the major HONO loss pathway at night,
54 especially over wet surfaces (He et al., 2006; VandenBoer et al., 2015). However, HONO
55 sources in the planetary boundary layer (PBL) are numerous. HONO is directly emitted from
56 combustion processes, such as automobile emissions (Li et al., 2008b) and biomass burning
57 (Burling et al., 2010; Trentmann et al., 2003). Soil emission via nitrification or denitrification
58 is another source of HONO, which might be important in agriculture region (Maljanen et al.,
59 2013; Oswald et al., 2013; Su et al., 2011). Due to the relatively short photolytic lifetime of
60 HONO, in the order of 10 min around summer noontime, the impacts of the direct emission
61 on HONO distribution and chemistry is highly localized and limited to the source region
62 ~~during the day. Recent studies have suggested that microbial activities produce nitrite through~~
63 ~~nitrification or denitrification in the soil, and soil emission may be a significant HONO source~~
64 ~~for the overlying atmosphere~~ (Maljanen et al., 2013; Oswald et al., 2013; Su et al., 2011).
65 ~~Since the emission of HONO from soils depends on multiple factors, such as the abundance of~~
66 ~~soil nitrate and ammonia, the soil pH and water content, and microbial types and activities, it~~

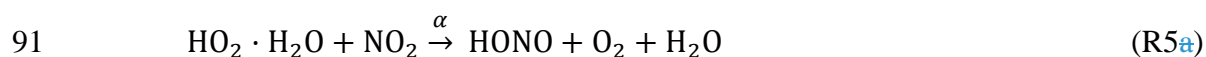
67 is expected that the strength of this HONO emission varies greatly in different environments
68 and thus needs to be further quantified (Oswald et al., 2013).

69 HONO is a unique species that is produced through heterogeneous reactions of
70 different precursors, such as NO₂ and HNO₃, on surfaces (R2 - R3):



73 Heterogeneous reactions of NO₂ with organics (R2) on the surfaces have been found to be
74 greatly accelerated by sunlight through photosensitization (George et al., 2005; Kleffmann,
75 2007; Stemmler et al., 2006, 2007) and these reactions on ground surfaces are likely the major
76 daytime HONO source in urban environments (Acker et al., 2006; Villena et al., 2011; Wong
77 et al., 2011). Laboratory studies have confirmed that HNO₃ undergoes photolysis in sunlight
78 at rates 2 - 3 orders of magnitude greater on the surface than in the gas phase (Baergen and
79 Donaldson, 2013; Du and Zhu, 2011; Ye et al., 2016a, b; Zhou et al., 2003; Zhu et al., 2008),
80 producing NO_x and HONO. In low-NO_x environments, photolysis of nitric acid/nitrate
81 deposited on the surface has been proposed to be the major daytime HONO source near the
82 ground surface (Ye et al., 2016b; Zhou et al., 2003, 2011).

83 Several processes within an air mass may lead to volume, or *in situ*, production of
84 HONO. The OH+NO reaction (R-1) in the gas phase may be a significant HONO source in
85 high NO_x and photochemically reactive atmospheres (Kleffmann, 2007; [Neuman et al., 2016](#);
86 Villena et al., 2011), but becomes negligible in low-NO_x environments (Li et al., 2014; Ye et
87 al., 2016b). Two additional gas-phase reactions have been ~~also~~ proposed to produce HONO
88 within the air column: between excited NO₂ (NO₂^{*}) and water vapor (R4) (Li et al., 2008a),
89 and between NO₂ and the hydroperoxyl-water complex (HO₂·H₂O) (R5a) (Li et al., 2014):



93 However, further laboratory evidence suggests that reaction (R4) is too slow to be important
94 (Carr et al., 2009; Wong et al., 2011). And recent airborne observations have demonstrated
95 that the HONO yield (α) from reaction (R5) is less than 0.03 (Ye et al., 2015). Heterogeneous
96 reactions of NO₂ (R2) on aerosol surfaces and photolysis of particulate nitrate (pNO₃)
97 associated with aerosol particles similar to (R3) also contribute *in situ* HONO production in
98 the air column.

99 ~~Most~~ ~~Almost all~~ HONO measurements ~~to date~~ have been made at ground stations. The
100 observed HONO concentrations reported in the literature represent the HONO levels in the
101 lower PBL under the significant but varying influence of ground surface processes. Thus, it is
102 difficult to distinguish the ground surface HONO sources from the *in situ* HONO sources.
103 Measurements of ~~the vertical profile of~~ HONO concentrations profiles and/or HONO fluxes
104 have suggested that ground surfaces can be major HONO sources for the overlying
105 atmosphere in many cases (He et al., 2006; Kleffmann et al., 2003 Stutz et al., 2002; Zhou et
106 al., 2011; VandenBoer et al., 2013; Young et al., 2012), but not in some other cases (Villena
107 et al., 2011). A recent HONO flux measurement has suggested that the HONO source from
108 the forest canopy contributed ~ 60% of the measured HONO budget at the measurement
109 height of 11 m above the forest canopy, and the *in situ* HONO production contributed the
110 remaining ~ 40% (Zhou et al., 2011). Similarly, observational and modeling studies implied a
111 presence of a volume HONO source at 130-m altitude above Houston, TX (Wong et al., 2012,
112 2013). The relative importance of *in situ* HONO production would be expected to increase
113 with altitude due to decreasing influence of the ground surface, at least during the day.
114 Airborne measurements in the air mass above the altitude influenced directly by ground
115 HONO sources should provide more direct and quantitative evidence for *in situ* HONO
116 production in the troposphere. Indeed, the limited number of airborne measurements available
117 have shown that HONO exists not only in substantial amounts in combustion and urban
118 plumes (Neuman et al., 2016) but also throughout the troposphere (Li et al., 2014; Ye et al.,
119 2015; Zhang et al., 2009).

120 Here we report airborne HONO measurement results and findings from five research
121 flights in the Southeast U.S. during the NOMADSS (Nitrogen, Oxidants, Mercury and
122 Aerosol Distributions, Sources and Sinks) 2013 summer field campaign aboard the
123 NSF/NCAR C-130 research aircraft.

124 **2 Experimental**

125 NOMADSS was an airborne field study under the “umbrella” of SAS (Southeast
126 Atmosphere Study). It consisted of nineteen research flights on board the NSF/NCAR C-130
127 aircraft from June 1, 2013 to July 15, 2013. Parameters observed included HONO, HNO₃,
128 particulate nitrate, NO_x, O₃, BrO, OH radicals, HO₂ radicals, RO₂ radicals, aerosol surface
129 area densities (size <1 μm), VOCs, photolysis frequencies, and other meteorology parameters.
130 Table 1 summarizes the instrumentation, time resolution, detection limit, accuracy, and

131 references for the measurements. The results from five out of nineteen flights are presented
132 here to discuss vertical HONO distribution and HONO chemistry in the Southeast U.S. The
133 flight tracks are shown in Figure 1.

135 2.1 LPAP measurements of HONO and pNO₃

136 HONO was measured by two long-path absorption photometric (LPAP) systems;
137 ~~which take turns to run a 30-min measurement and zero cycle,~~ based on the Griess-Saltzman
138 reaction (Zhang et al., 2012; Ye et al., 2016b). Briefly, ambient air was first brought into the
139 aircraft through a heated PFA inlet, with a residence time of 0.14 s. ~~and then~~ HONO was
140 scrubbed using de-ionized (DI) water in ~~a two~~ 10-turn glass coil samplers ~~to ensure high~~
141 ~~efficiency HONO sampling and~~ The scrubbed collected nitrite was then derivatized with 5
142 mM sulfanilamide (SA) and 0.5 mM N-(1-Naphthyl)-ethylene-diamine (NED) in 40 mM HCl,
143 to form an azo dye ~~within 5 min~~. The azo dye was then detected by light ~~absorbance~~
144 absorption at 540 nm using an 4-channel optic fiber spectrometer (LEDSpec, WPI) with two a
145 1-m liquid waveguide capillary flow cells (WPI). Each LPAP system ~~takes turns to~~ ran a 30-
146 min measurement and zero cycle, with 20 min sampling ambient air and 10 min sampling
147 “zero-HONO” air for baseline correction, and with a 15-min time offset between the two
148 sampling cycles. The combination of the data from the two systems provides continues
149 HONO concentration measurement. The “Zero-HONO” air was generated by directing the
150 sample stream through a Na₂CO₃-coated denuder to remove HONO while allowing most of
151 interfering species (NO_x, PAN, and particulate nitrite) to pass through and was sampled by the
152 ~~systems periodically to establish measurement baselines.~~ The absorbance signals were
153 sampled at a rate of 1 Hz, and were as averaged into 1-min or 3-min data for analysis.

154 Interference from NO_x, PAN, and particulate nitrite ~~if any~~, was corrected by
155 subtracting the baseline from the ambient air signal. Due to the low collecting efficiency of
156 these interfering species in the sampling coil and their low concentrations, the combined
157 interference was estimated to be less than 10% of the total signal. Potential interference from
158 peroxyntic acid (HO₂NO₂) was suppressed by heating the PFA sampling line to 50 °C ~~with a~~
159 ~~residence time of 0.8 14 s~~. The HO₂NO₂ steady state concentration ([HO₂NO₂]_{ss}) was
160 estimated to be less than 1 pptv at temperatures of 20 - 30 °C in the background PBL
161 (Gierczak et al., 2005), and thus interference from HO₂NO₂ was negligible. Whereas in power
162 plant ~~plumes~~ and urban plumes in the PBL or biomass burning plumes in the upper free

163 troposphere (FT), HO₂NO₂ interference was not negligible and thus a correction for HONO
164 measurement was made. An upper-limit HO₂NO₂-to-HONO conversion response efficiency
165 in LPAP was estimated to be 0.2 for our HONO measurement systems. The estimation was
166 made from the lowest ratio of the observed measured [HONO] HONO to the
167 corresponding [HO₂NO₂]_{SS} in cold air masses at high altitude to the calculated [HO₂NO₂]_{SS},
168 assuming no HONO existed in the air mass. [HO₂NO₂]_{SS} refers to the steady state
169 concentration of HO₂NO₂-HONO measurements concentration were then corrected by
170 subtracting a term of “0.2 × [HO₂NO₂]_{SS}” to ensure that HO₂NO₂ interference did not lead to
171 an overestimate in our HONO measurement, assuming an upper limit HO₂NO₂-to-HONO
172 conversion efficiency of 0.2 in our system. [HO₂NO₂]_{SS} refers to the steady state
173 concentration of HO₂NO₂, and the upper limit HO₂NO₂-to-HONO conversion efficiency of
174 0.2 was estimated from the ratio of the observed [HONO] to the calculated [HO₂NO₂]_{SS} in
175 cold, high altitude air masses under our measurement conditions. In the PBL, the correction
176 was below 10% of the total signal measured HONO concentrations in the PBL plumes.
177 However, there may be over-corrections in the cold free troposphere, due to the temperature
178 of 20–30 °C and low levels of [HO₂NO₂]_{SS} in the PBL.

179 The lower detection limit of LPAP-HONO measurement was estimated to be ≤1 pptv,
180 based on 3 times the standard deviation of the zero air signal (N >10). An overall uncertainty
181 of ±(1 + 0.2 [HONO]) pptv was estimated, combining the uncertainties in signal acquisition
182 and processing, air and liquid flow rates, standard preparation, and baseline correction. The
183 accuracy of HONO measurements was confirmed by comparison with a limb-scanning
184 Differential Optical Absorption Spectroscopy (DOAS) (Platt and Stutz, 2008). The agreement
185 between these two instruments was very good in wide power plant plumes where HONO
186 mixing ratios significantly exceeded the detection limits of both instruments (Ye et al.,
187 2016b).

188 Particulate nitrate (pNO₃) was quantitatively collected with a frit disc sampler after a
189 NaCl-coated denuder to remove HNO₃ (Huang et al., 2002). The collected nitrate was reduced
190 to nitrite by a Cd column, and determined using a LPAP systems (Zhang et al., 2012). “Zero-
191 pNO₃” air was generated to establish measurement baselines for pNO₃ by passing the ambient
192 air through a Teflon filter to remove aerosol particles and then a NaCl-coated denuder to
193 remove aerosol particles and HNO₃ before reaching the sampling unit of LPAP. Potential
194 interferences from HONO, NO_x and PAN were corrected by subtracting the baselines from
195 the ambient air signals. The lower detection limit of pNO₃ was estimated to be 2 pptv, based

196 on 3 times the standard deviation of the zero air signal (N >10). An overall uncertainty of $\pm(2$
197 + 0.3 [pNO₃]) pptv was estimated.

198 Noisy baselines were observed when the C-130 was flying in the clouds, due to the
199 sampling of cloud droplets by our sampling systems. Because of the lack of a valid way to
200 correct for this interference, all in-cloud measurement data of HONO and pNO₃ have been
201 excluded from the data analysis.

202 **2.2- Supporting measurements**

203 The mixing ratios of a large number of non-methane organic compounds (NMOCs)
204 were measured by Trace Organic Gas Analyzer (TOGA) (Hornbrook et al., 2011a) and
205 Proton-transfer-reaction mass spectrometry (PTR-MS) (Karl et al., 2003; de Gouw and
206 Warneke, 2007). The surface area density of fine particles was obtained by the measurement
207 measured by of a Scanning Mobility Particle Sizer (SMPS), under the assumption of preface
208 sphere of aerosol particle. The photolysis frequencies were determined by a Charged-coupled
209 device Actinic Flux Spectroradiometer instrument (CAFS) (Shetter et al., 2002). The mixing
210 ratios of HO_x and RO₂ radicals were measured by a method based on selected-ion chemical-
211 ionization mass spectrometry (SICIMS) (Hornbrook et al., 2011b; Mauldin et al., 2010). The
212 mixing ratios of ozone and NO_x were measured by ~~NCAR's~~ chemiluminescence instruments
213 (Ridley et al., 2004). Meteorology parameters were provided by state parameter
214 measurements on board the C-130.

215 ~~The results from five out of nineteen flights are presented here to discuss vertical HONO~~
216 ~~distribution and HONO chemistry in the Southeast U.S. The flight tracks are shown in Figure~~
217 ~~4.~~

218 **3 Results and Discussion**

219 **3.1 General data description**

220 Figure 2 shows the time series of HONO, NO_x, pNO₃ concentrations and the measurement
221 altitude for five selected research flights in the Southeast U.S. during the NOMADSS 2013
222 summer field study. Research flight (RF) #4, RF #5 and RF #17 are race track flights in the
223 background terrestrial areas designed to establish HONO distribution and explore HONO
224 chemistry in background air masses. RF #11 is a race track flight designed to intercept plumes
225 from local power plants and urban areas and explore HONO chemistry therein. All four flights
226 were conducted in the daytime, roughly from 14:00 to 22:00 UTC (10:00 to 18:00 EDT). RF

227 #18 is a race track flight conducted from 20:30 on July 12th to 03:30 on July 13th UTC (16:30
228 ~~on July 12th to 00:23:30 on July 12th-13th~~, 2013 EDT), aiming to study the potential night-time
229 HONO accumulation both in the PBL and the FT.

230 Table 2 summarizes the data statistics for HONO, NO_x and pNO₃ measurements in the
231 PBL and the FT, and Figure 3 shows composite vertical distributions of HONO, NO_x and
232 pNO₃ concentrations from the five flights in the Southeast U.S. during the NOMADSS 2013
233 summer field study. HONO, NO_x and pNO₃ concentrations show horizontal gradients in every
234 race track flight and vary in different race track flights, reflecting the inhomogeneity of air
235 masses in the region. However, there was no significant vertical gradient in HONO, NO_x and
236 pNO₃ concentrations ~~is apparent~~, which will be further discussed below. Except in a few
237 power plant plumes and urban plumes mostly encountered in RF #11 ~~(labelled as A-G)~~, most
238 of the data is representative of background terrestrial air masses. The range of the mixing ratio
239 of HONO is ~~13.1 – 3534.94~~ pptv. The mean ($\pm 1SD$) and median values of HONO
240 concentration are ~~5.46 (± 33.44)~~ pptv and 4.2 pptv in the FT, and ~~11.22 (± 4.33)~~ pptv and
241 ~~10.63~~ pptv in the PBL. HONO levels at ~ 4 pptv are typically found in the background FT,
242 but high HONO concentrations up to ~~1815.2~~ pptv are also observed in the elevated biomass
243 burning plumes. ~~Many biomass burning plumes were observed during other flights and will be~~
244 ~~discussed in a future paper.~~ HONO levels at ~ 11 pptv are representative of background
245 conditions in the PBL. High HONO levels up to ~~3534.94~~ pptv are observed in the power
246 plant plumes and urban plumes in RF #11 ~~(see section 3.4) and RF # 17. The HONO~~
247 ~~distribution and chemistry in these urban and power plant plumes in the Southeast U.S. are~~
248 ~~specifically discussed below, in comparison with the results for background conditions (RF #~~
249 ~~4, #5, and #17).~~ These measured HONO values are consistent with the range of 4 – 74 pptv in
250 the troposphere over Northern Michigan (Zhang et al., 2009), but are significantly lower than
251 ~~other 100 airborne observations (up to 150 pptv)~~ in the morning residual layer over an
252 industrial region of Northern Italy (Li et al., 2014), where the levels of HONO precursors,
253 such as NO_x and pNO₃, were much higher. The HONO concentrations were also consistent
254 with the levels reported for the same region during the Southeast Nexus Experiment on the
255 NOAA WP-3D aircraft (Neuman et al., 2016), that is, “indistinguishable from zero within the
256 15 parts per trillion by volume measurement uncertainty” in the background air and up to 150
257 pptv in the power plant plumes during the day. The lower HONO concentrations measured in
258 the power plant plumes in ~~our~~ this study than the daytime values reported by Neuman et al
259 (2016) probably reflects greater dilution of smaller plumes encountered by the C-130 than by

260 the WP-3D, as indicated by much lower NO_x levels observed, up to 1.8 ppbv vs up to 60
261 ppbv.

262 The range of the mixing ratio of NO_x is from several pptv to around 1.8 ppbv. The
263 mean (± 1 SD) and median values of NO_x concentration are ~~96-94~~ (\pm ~~5253~~) pptv and 92 pptv
264 in the FT, and ~~313-316~~ (\pm ~~174182~~) pptv and ~~278-279~~ pptv in the PBL. The mixing ratios of
265 NO_x are mostly between 50 - 150 pptv in the background conditions in the FT and between
266 200 - 500 pptv in the background conditions in the PBL. Similar to HONO, high values of
267 NO_x also occur in the urban and power plant plumes in the PBL (up to ~~1.6-8~~ ppbv) and in the
268 biomass burning plumes in the FT (up to 0.6 ppbv).

269 Fewer measurement data points are available for pNO₃, compared to those for NO_x
270 and HONO, due to air bubble formation in the flow cell of the pNO₃ system, especially at
271 high altitudes. The range of the mixing ratio of pNO₃ is from ~~2-3~~ pptv to ~~216-186~~ pptv, with
272 the mean (± 1 SD) and median values of ~~28-35~~ (\pm ~~2539~~) pptv and ~~21-15~~ pptv in the FT, and
273 ~~78-76~~ (\pm ~~4745~~) pptv and ~~70-66~~ pptv in the PBL. The pNO₃ levels were highly variable in both
274 the FT and the PBL. In the FT, the pNO₃ levels were often under 10 pptv, but high
275 concentrations up to ~~115-179~~ pptv were also observed in elevated biomass burning plumes. In
276 the PBL, high pNO₃ levels were sometimes observed in relative clean conditions; whereas,
277 low pNO₃ levels were observed in high HONO and NO_x power plant plumes. Both the N(V)
278 level (= [HNO₃] + [pNO₃]) and the partitioning between HNO₃ and pNO₃ seem to play roles
279 in determining the pNO₃ level.

280 **3.2 HONO contribution from ground-level sources**

281 There are several ground-level HONO sources that may contribute to the HONO
282 budget in the overlying atmosphere. They include anthropogenic sources, such as power plant
283 and automobile emissions (Li et al., 2008b; [Neuman et al., 2016](#)), and natural processes, such
284 as soil emission (Maljanen et al., 2013; Oswald et al., 2013; Su et al., 2011), heterogeneous
285 reactions of NO₂ (Acker et al., 2006; George et al., 2005; Ndour et al., 2008, 2009; Ramazan
286 et al., 2006) and surface HNO₃ photolysis (Ye et al., 2016b; Zhou et al., 2003,2011). Since
287 HONO photolytic lifetime is relatively short, e.g. 8 - 16 min in RF #4, RF #5, RF #11 and RF
288 #17, a steep negative vertical gradient of HONO concentration would be expected if a
289 significant contribution originated from the ground. The lack of a significant vertical gradient
290 in the measured HONO concentrations (Fig. 3a) thus suggests that the ground contribution is
291 either limited to the shallow layer of the boundary layer near the ground, below the C-130

292 lowest flight altitude of 300 m, or small relative to the *in situ* production of HONO in the air
293 column (Ye et al., 2017).

294 To further examine the potential HONO contribution from the ground sources, vertical
295 profiles of HONO, NO_x, and pNO₃, are compared with those of potential temperature (K) and
296 isoprene measured, for example, in the first race-track of RF#4 from 11:00 – 12:15 LT (Fig.
297 4). ~~Indeed, the measurements conducted in the PBL height (H) was from 300 m to ~ 1200 m
298 were above the unstable surface layer,~~ as indicated by the constant potential temperature (Fig.
299 4e). The vertical distribution of isoprene originating from the ground can be expressed with
300 the following equation (Eq.1):

$$301 \quad \ln\left(\frac{C}{C_0}\right) = -\frac{k\tau}{H}h = -\frac{h}{h^*} \quad (\text{Eq. 1})$$

302 where, C_0 and C are its concentrations near the ground and at the altitude h , k is the pseudo-
303 first order degradation rate constant, ~~H is the boundary layer height,~~ τ is the average mixing
304 time in the PBL, and h^* ($= H/(k\tau)$) is its characteristic transport height within one degradation
305 lifetime of isoprene. According to the best fit of (Eq.1) to the observed isoprene data (Fig. 4d),
306 its characteristic transport height h^* is estimated 692 m for isoprene. Assuming isoprene is
307 mainly oxidized by the OH radical whose average concentration is estimated at 3×10^6 mole
308 cm^{-3} in the PBL (Kaser et al., 2015), the pseudo-first order degradation rate constant of ~
309 $3.0 \times 10^{-4} \text{ s}^{-1}$ (or the degradation rate of ~ 0.93 h^{-1}) is determined for isoprene. Based on a
310 boundary layer height of ~1.2 km (Fig. 4e), an average PBL mixing time τ is estimated to be
311 ~1.6 h between 11:00 – 12:15 LT of RF #4. With a photolytic lifetime of ~ 11 min for HONO,
312 about 11% of the HONO originated from the ground level is expected to reach the altitude
313 of 300 m, the lowest flight altitude of the C-130 aircraft between 11:00 – 12:15 LT in RF
314 #4. ~~the estimated characteristic transport height of ground surface HONO is 138 m between~~
315 ~~11:00 – 12:15 LT in RF #4, well below 300 m, the lowest flight altitude of the C-130 aircraft~~
316 ~~during this field study. Therefore, the instrument on board the C-130 would not detect the~~
317 ~~HONO contribution from the ground sources during this race-track profiling around~~
318 ~~noontime. However, it is interesting to note that there was a slight increase in HONO~~
319 ~~concentration at the two lowest altitudes (Fig. 4a), which may be attributed to the increasing~~
320 ~~concentrations of its potential precursors, NO_x and pNO₃ (Fig. 4b, c), both which are much~~
321 ~~longer lived than HONO.~~

322 ~~Apart from the rapid photolytic loss of HONO, the rate of vertical mixing plays an important~~
323 ~~role in limiting the transport height of HONO in the PBL.~~ The vertical mixing of the PBL is
324 enhanced from the morning to the afternoon, as the ground surface is heated by solar radiation

325 gradually during the day. The average mixing time in the PBL is reduced from ~ 3 h in the
326 morning, to ~ 1.5 h around noontime, and to ~ 30 min in the afternoon, determined from
327 isoprene gradients from RF #4, #5 and #17. ~~The characteristic transport height of HONO~~
328 ~~would be ~ 500 m in the afternoon, i.e., some~~ About 50% of the ground emitted HONO could
329 survive and be transported to lower measurement altitudes, ~~and. Again, if this ground source~~
330 ~~contribution was significant, the HONO concentration profile should exhibit~~ thus may be
331 ~~detected by our profile measurements~~ a significant gradient, probably more pronounced than
332 that of isoprene due to its shorter lifetime. The lack of such a vertical HONO gradient in the
333 measured HONO concentration profiles (Fig. 3a) suggests that ~~However,~~ the contribution
334 from ground HONO sources to the observed HONO concentrations in the PBL above 300 m
335 ~~appear to be~~ is limited ~~insignificant,~~ ~~as indicated by the lack of consistent vertical HONO~~
336 ~~gradient above the altitude of 300 m (Fig. 3a) in all the race track flights.~~

337 The NO_x level was ≤ 0.5 ppbv in the PBL over the Southeast U.S. (Figure 2),
338 excluding the power plant plumes. Based on an upper limit HONO/NO_x ratio of 0.05 for
339 urban atmosphere at ground level (Villena et al., 2011), the initial HONO concentration would
340 be ≤ 25 pptv in the source air mass on the ground level. With a transport time of ≥ 0.5 h,
341 i.e., ≥ 3 times of the HONO photolysis lifetime, the contribution from the ground HONO
342 source would be ≤ 1 pptv. This analysis supports the conclusion that contribution of surface
343 HONO source to the PBL HONO budget is insignificant.

345 3.3 Daytime HONO chemistry in low NO_x areas

346 After removing the data measured in the urban and power plant plumes, the daytime HONO
347 concentrations are ~~mostly~~ within the range of 5 - 15 pptv throughout the PBL in the
348 background terrestrial areas in the five race-track research flights. Photolysis ~~of HONO is its~~
349 ~~the~~ dominant sink for HONO, with a photolysis lifetime of 8 - 16 min during these four
350 daytime flights (RF #4, RF #5, RF #11, and RF #17). Therefore, there must be a significant
351 volume HONO source, up to ~~200-173~~ pptv h⁻¹, within the air mass to sustain the observed
352 HONO concentrations.

353 Both NO_x and pNO₃ are potential HONO precursors in the air column. ~~Figure 5 S1~~
354 ~~shows the correlation analysis of HONO with NO_x and pNO₃ in the background terrestrial air~~
355 ~~masses during the five flights.~~ While HONO correlates ~~relatively well~~ moderately with NO_x (r^2
356 = ~~0.5245, Fig S1~~), ~~with a fitted HONO/NO_x ratio around 0.04~~, it only weakly correlates with

357 pNO₃ (R² = 0.147) (Fig. 5). It may appear at first that NO_x is a more important HONO
 358 precursor than pNO₃. However, the detailed analysis below suggests that NO_x is only a minor
 359 precursor to the observed HONO, and photolysis of pNO₃ is the major *in situ* HONO source.

360 The upper limit of photo-stationary state HONO concentration ([HONO]_{pss}) was
 361 calculated using Equation 2 that takes into account all the known HONO source contributions
 362 from NO_x-related reactions, including gaseous reactions of OH and NO (R-1), excited NO₂
 363 (NO₂^{*}) and water vapor (R4) (Carr et al., 2009; Li et al., 2008a), NO₂ and the hydroperoxyl-
 364 water complex (HO₂·H₂O) with an upper limit HONO yield of 3% (R5a)(Li et al., 2014; Ye et
 365 al., 2015), and heterogeneous reaction of NO₂ on aerosol surfaces (R2) using an upper limit
 366 uptake coefficient of 10⁻⁴ reported in the literature (George et al., 2005; Monge et al., 2010;
 367 Ndour et al., 2008, 2009; Stemmler et al., 2006, 2007):

$$368 \quad [\text{HONO}]_{pss} = \frac{k_{-1}[\text{NO}][\text{OH}] + k_4[\text{NO}_2^*][\text{H}_2\text{O}] + \alpha k_5[\text{NO}_2\text{NO}_2^*][\text{HO}_2 \cdot \text{H}_2\text{O}] + k_2 S_{aerosol}[\text{NO}_2]}{J_{\text{HONO}} + k_{\text{OH-HONO}}[\text{OH}]} \quad (\text{Eq. 2})$$

370 where $S_{aerosol}$ is the aerosol surface area density. It should be noted that the upper limit values
 371 of rate constants were used in the calculation to avoid the underestimation of [HONO]_{pss}
 372 value. Under typical daytime conditions in the PBL with the median measured values of
 373 reactants, the upper limit [HONO]_{pss} value is less than 2 pptv, much lower than the median
 374 measured HONO concentration of ~ 11 pptv. Figure 65a shows the relationship (r² =
 375 0.443840) between the photolytic HONO loss rate with the sum of HONO production rates
 376 from all the NO_x-related reactions calculated with upper-limit reaction rate constants. A slope
 377 of about 0.19 indicates that the contribution from these NO_x-related reactions to the volume
 378 HONO source is minor in the background troposphere, despite the good correlation between
 379 HONO and NO_x. The high HONO/NO_x ratios up to 0.24 in the low-NO_x air masses are
 380 indicative of more important contributions from other HONO precursors, such as pNO₃.

381 Photolysis of HNO₃ on surfaces has been found to proceed at a much higher rate than
 382 in the gas phase (Baergen and Donaldson, 2013; Du and Zhu, 2011; Ramazan et al., 2004; Ye
 383 et al., 2016b; Zhou et al., 2003; Zhu et al., 2008), with HONO as the major product on
 384 environmental surfaces (Ye et al., 2016a, 2017). Furthermore, photolysis of particulate nitrate
 385 has been found to be the major daytime HONO source in the marine boundary layer (Ye et al.,
 386 2016b). To examine the role of particulate nitrate as a potential HONO source in the
 387 troposphere, aerosol samples over the terrestrial areas were collected and on Teflon
 388 filters on board the C-130 aircraft during the NOMADSS 2013 summer field study and were

389 used in the light-exposure experiments to determine the photolysis rate constants for
 390 particulate nitrate in the laboratory. The determined pNO₃ photolysis rate constant ($J_{pNO_3}^N$)
 391 varies over a wide range, from $8.3 \times 10^{-5} \text{ s}^{-1}$ to $3.1 \times 10^{-4} \text{ s}^{-1}$, with a median of $2.0 \times 10^{-4} \text{ s}^{-1}$
 392 and a mean (± 1 ~~standard deviation~~SD) of $1.9 (\pm 1.2) \times 10^{-4} \text{ s}^{-1}$, when normalized to tropical
 393 noontime conditions at ground level (solar zenith angle = 0°), and the average HONO to NO₂
 394 relative yield is 2.0 (Ye et al., 2017). Figure 6b shows the relationship between the photolytic
 395 HONO loss rate ($J_{HONO} \times [HONO]$) and the volume HONO production rates from pNO₃
 396 photolysis ($\frac{2}{3} \times J_{HNO_3} \times J_{pNO_3} \times [pNO_3]$). The median $J_{pNO_3}^N$ of $\sim 2.0 \times 10^{-4} \text{ s}^{-1}$ was used to
 397 calculate the ambient J_{pNO_3} by scaling to J_{HNO_3} :

$$398 \quad J_{pNO_3} = J_{pNO_3}^N \times \frac{J_{HNO_3}}{7.0 \times 10^{-7} \text{ s}^{-1}} \quad (\text{Eq. 3}),$$

399 where J_{HNO_3} is the photolysis rate constant of gas-phase HNO₃ calculated from light intensity
 400 measurement on the C-130 aircraft, and $7.0 \times 10^{-7} \text{ s}^{-1}$ is the photolysis rate constant of gas-
 401 phase HNO₃ under the tropical noontime condition at ground level (solar zenith angle = 0°). A
 402 slope of 0.697 can be derived from Figure 56b, suggesting that pNO₃ photolysis is the major
 403 volume HONO source. However, the r^2 of 0.3941 is not as strong as expected from pNO₃
 404 photolysis being the major volume HONO source. It may be in part due to the use of a single
 405 median $J_{pNO_3}^N$ value of $\sim 2.0 \times 10^{-4} \text{ s}^{-1}$ in the calculations of the ambient J_{pNO_3} and the
 406 production rates of HONO in Figure 5b; the actual $J_{pNO_3}^N$ values are highly variable, ranging
 407 from $8.3 \times 10^{-5} \text{ s}^{-1}$ to $3.1 \times 10^{-4} \text{ s}^{-1}$ (Ye et al., 2017). HONO source contribution from
 408 particulate nitrate photolysis—the fact that only a single median $J_{pNO_3}^N$ value of $\sim 2.0 \times 10^{-4} \text{ s}^{-1}$
 409 is used in the calculations of the ambient J_{pNO_3} and the production rates of HONO in Figure
 410 6b, while the actual pNO₃ photolysis rate constants determined from seven NOMADSS
 411 aerosol samples are highly variable, ranging from $8.3 \times 10^{-5} \text{ s}^{-1}$ to $3.1 \times 10^{-4} \text{ s}^{-1}$ (Ye et al.,
 412 2017). The production rates of HONO in Figure 56b are thus only rough estimates of the *in*
 413 situ HONO production rates from pNO₃ photolysis in different air masses.

414 HONO photolysis has been found to be an important or even a major OH primary
 415 source in the atmosphere near the ground surface (Elshorbany et al., 2010; He et al., 2006;
 416 Kleffmann et al., 2003; Villena et al., 2011; Zhou et al., 2011). However, HONO is not a
 417 significant daytime OH precursor in the background troposphere away from the ground
 418 surface. Based on the measurement results in this study, the mean (\pm SD) contribution of
 419 HONO photolysis to the OH source budget (mean \pm SD) is 52-53 (\pm 22-21) pptv h⁻¹ in the
 420 PBL and 28-44 (\pm 20-26) pptv h⁻¹ in the FT (Table S1), respectively, less than 10% of the OH

421 production contributed by O₃ photolysis. ~~However, s~~ Since HONO is mainly produced from
422 photolysis of particulate nitrate, it becomes an important intermediate product of a
423 photochemical renoxification process recycling nitric acid and nitrate back to NO_x. The
424 regenerating rate of NO_x of about ~~38 (± 23)~~ 52 pptv h⁻¹ via ~~HONO-pNO₃~~ photolysis (Table S1)
425 is equivalent to an air column NO_x source of ~ ~~232.3~~ ×10⁻⁶ mol m⁻² h⁻¹ in the 1.5- km PBL, a
426 considerable supplementary NO_x source in the low-NO_x background area.

It should be pointed out that particulate nitrate is in a dynamic equilibrium with gas-phase HNO₃, the later accounts for a larger (or even dominant) fraction of total nitrate (pNO₃+HNO₃) and is photochemically inert. The overall photolysis of pNO₃+HNO₃ would be much slower than indicated by J_{pNO₃}. In addition, oxidation of NO_x via several reactions will replenish the pNO₃+HNO₃ reservoir. The results reported here and in earlier papers (Reed et al., 2017; Ye et al., 2016a) suggest that there is a rapid cycling in reactive nitrogen species in the low-NO_x atmosphere, sustaining the observed levels of HONO and pNO₃.

434 3.4 HONO chemistry in plumes

435 One of the objectives of RF #11 was to study the chemistry of HONO in urban and coal fired
436 power plant plumes. The arrows and corresponding labels in Figures 2 ~~and 7~~ indicate the
437 urban plumes (~~A~~U1-U3 ~~C~~) and power plant plumes (~~D~~GPI-P4). CO and benzene were used to identify influence from urban plumes, SO₂ to identify influence from power plant plumes, and acetonitrile to identify the influence of biomass burning plumes (Fig. S2).
438 Benzene was used as the tracer of urban plumes (Liu et al., 2012; Shaw et al., 2015). ~~The~~
441 Benzene peaks were observed in all urban plumes (~~A~~U1-U3 ~~and C~~) ~~B~~ were identified as
442 urban plumes for benzene and CO, but not in the peaks from cities of Birmingham (U1, U3)
443 and Montgomery (U23) in Alabama, respectively, and power plant plumes (~~D~~ = ~~G~~CPI-P4
444 and ~~D~~) were identified as power plant plumes from power plants in Monroe county (P1-P3)
445 and Putman county (P4) in Georgia, respectively. The influence of biomass burning plumes
446 was negligible as acetonitrile concentration was low and stable. The power plant plumes were
447 generated from high-intensity point sources, and thus had features of narrow but high peaks of
448 both HONO and NO_x concentrations in the time-series plots (Figs. 2, 6 & S22, ~~S1~~ ~~and 7~~). In
449 contrast, the urban plumes were generated from area sources and thus were shown as broad
450 peaks of HONO and NO_x in the time-series plot with low levels of NO_x (mostly below 500
451 pptv) (Figs. 2, 6 & S12). There were a few sharp but small NO_x peaks within the broad urban
452 plumes, reflecting the contributions of some point sources in the urban areas. The observed

453 HONO/NO_x ratio was ~~around 0.02~~0.019 ($\pm 0.004\%$) in the power plant plumes (e.g., DP4)
454 ~~(P4)~~, and ~~lower than that of (0.057 ($\pm 1.9\%$))~~0.0019 in urban plumes ~~and in background~~
455 ~~terrestrial air masses~~, significantly higher than the typical HONO/NO_x emission ratio of
456 ~~~0.002 in the fresh power plant plumes (Neuman et al., 2016) and ≤ 0.01 in automobile~~
457 ~~exhaust (Kurtenbach et al., 2001; Li et al., 2008b). The elevated HONO/NO_x ratios observed~~
458 ~~in the plumes suggest that the observed HONO was mostly produced from precursors within~~
459 ~~the air mass during the transport.~~ Based on the distances between measurement locations from
460 the power plants or the ~~centres~~ of urban areas and ~~the observed~~ wind speed, the
461 transport times of these ~~power plant~~ plumes were estimated to be ≥ 1 h, ~~over~~ ~5 times longer
462 than HONO photolysis lifetime of 8 - 16 min, ~~again suggesting~~. Therefore, ~~that~~ most of the
463 observed HONO in the ~~power plant~~ plumes was produced *in situ* within the air masses. ~~Since~~
464 ~~the typical emission ratio of HONO/NO_x is less than 0.01 in the fresh power plant plumes and~~
465 ~~automobile engines (Kurtenbach et al., 2001; Li et al., 2008b), the elevated HONO/NO_x ratios~~
466 ~~observed in the plumes suggest the presence of other HONO precursors, such as pNO₃.~~

467 Figure 67b shows the time-series plot of HONO budgets within the air masses sampled
468 by the C-130 aircraft during flight RF# 11, comparing its photolysis loss rate with its
469 production rates from pNO₃ photolysis and from all the NO_x-related reactions combined.
470 Photolysis of particulate nitrate appears to be the major volume HONO source in all urban
471 plumes and in most of the power plant plumes except for plume G-DP4 observed here (Fig.
472 7b). NO_x was generally more important as a HONO precursor in the power plant plumes than
473 in the urban plumes and in low-NO_x background ~~terrestrial~~ air masses, due to higher levels of
474 NO_x (up to 1.6-8 ppb in Figs. 7a2c and 6S2), OH radical and aerosol surface density. For
475 example, all the NO_x-related reactions combined contributed up to 52% of the total volume
476 HONO source required to sustain the observed HONO concentration in plume G-P4 (Fig.
477 7b6). In fresh ~~and larger~~ power plant plumes encountered during the RF #7 to Ohio River
478 Valley (X. Zhou, unpublished data), over 20 ppb NO_x was detected, and the NO_x-related
479 reactions, ~~mainly the NO+OH reaction~~, were found to account for almost all the required
480 HONO source ~~strength~~ to sustain the observed HONO, ~~in agreement with~~ Neuman et al.
481 (2016). The power plant plumes undergo rapid physical and photochemical evolution during
482 the day, such as dilution and NO_x-~~into~~ HNO₃ conversion. Thus, the relative contributions
483 from NO_x-related reactions and particulate nitrate photolysis as HONO sources change rapidly
484 as the plumes age.

485 3.5 Night-time HONO chemistry

486 Nighttime HONO accumulation ~~near the ground surface during the nighttime~~ has been widely
487 observed at the ground level (Kleffmann et al., 2003; Oswald et al., 2015; 2008; Stutz et al.,
488 2002, 2010; VandenBoer et al., 2013, 2014, 2015), contributed by various anthropogenic and
489 natural HONO sources on the ground. The main objective of RF #18 was to study the night-
490 time HONO evolution in both the nocturnal residual layer and the nocturnal FT. After sunset,
491 the surface cooling promotes the formations of a inversion layer near the ground surface and a
492 nocturnal residual layer above; the contribution from ground HONO sources then becomes
493 negligible to the air masses beyond the surface inversion layer. Meanwhile, no effective
494 HONO sinks, such as photolysis, oxidation by OH and dry deposition, exist in the nocturnal
495 residual layer. Thus the HONO accumulation, if any, is a net contribution from dark
496 heterogeneous NO₂ reaction on aerosol surfaces (R2).

497 The C-130 flew in an elongated race track pattern along a north-south direction, about
498 140 km from Nashville, TN (Fig. 1), alternating between the PBL (1200 m) and the FT (2500
499 m), from late afternoon to midnight local time (Fig. 2). In the FT, HONO and NO_x
500 concentrations were relatively stable throughout the afternoon and the night, staying around 4
501 ppt and 90 pptv respectively. The lack of night-time HONO accumulation is expected from
502 the low levels of HONO precursors, mostly NO₂, and surface area of aerosol particles in the
503 FT (Fig. 2).

504 The conditions in the PBL were far more variable and complicated. There were strong
505 horizontal gradients of NO_x, pNO₃ and HONO in the PBL, with higher concentrations at the
506 southern end and lower concentrations at the northern end of the flight track. Back-trajectory
507 analysis using NOAA's HYSPLIT model (Stein et al., 2015) indicates that the encountered air
508 masses in the PBL at the southern end passed over Nashville, about 140 km northeast of the
509 sample area, with a transport time of about 6 h (Fig. ~~8a~~S233a), while the air masses at the
510 northern end stayed to north of Nashville (Fig. ~~8b~~S323b). Therefore, the anthropogenic
511 emissions from the metropolitan area of Nashville contributed to the higher concentrations of
512 pollutants observed at the southern end of the flight track. There were also trends of
513 increasing concentrations of NO_x, pNO₃ and HONO with time after the sunset (Fig. 2). This
514 was probably a result of less dispersion and dilution of anthropogenic pollutants, including
515 NO_x, as the PBL became more stable after sunset. Furthermore, as time progressed from late
516 afternoon into evening and night, the air masses were less photochemically aged during the

517 transport from the source areas, due to the decreasing solar light intensity and shorter solar
518 light exposure time.

519 Because of the large spatial and temporal variations in the concentrations of HONO and
520 its precursors in the PLB (Fig. 2), it is difficult to directly evaluate the nighttime HONO
521 accumulation from HONO measurements alone. The concentration ratio of HONO and its
522 dominant nighttime precursor, NO₂, can be used as an indicator of nighttime HONO
523 accumulation. As the air masses at measurement altitude of 1200 m decoupled from the
524 ground-level processes after sunset, the HONO production ($P(\text{HONO})$) from heterogeneous
525 NO₂ reaction (R2) on aerosol surface becomes the only HONO source, and can be expressed
526 by the following equations (Eq. 4 and Eq. 5):

$$527 \quad P(\text{HONO}) = \frac{1}{4} \times \left[\frac{s}{v} \right] \times \sqrt{\frac{8RT}{\pi M}} \times \gamma \times [\text{NO}_2] \quad (\text{Eq.4})$$

$$528 \quad \frac{P(\text{HONO})}{[\text{NO}_2]} = \frac{1}{4} \times \left[\frac{s}{v} \right] \times \sqrt{\frac{8RT}{\pi M}} \times \gamma \quad (\text{Eq.5})$$

529 where $\left[\frac{s}{v} \right]$ is the specific aerosol surface area density, R is the gas constant, K the absolute
530 temperature, M the molecular weight of NO₂, and γ is the dark uptake coefficient of NO₂
531 leading to HONO production. The NO₂-normalized HONO accumulation over time, $\Delta \frac{[\text{HONO}]}{[\text{NO}_2]}$,
532 can then be calculated by equation (Eq. 6):

$$533 \quad \Delta \frac{[\text{HONO}]}{[\text{NO}_2]} \sim \frac{1}{4} \times \left[\frac{s}{v} \right] \times \sqrt{\frac{8RT}{\pi M}} \times \gamma \times \Delta t \quad (\text{Eq. 6})$$

534 Assuming a dark uptake coefficient γ of 1×10^{-5} of NO₂ on aerosol (George et al., 2005;
535 Monge et al., 2010; Ndour et al., 2008; Stemmler et al., 2006, 2007) with a $\left[\frac{s}{v} \right]$ value of $\sim 10^{-4}$
536 m⁻¹, a relative HONO accumulation rate, $\Delta \frac{[\text{HONO}]}{[\text{NO}_2]} / \Delta t$ of $\sim 0.0003 \text{ h}^{-1}$ is estimated using the
537 equation (Eq. 6), equivalent to a HONO accumulation of 0.13 pptv hr⁻¹ at a constant NO₂
538 concentration of 400 pptv. Such a low HONO accumulation rate is below our measurement
539 detection limit. Indeed, the calculated HONO to the NO_x ratio using the measurement data
540 stayed almost unchanged with time (Fig. 97), well within the observational variability after
541 the sunset, suggesting no significant volume production of HONO in the nocturnal boundary
542 layer.

543 **4 Conclusions**

544 Substantial levels of HONO existed during the day in both the PBL (median ~ 11 pptv) and
545 the FT (median ~ 4 pptv) over the Southeast U.S. during the NOMADSS 2013 summer field

546 study. ~~It appears that~~ The ground HONO sources did not significantly contribute to the
547 HONO budget in the PBL above the minimum measurement heights of 300 m. HONO
548 budget analysis suggests that photolysis of particulate nitrate was the major volume HONO
549 source (~69%)~~in the low NO_x background air masses~~, while the sum of known NO_x-related
550 reactions a minor HONO source (~19% \leq 20%) in the low-NO_x background air masses.
551 HONO was not a significant daytime OH precursor in the ~~rural troposphere~~PBL away from
552 the ground surface; however, HONO ~~mainly produced from~~was an important intermediate
553 product of photolysis of particulate nitrate ~~could significant provide in a the~~ renoxification
554 pathway process. Up to several tens pptv of HONO were observed in ~~coal-fired~~ power plant
555 plumes and urban plumes during the day; ~~the major HONO precursor could be either, mostly~~
556 produced in situ from precursors including NO_x ~~or and~~ pNO₃ ~~depending on the chemical~~
557 ~~characteristics and photochemical age of the plumes. Na.~~ No significant night-time HONO
558 accumulation was observed in the nocturnal residual layer and the free troposphere,
559 ~~suggesting no significant night time volume HONO source~~ due to low levels of NO_x and
560 specific aerosol surface area.

561

562 **Acknowledgements**

563 This research is funded by National Science Foundation (NSF) grants (AGS-1216166, AGS-
564 1215712, and AGS-1216743). We would like to acknowledge operational, technical, and
565 scientific support provided by NCAR, sponsored by the National Science Foundation. The
566 data are available in our project data archive
567 (http://data.eol.ucar.edu/master_list/?project=SAS). Any opinions, findings, and conclusions
568 or recommendations expressed in this paper are those of the authors and do not necessarily
569 reflect the views of NSF.

570

571 **References**

572 Acker, K., Moller, D., Wieprecht, W., Meixner, F. X., Bohn, B., Gilge, S., Plass-Dulmer, C.,
573 and Berresheim, H.: Strong daytime production of OH from HNO₂ at a rural mountain site,
574 Geophys. Res. Lett., 33, Artn L02809, 10.1029/2005gl024643, 2006.
575 Baergen, A. M., and Donaldson, D. J.: Photochemical renoxification of nitric acid on real
576 urban grime, Environ. Sci. Technol., 47, 815-820, 10.1021/es3037862, 2013.

577 Burling, I. R., Yokelson, R. J., Griffith, D. W. T., Johnson, T. J., Veres, P., Roberts, J. M.,
578 Warneke, C., Urbanski, S. P., Reardon, J., Weise, D. R., Hao, W. M., and de Gouw, J.:
579 Laboratory measurements of trace gas emissions from biomass burning of fuel types from
580 the southeastern and southwestern United States, *Atmos. Chem. Phys.*, 10, 11115-11130,
581 2010.

582 Carr, S., Heard, D. E., and Blitz, M. A.: Comment on "Atmospheric hydroxyl radical
583 production from electronically excited NO₂ and H₂O", *Science*, 324, 2009.

584 de Gouw, J., and Warneke, C.: Measurements of volatile organic compounds in the earths
585 atmosphere using proton-transfer-reaction mass spectrometry, *Mass Spectrom. Rev.*, 26,
586 223-257, 2007.

587 Du, J., and Zhu, L.: Quantification of the absorption cross sections of surface-adsorbed nitric
588 acid in the 335-365 nm region by Brewster angle cavity ring-down spectroscopy, *Chem.*
589 *Phys. Lett.*, 511, 213-218, 10.1016/j.cplett.2011.06.062, 2011.

590 Elshorbany, Y. F., Kleffmann, J., Kurtenbach, R., Lissi, E., Rubio, M., Villena, G., Gramsch,
591 E., Rickard, A. R., Pilling, M. J., and Wiesen, P.: Seasonal dependence of the oxidation
592 capacity of the city of Santiago de Chile, *Atmos. Environ.*, 44, 5383-5394,
593 10.1016/j.atmosenv.2009.08.036, 2010.

594 Finlayson-Pitts, B. J., and J. N. Pitts, Jr.: *Chemistry of the Upper and Lower Atmosphere:*
595 *Theory, Experiments, and Applications*, Academic Press, San Diego, California, 2000.

596 Flagan, R. C.: Electrical mobility methods for sub-micrometer particle characterization. In
597 *Aerosol Measurement: Principles, Techniques, and Applications*, Third Edition (eds P.
598 Kulkarni, P. A. Baron and K. Willeke), pp339-364, John Wiley & Sons, New York, 2002.

599 George, C., Strekowski, R. S., Kleffmann, J., Stemmler, K., and Ammann, M.:
600 Photoenhanced uptake of gaseous NO₂ on solid-organic compounds: a photochemical
601 source of HONO?, *Faraday Discuss.*, 130, 195-210, 2005.

602 Gierczak, T., Jimenez, E., Riffault, V., Burkholder, J. B., and Ravishankara, A. R.: Thermal
603 decomposition of HO₂NO₂ (peroxynitric acid, PNA): Rate coefficient and determination of
604 the enthalpy of formation, *J. Phys. Chem. A*, 109, 586-596, 2005.

605 ~~Handley, S. R., Clifford, D., and Donaldson, D. J.: Photochemical loss of nitric acid on~~
606 ~~organic films: A possible recycling mechanism for NO_x, *Environ. Sci. Technol.*, 41, 3898-~~
607 ~~3903, 10.1021/es062044z, 2007.~~

608 He, Y., Zhou, X. L., Hou, J., Gao, H. L., and Bertman, S. B.: Importance of dew in controlling
609 the air-surface exchange of HONO in rural forested environments, *Geophys. Res. Lett.*, **33**,
610 2006.

611 Hornbrook, R. S., Blake, D. R., Diskin, G. S., Fried, A., Fuelberg, H. E., Meinardi, S.,
612 Mikoviny, T., Richter, D., Sachse, G. W., Vay, S. A., Walega, J., Weibring, P.,
613 Weinheimer, A. J., Wiedinmyer, C., Wisthaler, A., Hills, A., Riemer, D. D., and Apel, E.
614 C.: Observations of nonmethane organic compounds during ARCTAS - Part 1: Biomass
615 burning emissions and plume enhancements, *Atmos. Chem. Phys.*, **11**, 11103-11130,
616 2011a.

617 Hornbrook, R. S., Crawford, J. H., Edwards, G. D., Goyea, O., Mauldin, R. L., Olson, J. S.,
618 and Cantrell, C. A.: Measurements of tropospheric HO₂ and RO₂ by oxygen dilution
619 modulation and chemical ionization mass spectrometry, *Atmos. Meas. Tech.*, **4**, 735-756,
620 2011b.

621 Huang, G., Zhou, X., Deng, G., Qiao, H., and Civerolo, K.: Measurements of atmospheric
622 nitrous acid and nitric acid, *Atmos. Environ.*, **36**, 2225-2235, 2002.

623 Kaser, L., Karl, T., Yuan, B., Mauldin, R. L. III, Cantrell, C. A., Guenther, A. B., Patton, E.
624 G., Weinheimer, A. J., Knote, C., Orlando, J., Emmons, L., Apel, E., Hornbrook, Shertz,
625 R., S., Ullmann, K., Hall, S., Graus, M., de Gouw, J., Zhou, X., and Ye, C.: chemistry-
626 turbulence interactions and mesoscale variability influence the cleansing efficiency of the
627 atmosphere, *Geophys. Res. Lett.*, **42**, doi:10.1002/2015GL066641, 2015.

628 Karl, T., Jobson, T., Kuster, W.C., Williams, E., Stutz, J., Shetter, R., Hall, S.R., Goldan, P.,
629 Fehsenfeld, F., and W. Lindinger, W.: The use of Proton-Transfer-Reaction Mass
630 Spectrometry to Characterize VOC Sources at the La Porte Super Site during the Texas Air
631 Quality Study 2000, *J. Geophys. Res.*, **108**, doi: 10.1029/2002JD003333, 2003.

632 Kleffmann, J., Kurtenbach, R., Lorzer, J., Wiesen, P., Kalthoff, N., Vogel, B., and Vogel, H.:
633 Measured and simulated vertical profiles of nitrous acid - Part I: Field measurements,
634 *Atmos. Environ.*, **37**, 2949-2955, 2003.

635 Kleffmann, J.: Daytime sources of nitrous acid (HONO) in the atmospheric boundary layer,
636 *Chemphyschem*, **8**, 1137-1144, 10.1002/cphc.200700016, 2007.

637 Kurtenbach, R., Becker, K. H., Gomes, J. A. G., Kleffmann, J., Lorzer, J. C., Spittler, M.,
638 Wiesen, P., Ackermann, R., Geyer, A., and Platt, U.: Investigations of emissions and
639 heterogeneous formation of HONO in a road traffic tunnel, *Atmos. Environ.*, **35**, 3385-
640 3394, Doi 10.1016/S1352-2310(01)00138-8, 2001.

641 Li, S. P., Matthews, J., and Sinha, A.: Atmospheric hydroxyl radical production from
642 electronically excited NO₂ and H₂O, *Science*, 319, 1657-1660, 2008a.

643 Li, X., Rohrer, F., Hofzumahaus, A., Brauers, T., Haseler, R., Bohn, B., Broch, S., Fuchs, H.,
644 Gomm, S., Holland, F., Jager, J., Kaiser, J., Keutsch, F. N., Lohse, I., Lu, K. D., Tillmann,
645 R., Wegener, R., Wolfe, G. M., Mentel, T. F., Kiendler-Scharr, A., and Wahner, A.:
646 Missing gas-phase source of HONO inferred from Zeppelin measurements in the
647 troposphere, *Science*, 344, 292-296, 2014.

648 Li, Y. Q., Schwab, J. J., and Demerjian, K. L.: Fast time response measurements of gaseous
649 nitrous acid using a tunable diode laser absorption spectrometer: HONO emission source
650 from vehicle exhausts, *Geophys. Res. Lett.*, 35, 2008b.

651 ~~[Liu, W., Hsieh, H., Chen, S., Chang, J.S., Lin, N., Chang, C., and Wang, J.: Diagnosis of air](#)~~
652 ~~[quality through observation and modeling of volatile organic compounds \(VOCs\) as](#)~~
653 ~~[pollution tracers. *Atmos. Environ.*, 55, 56-63, 2012.](#)~~

654 Maljanen, M., Yli-Pirila, P., Hytonen, J., Joutsensaari, J., and Martikainen, P. J.: Acidic
655 northern soils as sources of atmospheric nitrous acid (HONO), *Soil. Biol. Biochem.*, 67,
656 94-97, 10.1016/j.soilbio.2013.08.013, 2013.

657 Mauldin, R., Kosciuch, E., Eisele, F., Huey, G., Tanner, D., Sjostedt, S., Blake, D., Chen, G.,
658 Crawford, J., and Davis, D.: South Pole Antarctica observations and modeling results: New
659 insights on HO_x radical and sulfur chemistry, *Atmos. Environ.*, 44, 572-581, 2010.

660 Monge, M. E., D'Anna, B., Mazri, L., Giroir-Fendler, A., Ammann, M., Donaldson, D. J., and
661 George, C.: Light changes the atmospheric reactivity of soot, *P. Natl. Acad. Sci. USA*, 107,
662 6605-6609, 2010.

663 Ndour, M., D'Anna, B., George, C., Ka, O., Balkanski, Y., Kleffmann, J., Stemmler, K., and
664 Ammann, M.: Photoenhanced uptake of NO₂ on mineral dust: Laboratory experiments and
665 model simulations, *Geophys. Res. Lett.*, 35, 2008.

666 Ndour, M., Nicolas, M., D'Anna, B., Ka, O., and George, C.: Photoreactivity of NO₂ on
667 mineral dusts originating from different locations of the Sahara desert, *Phys. Chem. Chem.*
668 *Phys.*, 11, 1312-1319, 2009.

669 ~~[Neuman, J.A., Trainer, M., Brown, S.S., Min, K.-E., Nowak, J.B., Parrish, D.D., Peischl, J.,](#)~~
670 ~~[Pollack, I.B., Roberts, J.M., Ryerson, T.B., and Veres, P.R.: HONO emission and](#)~~
671 ~~[production determined from airborne measurements over the Southeast U.S., *J. Geophys.*](#)~~
672 ~~[Res.-Atmos., 121, 9237-9250, 2016.](#)~~

673 Oswald, R., Behrendt, T., Ermel, M., Wu, D., Su, H., Cheng, Y., Breuninger, C., Moravek,
674 A., Mougín, E., Delon, C., Loubet, B., Pommerening-Roser, A., Sorgel, M., Poschl, U.,
675 Hoffmann, T., Andreae, M. O., Meixner, F. X., and Trebs, I.: HONO emissions from soil
676 bacteria as a major source of atmospheric reactive nitrogen, *Science*, 341, 1233-1235,
677 10.1126/science.1242266, 2013.

678 Oswald, R., Ermel, M., Hens, K., Novelli, A., Ouwersloot, H. G., Paasonen, P., Petaja, T.,
679 Sipila, M., Keronen, P., Back, J., Konigstedt, R., Beygi, Z. H., Fischer, H., Bohn, B.,
680 Kubistin, D., Harder, H., Martinez, M., Williams, J., Hoffmann, T., Trebs, I., and Sorgel,
681 M.: A comparison of HONO budgets for two measurement heights at a field station within
682 the boreal forest in Finland, *Atmos. Chem. Phys.*, 15, 799-813, 10.5194/acp-15-799-2015,
683 2015.

684 Platt, U., and Stutz, J.: *Differential Optical Absorption Spectroscopy: Principles and*
685 *Applications*, Springer, Berlin., 2008.

686 Ramazan, K. A., Syomin, D., and Finlayson-Pitts, B. J.: The photochemical production of
687 HONO during the heterogeneous hydrolysis of NO₂, *Phys. Chem. Chem. Phys.*, 6, 3836-
688 3843, 10.1039/b402195a, 2004.

689 Ramazan, K. A., Wingen, L. M., Miller, Y., Chaban, G. M., Gerber, R. B., Xantheas, S. S.,
690 and Finlayson-Pitts, B. J.: New experimental and theoretical approach to the heterogeneous
691 hydrolysis of NO₂: Key role of molecular nitric acid and its complexes, *J. Phys. Chem. A*,
692 110, 6886-6897, 10.1021/jp056426n, 2006.

693 Reed, C., Evans, M.J., Crilley, L.R., Bloss, W.J., Sherwen, T., Read, K.A., Lee, J.D., and
694 Carpenter, L.J.: Evidence for renoxification in the tropical marine boundary layer, *Atmos.*
695 *Chem. Phys.*, 17, 4081–4092, 2017.

696 Ridley, B., Ott, L., Pickering, K., Emmons, L., Montzka, D., Weinheimer, A., Knapp, D.,
697 Grahek, F., Li, L., Heymsfield, G., McGill, M., Kucera, P., Mahoney, M. J., Baumgardner,
698 D., Schultz, M., and Brasseur, G.: Florida thunderstorms: A faucet of reactive nitrogen to
699 the upper troposphere, *J. Geophys. Res.-Atmos.*, 109, 2004.

700 ~~Shaw, M. D., Lee, J. D., Davison, B., Vaughan, A., Purvis, R. M., Harvey, A.; Lewis, A. C.,~~
701 ~~and Hewitt, C. N.: Airborne determination of the temporo-spatial distribution of benzene,~~
702 ~~toluene, nitrogen oxides and ozone in the boundary layer across Greater London, UK.~~
703 ~~*Atmos. Chem. Phys.*, 15, 5083–5097, 2015.~~

704 Shetter, R. E., Cinquini, L., Lefer, B. L., Hall, S. R., and Madronich, S.: Comparison of
705 airborne measured and calculated spectral actinic flux and derived photolysis frequencies
706 during the PEM Tropics B mission, *J. Geophys. Res.-Atmos.*, 108, 2002.

707 Stemmler, K., Ammann, M., Donders, C., Kleffmann, J., and George, C.: Photosensitized
708 reduction of nitrogen dioxide on humic acid as a source of nitrous acid, *Nature*, 440, 195-
709 198, 10.1038/nature04603, 2006.

710 Stemmler, K., Ndour, M., Elshorbany, Y., Kleffmann, J., D'Anna, B., George, C., Bohn, B.,
711 and Ammann, M.: Light induced conversion of nitrogen dioxide into nitrous acid on
712 submicron humic acid aerosol, *Atmos. Chem. Phys.*, 7, 4237-4248, 2007.

713 Stein, A. F., Draxler, R. R., Rolph, G. D., Stunder, B. J. B., Cohen, M. D., and Ngan, F.:
714 NOAA's HYSPLIT atmospheric transport and dispersion modeling system. *Bul. Amer.*
715 *Meteorol. Soc.*, 96, 2059-2077, 10.1175/BAMS-D-14-00110.1, 2015.

716 Stutz, J., Alicke, B., and Neftel, A.: Nitrous acid formation in the urban atmosphere: Gradient
717 measurements of NO₂ and HONO over grass in Milan, Italy, *J. Geophys. Res.-Atmos.*,
718 107, Artn 8192,10.1029/2001jd000390, 2002.

719 Stutz, J., Oh, H. J., Whitlow, S. I., Anderson, C., Dibbb, J. E., Flynn, J. H., Rappengluck, B.,
720 and Lefer, B.: Simultaneous DOAS and mist-chamber IC measurements of HONO in
721 Houston, TX, *Atmos. Environ.*, 44, 4090-4098, 2010.

722 Su, H., Cheng, Y. F., Oswald, R., Behrendt, T., Trebs, I., Meixner, F. X., Andreae, M. O.,
723 Cheng, P., Zhang, Y., and Poschl, U.: Soil Nitrite as a Source of Atmospheric HONO and
724 OH Radicals, *Science*, 333, 1616-1618, 10.1126/science.1207687, 2011.

725 Trentmann, J., Andreae, M. O., and Graf, H. F.: Chemical processes in a young biomass-
726 burning plume, *J. Geophys. Res.-Atmos.*, 108, 2003.

727 VandenBoer, T. C., Brown, S. S., Murphy, J. G., Keene, W. C., Young, C. J., Pszenny, A. A.
728 P., Kim, S., Warneke, C., de Gouw, J. A., Maben, J. R., Wagner, N. L., Riedel, T. P.,
729 Thornton, J. A., Wolfe, D. E., Dube, W. P., Ozturk, F., Brock, C. A., Grossberg, N., Lefer,
730 B., Lerner, B., Middlebrook, A. M., and Roberts, J. M.: Understanding the role of the
731 ground surface in HONO vertical structure: High resolution vertical profiles during
732 NACHTT-11, *J. Geophys. Res.-Atmos.*, 118, 10155-10171, 2013.

733 VandenBoer, T. C., Markovic, M. Z., Sanders, J. E., Ren, X., Pusede, S. E., Browne, E. C.,
734 Cohen, R. C., Zhang, L., Thomas, J., Brune, W. H., and Murphy, J. G.: Evidence for a
735 nitrous acid (HONO) reservoir at the ground surface in Bakersfield, CA, during CalNex
736 2010, *J. Geophys. Res.-Atmos.*, 119, 9093-9106, 10.1002/2013JD020971, 2014.

737 VandenBoer, T. C., Young, C. J., Talukdar, R. K., Markovic, M. Z., Brown, S. S., Roberts, J.
738 M., and Murphy, J. G.: Nocturnal loss and daytime source of nitrous acid through reactive
739 uptake and displacement, *Nature Geosci.*, 8, 55-60, 2015.

740 [VandenBoer, T.C., Brown, S.S., Murphy, J.G., Keene, W.C., Young, C.J., Pszenny, A.A.P.,](#)
741 [Kim, S., Warneke, C., Gouw, Joost de, Maben, J.R., Wagner, N.L., Riedel, T.P., Thornton,](#)
742 [J.A., Wolfe, D.E., Dube, W.P., Ozturk, F., Brock, C.A., Grossberg, N., Lefer, B., Lerner,](#)
743 [B., Middlebrook, A.M., and Roberts, J.M.: Understanding the role of the ground surface in](#)
744 [HONO vertical structure: High resolution vertical profiles during NACHTT-11, J.](#)
745 [Geophys. Res.-Atmos.](#), 118, 10,155–10,171, doi:10.1002/jgrd.50721, 2013.

746

747 Villena, G., Kleffmann, J., Kurtenbach, R., Wiesen, P., Lissi, E., Rubio, M. A., Croxatto, G.,
748 and Rappengluck, B.: Vertical gradients of HONO, NO_x and O₃ in Santiago de Chile,
749 *Atmos. Environ.*, 45, 3867-3873, 2011.

750 Wong, K. W., Oh, H. J., Lefer, B. L., Rappengluck, B., and Stutz, J.: Vertical profiles of
751 nitrous acid in the nocturnal urban atmosphere of Houston, TX, *Atmos. Chem. Phys.*, 11,
752 3595-3609, 2011.

753 Wong, K. W., Tsai, C., Lefer, B., Haman, C., Grossberg, N., Brune, W. H., Ren, X., Luke,
754 W., and Stutz, J.: Daytime HONO vertical gradients during SHARP 2009 in Houston, TX,
755 *Atmos. Chem. Phys.*, 12, 635-652, 2012.

756 Wong, K. W., Tsai, C., Lefer, B., Grossberg, N., and Stutz, J.: Modeling of daytime HONO
757 vertical gradients during SHARP 2009, *Atmos. Chem. Phys.*, 13, 3587-3601, 2013.

758 [Wu, C., and Yu, J.Z.: Evaluation of linear regression techniques for atmospheric applications:](#)
759 [the importance of appropriate weighting, *Atmos. Meas. Tech.*, 11, 1233–1250, 2018.](#)

760 Ye, C. X., Zhou, X. L., Pu, D., Stutz, J., Festa, J., Spolaor, M., Cantrell, C., Mauldin, R. L.,
761 Weinheimer, A., and Haggerty, J.: Comment on "Missing gas-phase source of HONO
762 inferred from Zeppelin measurements in the troposphere", *Science*, 348,
763 10.1126/science.aaa1992, 2015.

764 Ye, C. X., Gao, H. L., Zhang, N., and Zhou, X.: Photolysis of nitric Acid and nitrate on
765 natural and artificial surfaces, *Environ. Sci. Technol.*, 50, 3530-3536, 2016a.

766 Ye, C. X., Zhou, X. L., Pu, D., Stutz, J., Festa, J., Spolaor, M., Tsai, C., Cantrell, C., Mauldin,
767 R. L., Campos, T., Weinheimer, A., Hornbrook, R. S., Apel, E. C., Guenther, A., Kaser, L.,
768 Yuan, B., Karl, T., Haggerty, J., Hall, S., Ullmann, K., Smith, J. N., Ortega, J., and Knote,

769 C.: Rapid cycling of reactive nitrogen in the marine boundary layer, *Nature*, 532, 489-491,
770 2016b.

771 Ye, C., Zhang, N., Gao, H., and Zhou, X.: Photolysis of particulate nitrate as a source of
772 HONO and NO_x, *Environ Sci Technol*, DOI: 10.1021/acs.est.7b00387, 2017.

773 [Young, C.J., Washenfelder, R.A., Roberts, J.M., Mielke, L.H., Osthoff, H.D., Tsai, C.,](#)
774 [Pikelnaya, O., Stutz, J., Veres, P.R., Cochran, A.K., VandenBoer, T.C., Flynn, J.,](#)
775 [Grossberg, N., Haman, C.L., Lefer, B., Stark, B., Martin, G., Gouw, Joost de., Gilman, J.B.,](#)
776 [Kuster, W.C., and Brown, S.S.: Vertically Resolved Measurements of Nighttime Radical](#)
777 [Reservoirs in Los Angeles and Their Contribution to the Urban Radical Budget, *Environ.*](#)
778 [Sci. Technol.](#), 46 (20), 10965–10973, 2012.

779 Zhang, N., Zhou, X., Shepson, P. B., Gao, H., Alaghmand, M., and Stirm, B.: Aircraft
780 measurement of HONO vertical profiles over a forested region, *Geophys. Res. Lett.*, 36,
781 Artn L15820,10.1029/2009gl038999, 2009.

782 Zhang, N., Zhou, X., Bertman, S., Tang, D., Alaghmand, M., Shepson, P. B., and Carroll, M.
783 A.: Measurements of ambient HONO concentrations and vertical HONO flux above a
784 northern Michigan forest canopy, *Atmos. Chem. Phys.*, 12, 8285-8296, 2012.

785 Zhou, X., Civerolo, K., Dai, H., Huang, G., Schwab, J., and Demerjian, K.: Summertime
786 nitrous acid chemistry in the atmospheric boundary layer at a rural site in New York State,
787 *J. Geophys. Res.*, 107, doi:10.1029/2001JD001539, 2002.

788 Zhou, X., Gao, H., He, Y., Huang, G., Bertman, S. B., Civerolo, K., and Schwab, J.: Nitric
789 acid photolysis on surfaces in low-NO_x environments: Significant atmospheric
790 implications, *Geophys. Res. Lett.*, 30, Artn 2217,10.1029/2003gl018620, 2003.

791 Zhou, X., Zhang, N., TerAvest, M., Tang, D., Hou, J., Bertman, S., Alaghmand, M., Shepson,
792 P. B., Carroll, M. A., Griffith, S., Dusanter, S., and Stevens, P. S.: Nitric acid photolysis on
793 forest canopy surface as a source for tropospheric nitrous acid, *Nature Geosci.*, 4, 440-443,
794 10.1038/NGEO1164, 2011.

795 Zhu, C. Z., Xiang, B., Zhu, L., and Cole, R.: Determination of absorption cross sections of
796 surface-adsorbed HNO(3) in the 290-330 nm region by Brewster angle cavity ring-down
797 spectroscopy, *Chem. Phys. Lett.*, 458, 373-377, 2008.

798
799

800 Table 1. Measurements from the NOMADSS 2013 summer study used in this analysis.

Parameters	Instrument	Time Resolution	Detection Limit	Accuracy	References
HONO	LPAP	200 s	1 pptv	20%	(1, 2)
pNO₃	LPAP	360 s	2 pptv	30%	(1, 2, 3)
HNO₃	LPAP	20 min	2 pptv	30%	(1, 2, 3)
NO	CI	1 s	20 pptv	10%	(4)
NO₂	CI	1 s	40 pptv	15%	(4)
O₃	CI	1 s	100 pptv	5%	(4)
OH	SICIMS	30 s	*5×10 ⁴	30%	(5, 6)
HONO	DOAS	60 s	~ 30 pptv	20%	(7)
Photolysis Frequencies	CAFS	6 s		10-15%	(8)
Surface area density	SMPS/UHSAS	65 s/1 s		20%	(9)
VOCs	PTRMS	15 s		20%	(10, 11)
VOCs/organic nitrates	TOGA	20 s		20%	(12)

801 *in molecules cm⁻³

802 LPAP: long-path absorption photometric (LPAP) systems

803 CI: 4-channel chemiluminescence instrument

804 SICIMS: selected-ion chemical-ionization mass spectrometer

805 DOAS: Differential Optical Absorption Spectroscopy

806 CAFS: Charged-coupled device Actinic Flux Spectroradiometer

807 SMPS: Scanning Mobility Particle Sizer

808 UHSAS: Ultra-High Sensitivity Aerosol Spectrometer

809 PTRMS: Proton Transfer Reaction Mass Spectrometry

810 TOGA: Trace Organic Gas Analyzer

811 References: (1) Zhang et al., 2012; (2) Ye et al., 2016b; (3) Huang et al., 2002; (4) Ridley et

812 al., 2004; (5) Hornbrook et al., 2011b; (6) Mauldin et al., 2010; (7) Platt and Stutz, 2008;

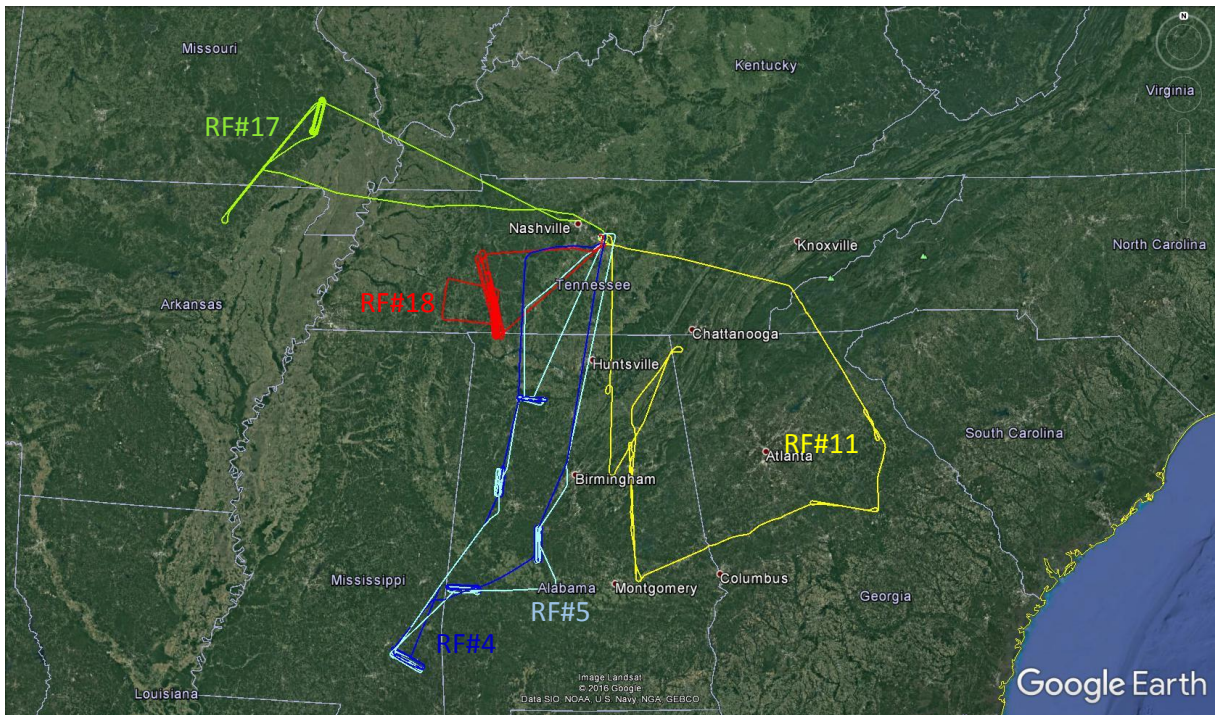
813 (8) Shetter et al., 2002; (9) Flagan, 2011; (10) Karl et al., 2003; (11) de Gouw and

814 Warneke, 2007; (12) Hornbrook et al., 2011a.

815 Table 2. Data statistics for HONO, NO_x and pNO₃ measurements both in the PBL and the FT
 816 from the five Southeast U.S. research flights during the NOMADSS 2013 summer field study.
 817 The statistics analysis is based on 1-min NO_x data, 3-min HONO data and 6-min pNO₃ data.
 818

		HONO, pptv	NO_x, pptv	pNO₃, pptv
PBL	Range	3.1 – 34.4 (n=356)	81 – 1774 (N=904)	9 – 186 (N=121)
	Mean ± (SD)	11.2 ± 4.3	316 ± 182	76 ± 45
	<u>Median</u>	<u>10.3</u>	<u>279</u>	<u>66</u>
	<u>Median</u> N	<u>10.3</u> <u>356</u>	<u>279</u> <u>904</u>	<u>66</u> <u>121</u>
FT	Range	1.3 - 15.2 (N=157)	<10 – 582 (N=655)	3 – 179 (N=46)
	Mean (±_SD)	5.6 ± 3.4	94 ± 53	35 ± 39
	<u>Median</u>	<u>4.2</u>	<u>92</u>	<u>15</u>
	<u>Median</u> N	<u>4.2</u> <u>157</u>	<u>92</u> <u>655</u>	<u>15</u> <u>46</u>

819
820

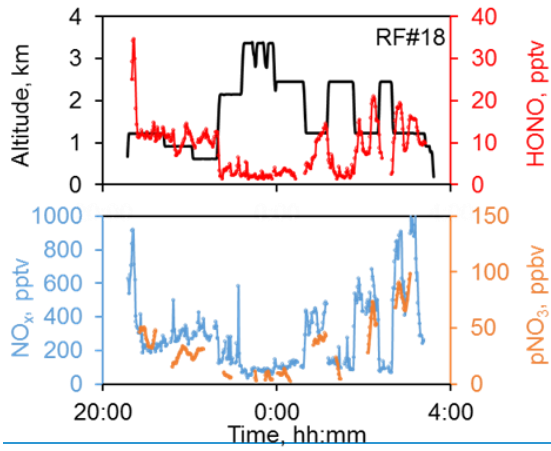
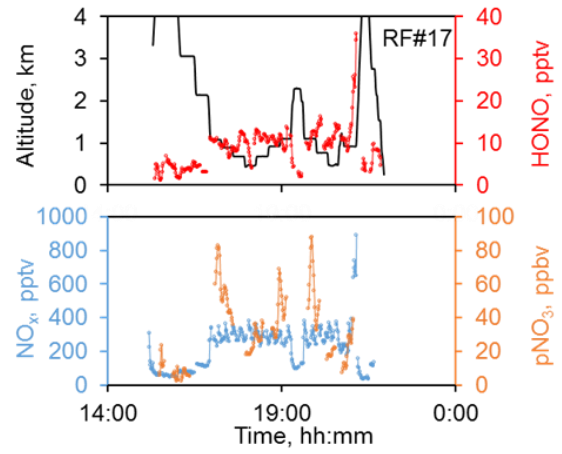
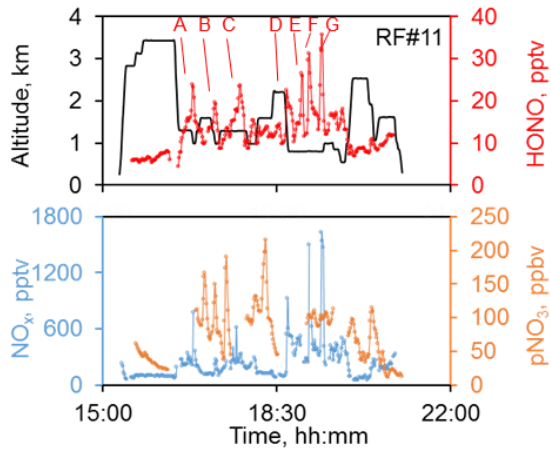
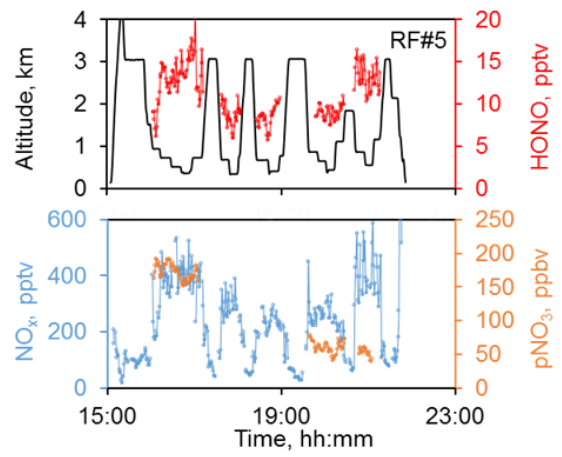
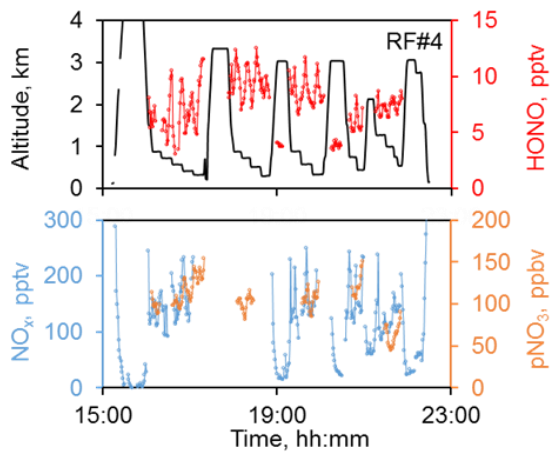


821

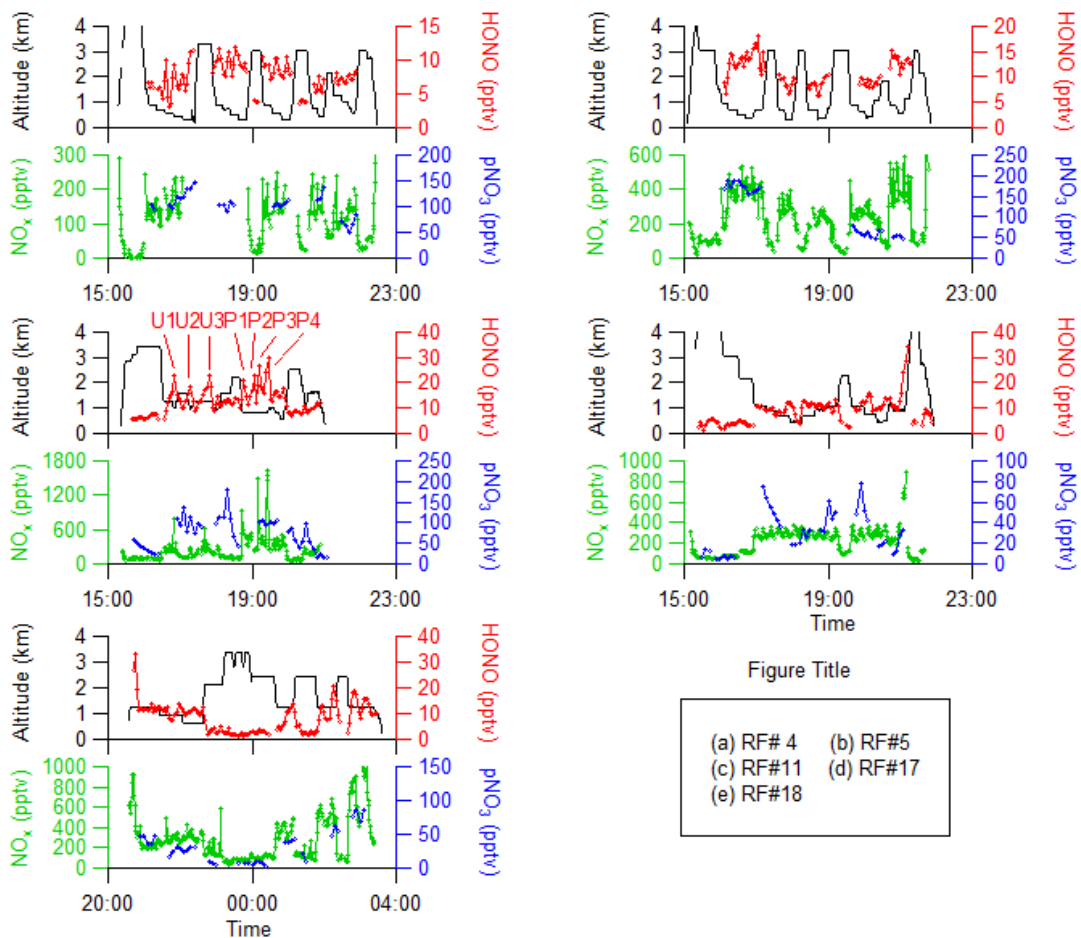
822 Figure 1. Flight tracks in the Southeast US during the NOMADSS 2013 summer study. The
 823 flight start time and end time in UTC (= EDT+4) are: RF#4 (blue): 15:12 and 22:30, June 12,
 824 2013; RF#5 (light blue): 15:04 and 21:52, June 14, 2013; RF#11 (yellow): 15:20 and 21:02,
 825 June 29, 2013; RF#17 (green): 15:07 and 21:57, July 11, 2013; RF#18 (red): 20:32, July 12,
 826 2013, and 03:37, July 13, 2013.

827

828



829

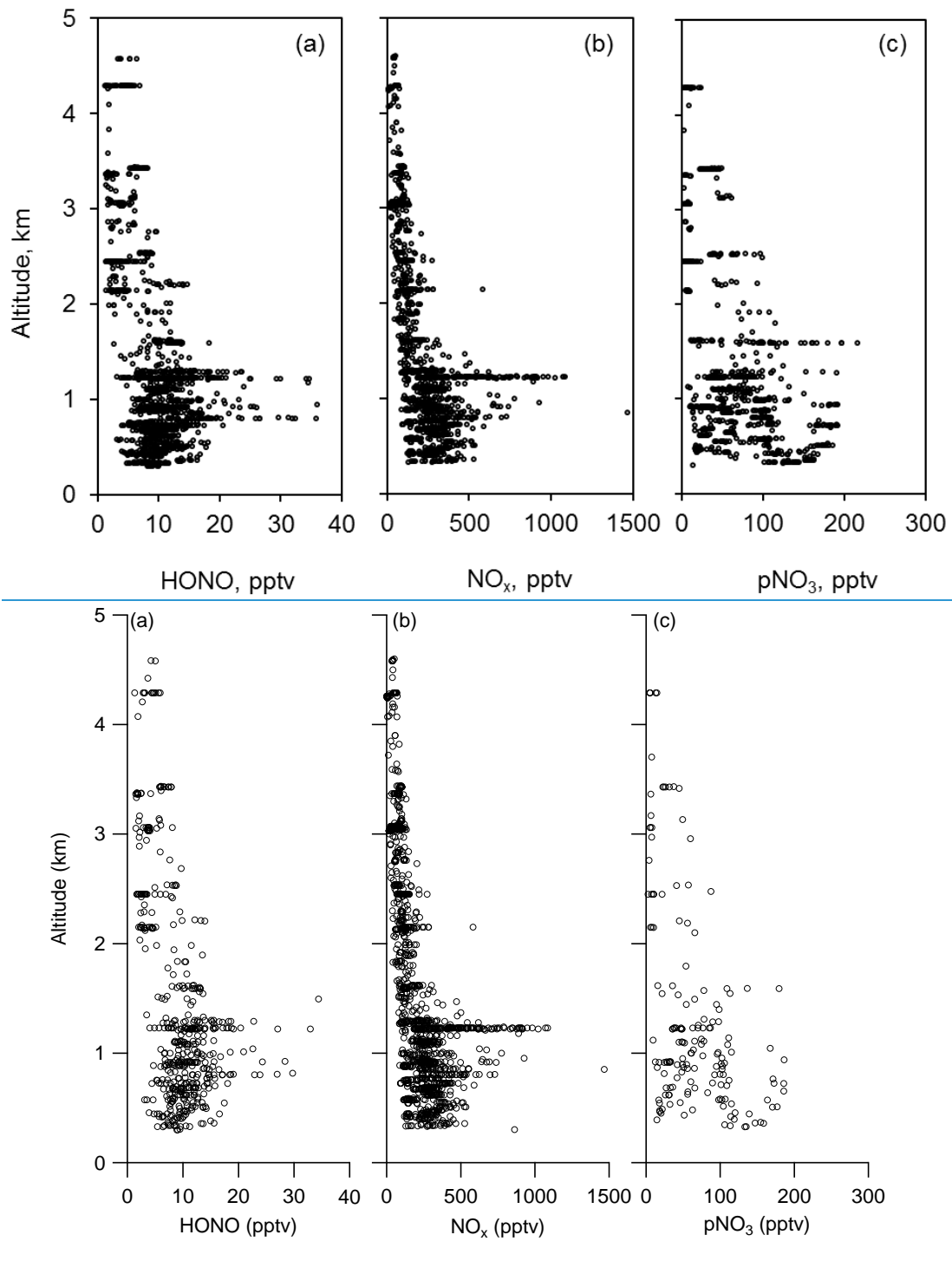


830

831

832 Figure 2. Time series of altitude, HONO, NO_x and pNO₃ in five flights (RF #4, RF #5, RF
 833 #11, RF #17 and #18) in the Southeast US during the NOMADSS 2013 summer study. In RF
 834 #11, the plumes U1 and U3 were from Birmingham, AL; the plume U2 was from
 835 Montgomery, AL; the plumes P1-P3 were from a power plant in Monroe County, GA; and the
 836 plume P4 was from a power plant in Putnam country, GA. A-C indicate urban plumes, and
 837 D-G indicate coal-fired power plant plumes. The time is in UTC.

838



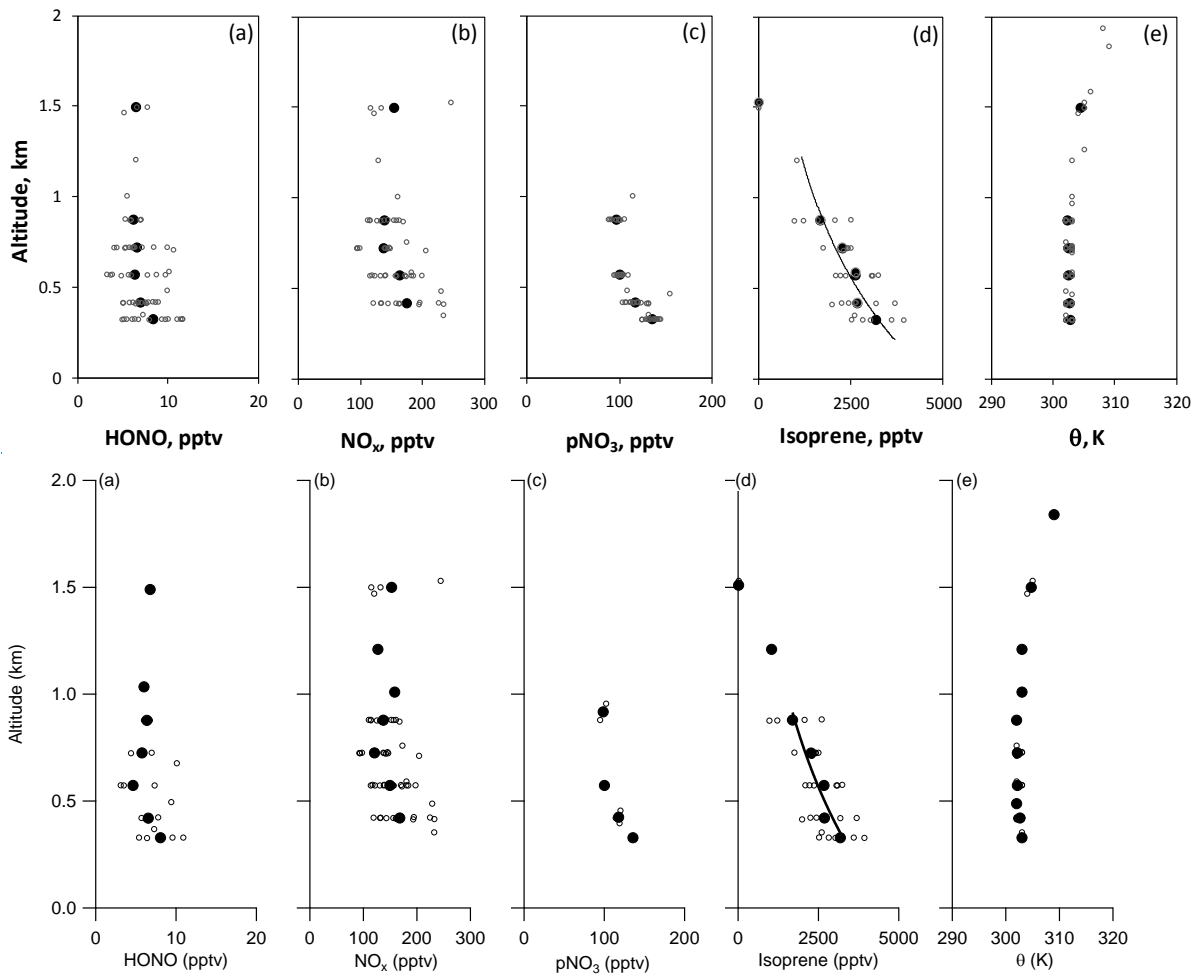
839

840

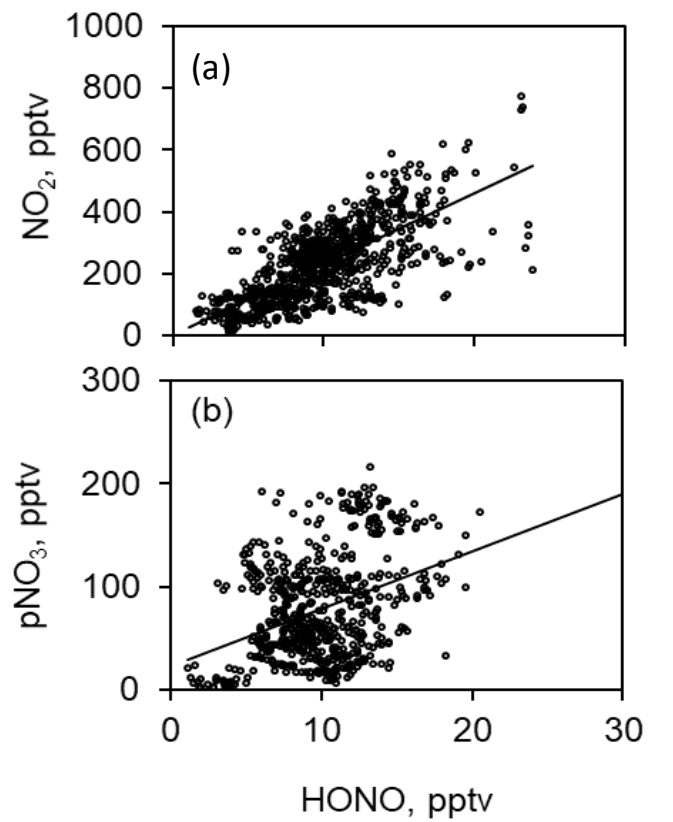
841 Figure 3. Vertical distributions of concentrations of HONO (a), NO_x (b), and pNO₃ (c) in the
 842 five selected flights in the Southeast US during the NOMADSS 2013 summer study.

843

844



848 Figure 4. Vertical distributions of concentrations of HONO (a), NO_x (b), pNO₃ (c), isoprene
 849 (d) and potential temperature (e) in the PBL during the first race-track of RF#4 from 11:00 –
 850 12:15 LT (16:00 – 17:15 UTC), June 12, 2013. The small open circles represent the 1-min
 851 data points, the large solid circles the mean values for each race-track measurement altitude.
 852 The line in (d) is the best fit of (Eq. 1) to the isoprene data: $C = 4700e^{-h/0.895}$ $h = 5.97 - 0.692$
 853 h , $r^2 = 0.93$.



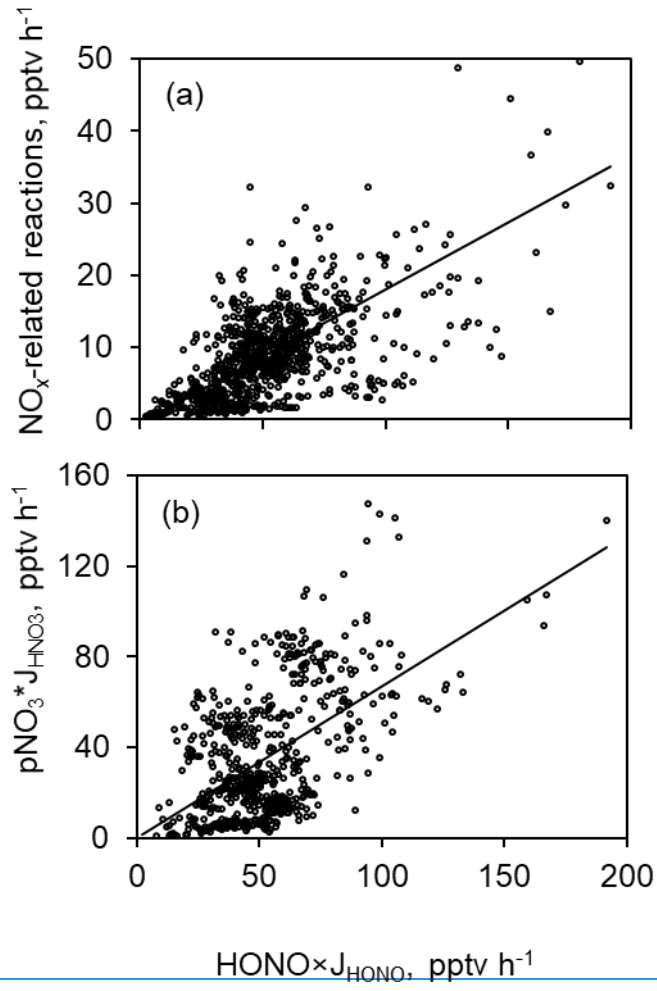
854

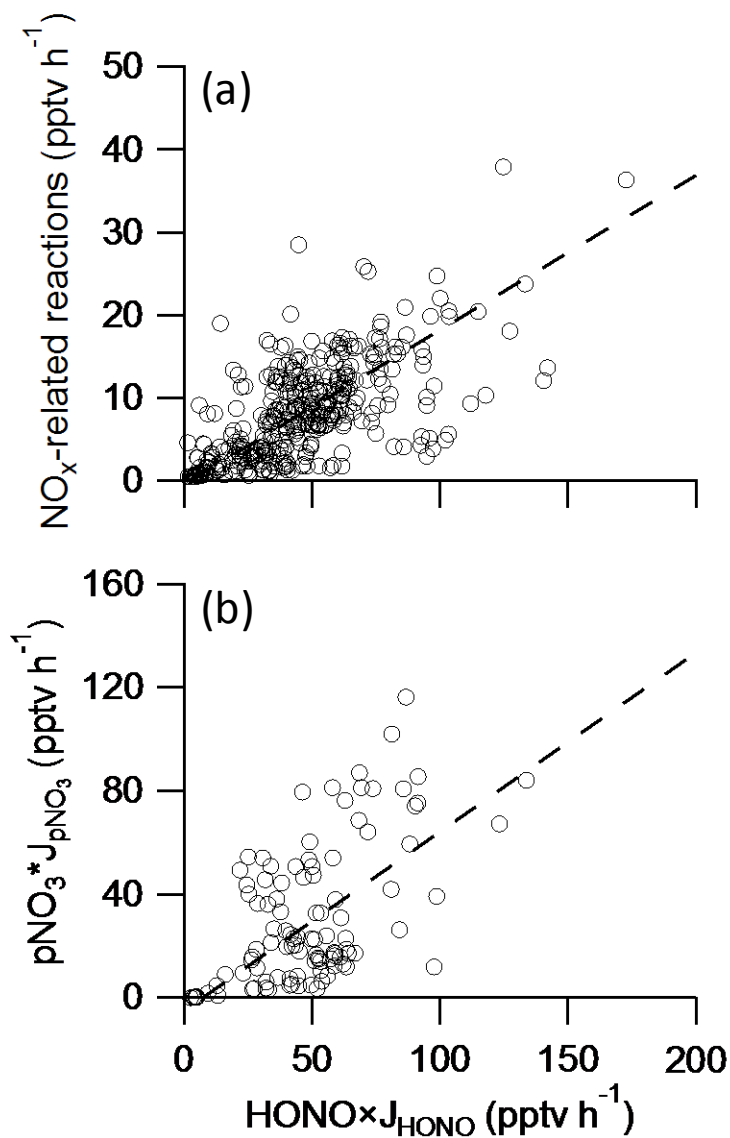
855

856 [Figure 5. Correlation analysis of HONO with NO_x \(a, \$r^2=0.52\$ \) and pNO₃ \(b, \$r^2=0.14\$ \) in the](#)
857 [southeast US during the NOMADSS 2013 summer study. Data points in the urban and power](#)
858 [plant plumes have been excluded.](#)

859

860



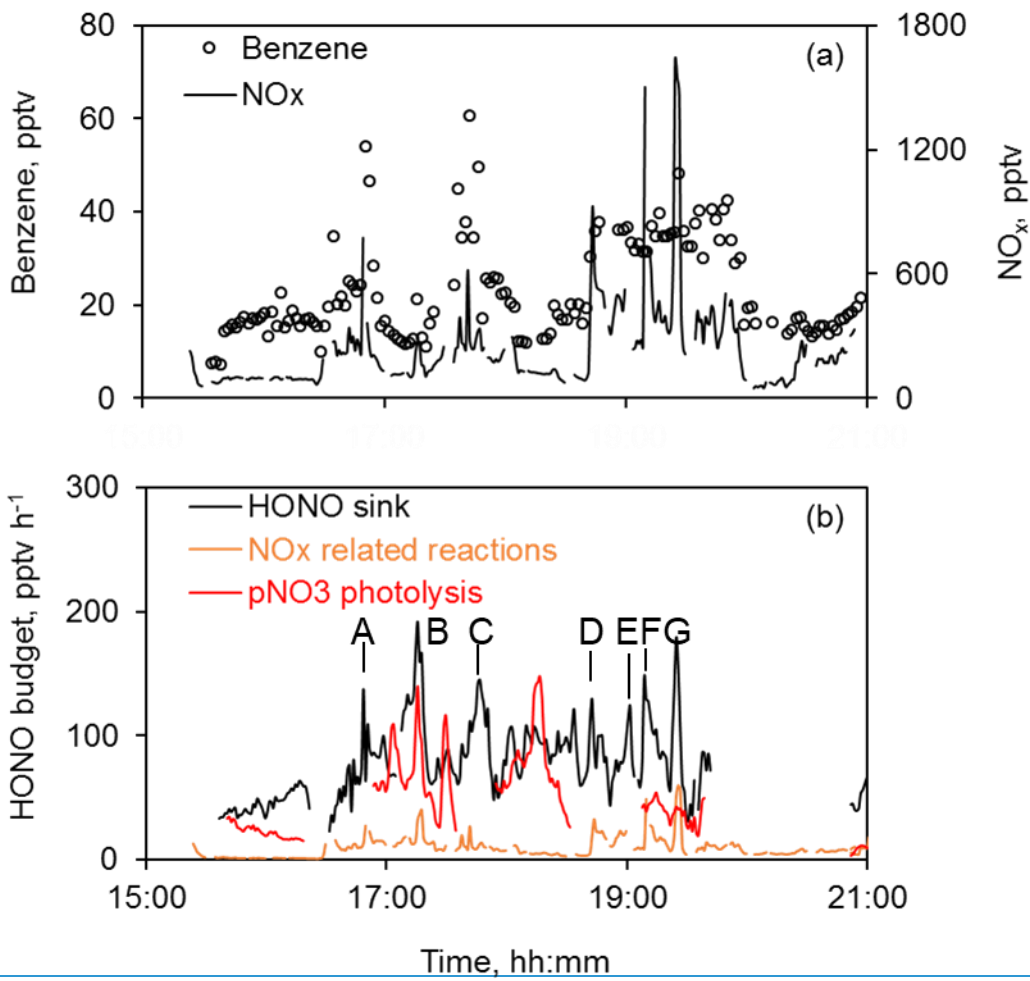


862

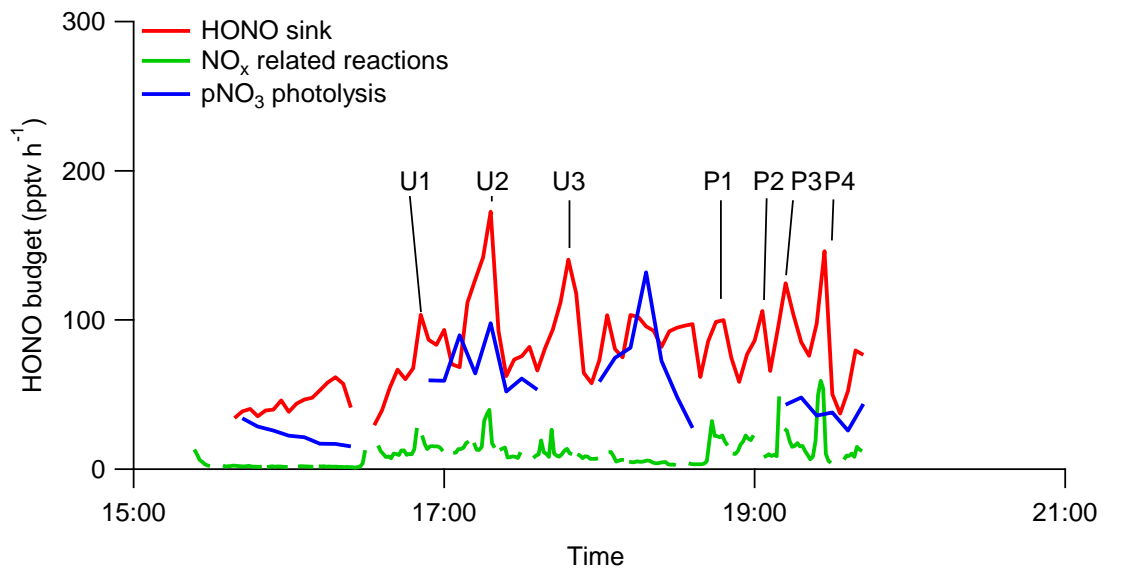
863 Figure 65. Correlation analysis of main HONO sink (“ $\text{HONO} \times \text{J}_{\text{HONO}}$ ”) with contribution from
 864 NO_x related reactions (a) and with contribution from particulate nitrate photolysis,
 865 $\text{pNO}_3 \times \text{J}_{\text{pNO}_3}$ (ab) and with contribution from NO_x -related reactions (b) in the southeast US
 866 during the NOMADSS 2013 summer study. The line represents the Deming least-squares
 867 fitting regression (Wu and Yu, 2018) (R^2 $r^2=0.4440$, intercept = $-0.57-0.51$ and slope = $0.19-19$
 868 for Figure 6a; R^2 $r^2=0.3134$, intercept = $0.05-5.0$ and slope = $0.67-69$ for Figure 6b).

869

870



871



872

873 Figure 76. HONO budget analysis in RF #11 in the Southeast US during the NOMADSS 2013
874 summer study. “HONO sink” is the HONO loss rate contributed by photolysis and the

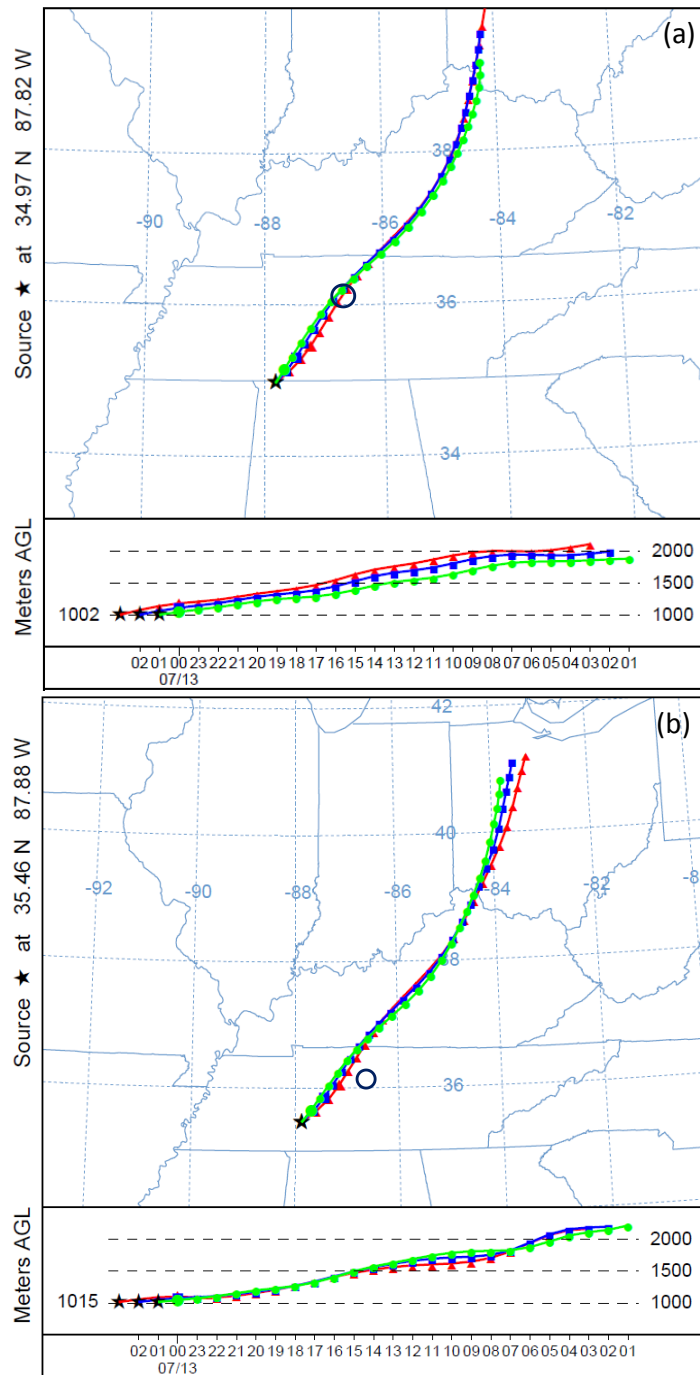
875 reaction of HONO with OH radicals, “NO_x related reactions” is the sum of HONO production
876 rates by from all known NO_x reactions, and “pNO₃ photolysis” is the HONO ~~source~~
877 production rate from contributed by photolysis of pNO₃. The calculations are based on 1-min
878 NO_x data, 3-min HONO data and 6-min pNO₃ data.

879

880

881

882



883

884

885

886

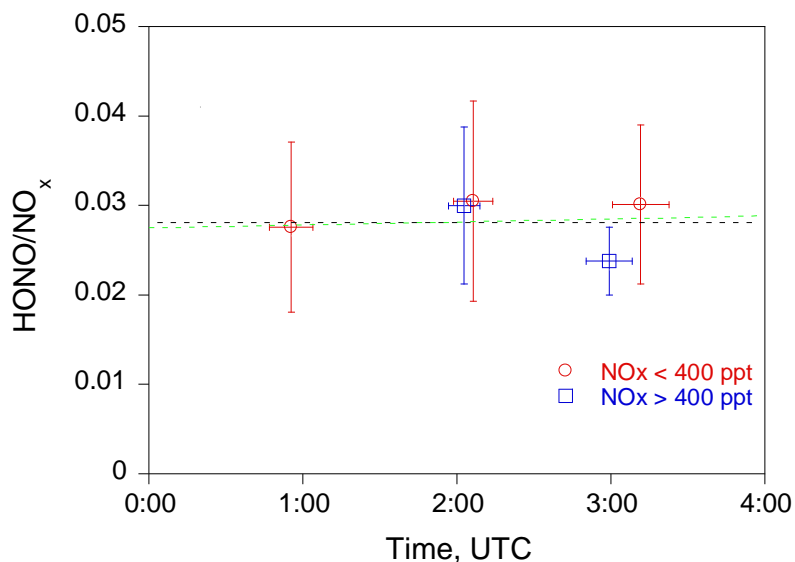
887

888

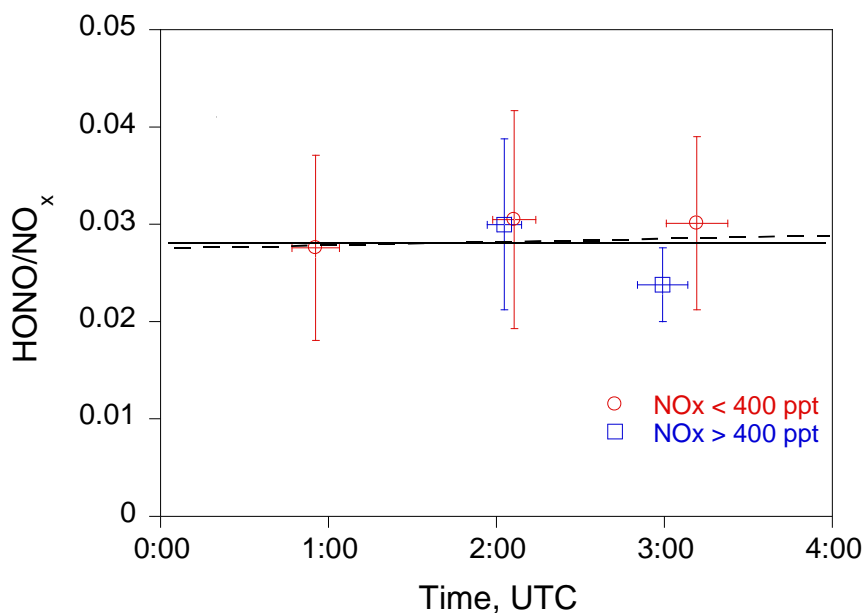
889

890

Figure 8. Back trajectory analysis of air masses encountered in the PBL in RF #18 in the Southeast US during the NOMADSS 2013 summer study. The air masses arriving at the southern point of the flight tracks were found to pass over the metropolitan area of Nashville (the black circle, panel a), while those at the northern point to stay to the north of the area. The back trajectory analysis was made using NOAA's online HYSPLIT model (http://www.arl.noaa.gov/HYSPLIT_info.php).



891



892

893 Figure 97. The evolution of HONO/NO_x ratio in the nocturnal boundary layer during the
 894 RF#18. The red circles and blue squares are the median HONO/NO_x values under the
 895 conditions of NO_x ≤ 400 pptv and NO_x > 400 pptv, respectively. The horizontal bars indicate
 896 the averaging time periods and the vertical bars the one standard deviation of HONO/NO_x
 897 ratios. The ~~black dashed~~ solid line is the least squared fit to the data, and the ~~green~~ dashed
 898 line indicates a slope of 3 × 10⁻⁴ hr⁻¹. The sunset time at the sampling location was 0:40 UTC.

899